

Aus der Klinik für Dermatologie, Venerologie und Allergologie,
Universitätsklinikum des Saarlandes, Homburg/Saar
Betreuer: Prof. Dr. Jörg Reichrath

**Regulation of circadian clock genes by
UVB radiation and vitamin D: a pilot
study in human epidermal keratinocytes
during different stages of skin
photocarcinogenicity.**

**Dissertation zur Erlangung des Grades eines Doktors der
Medizin der Medizinischen Fakultät**

der UNIVERSITÄT DES SAARLANDES
2022

vorgelegt von: Leandros Lamnis

geb. am: 04.04.1996 in Thessaloniki, Griechenland

Abstract

Several cellular processes are constantly under regulation of a timekeeping system, known as the circadian clock (CC), with the main regulatory genes involved referred to as the circadian clock genes (CCGs). In spite of a master pacemaker existing in the suprachiasmatic nucleus (SCN) of the hypothalamus, several clock systems have been shown to operate independently in peripheral tissues, including the skin. CCGs interact with cellular processes by both regulating them and being regulated by them, a prime example of this being the bilateral relationship between CC and ultraviolet B radiation (UV-B): On one hand, UV-radiation regulates expression of CCGs in many cell types, and on the other, it has recently been shown that expression of CCGs modulates susceptibility for UV-B-induced cellular damage, including the formation of pyrimidine dimers and other DNA-lesions that are a hallmark of photocarcinogenesis. It was the aim of this study to gain further insights into the CCGs' putative role for UVB-induced skin photocarcinogenesis. In particular, we aimed to investigate UV-effects on CC and whether these may at least in part be mediated by 1,25(OH)₂D₃ (D₃), the active form of vitamin D, that both depends on UV-B for its synthesis and is known to protect the skin from UV-B's damaging properties.

We treated cells with D₃, UV-B and a combination of the two and measured expression of two core clock genes, brain and muscle ARNT-like 1 (BMAL1) and Period-2 (Per2), both over several time points and in cells representing: normal (Normal Human Epidermal Keratinocytes – NHEK; p53 wild type), precancerous (HaCaT keratinocytes; mutated p53 status) and cancerous keratinocytes (Squamous Cell Carcinoma SCL-1; p53 null status). We also assessed the role of vitamin D receptor (VDR) and aryl hydrocarbon receptor (AhR) pathways by measuring UVB-induced damage, repair and cellular toxicity after treatment with D₃ and UVB and under chemical antagonization of either/both VDR and/or AhR.

Untreated HaCaT cells showed circadian rhythmicity (length of individual periods approximately 24 hours) for expression of BMAL1 and Per2, that were induced by UVB ($p < 0,001$), which also resulted in significant increase in cellular toxicity 24h after treatment ($p < 0,05$). In contrast, treatment with 1,25-dihydroxyvitamin D had only marginal effects (no visual effect on expression of BMAL1, trend for a marginal reduction of expression of Per2). While UV-B induced expression of Per2 in NHEK, HaCaT and SCL-1 cells, UVB-induced upregulation of BMAL1 was only detected in NHEKs and HaCaT, but not in SCL-1 cells. In regards to direct effects and interaction of UVB and D₃ and the roles of VDR and AhR on DNA damage and repair, no safe conclusions can be drawn from this study.

HaCaT keratinocytes express BMAL1 and Per2 with circadian rhythmicity. Our findings do not support the hypothesis that the UVB-induced upregulation of these CCGs may be mediated via UVB-induced synthesis of vitamin D. Comparing epidermal keratinocytes representing different stages of skin photocarcinogenesis, we provide further evidence for an independently operating timekeeping system in human skin cells, that is physiologically regulated by UVB. The destruction of this mechanism in malignant keratinocytes points to a contribution of CCGs for skin photocarcinogenesis.

Table of Contents

Tables	6
Figures' Table of contents	8
Abbreviations:	9
1. Introduction	10
1.1 Review of the literature	10
1.1.1 Overview of circadian clock physiology and its role in skin	10
1.1.2 The relevance of UV-R in cancer formation and its relationship with the circadian clock	12
1.1.3 Skin as an endocrine organ: the role of D ₃	14
1.1.4 UVB, p53 and vitamin D ₃	16
1.1.5 The role of AhR in circadian clock physiology, UVB stress response and vitamin D ₃ related pathways	16
1.2 Goals of research	18
2. Methods and Materials	20
2.1 Basic Laboratory Principles	20
2.2 Cell culture	20
Eucariotic cell lines used and their purpose	20
2.3 Defrosting Cells	21
2.4 Culturing Cells	22
2.5 Subculturing / Passaging of Cells	22
2.6 Methodology of cell treatment	25
Conditions tested	29
2.7 Harvesting of cells and Storage of samples	30
2.8 Isolation of mRNA	31
2.9 Reverse Transcription of mRNA to cDNA	31
2.10 Measurement of Gene Expression with RT-qPCR	32
2.11 Isolation of DNA	34
2.12 Dot Blot Assays	34
2.13 ELISA	35
2.14 Preparation of TE-Buffer	38
2.15 Preparation of samples for LDH-Assays of cellular toxicity	38
2.16 Statistical Analysis	38
2.17 Kit Components:	43
3. Results	45
3.1 Preexaminations	45
3.2 Expression of core CCGs BMAL1 and Per2 shows circadian rhythmicity in HaCaT keratinocytes	46
3.3 Circadian activity of core CCGs BMAL1 and Per2 may differ between normal (HaCaT) and cancerous (SCL-1) keratinocytes. A reference test-run	47
3.4 UVB radiation significantly upregulates both BMAL1 and Per2 in HaCaT keratinocytes, while 1,25(OH) ₂ D ₃ only mediated a marginal downregulation effect in Per2 and only between non-radiated samples	48
3.5 Cancerous SCL-1 cells show an overall decreased expression of BMAL1 and a further suppression following UVB radiation as opposed to an upregulation observed in HaCaT and even more strongly in NHEK keratinocytes, while no such cell-specific differences were observed for Per2	55
3.5.1 BMAL1	55
3.5.2 Per2	60

3.6	No significant effect was noticed after administration of AhR and VDR antagonists in HaCaT and NHEK cells regarding UVB-induced DNA damage, repair and LDH-toxicity.....	62
4.	Discussion.....	69
	Low-dosed UVB radiation upregulates CCGs in HaCaT keratinocytes and increases cellular toxicity.....	69
	1,25(OH) ₂ D ₃ shows no effect in BMAL1 expression but is significantly implicated in the downregulation of Per2 between non-radiated HaCaT keratinocytes.....	73
	BMAL1 shows a weaker expression profile in SCL-1 compared to HaCaT/NHEK. Low-dosed UVB radiation affects BMAL1 expression differently based on cell type, showing higher activation in NHEK than HaCaT and a suppression in SCL-1.	74
	The unclear role of 1,25(OH) ₂ D ₃ in UVB-induced DNA-damage response and repair in our study model.....	77
	A potential damaging effect of 1,25(OH) ₂ D ₃ in NHEK experiments. Increase of 6-4PP but not of CPDs in non-radiated 1,25(OH) ₂ D ₃ -treated NHEKs: A limited sample size error or a new pathway?	80
	Clinical vs Experimental photoprotectivity of 1,25(OH) ₂ D ₃ and the relevance of VDR / AhR chemical antagonization. Is AhR antagonization inducing 6-4PP clearance?	80
	Limitations:	83
	Implications / Impact of research	83
	Future Recommendations:	84
	Conclusions:	85
	References.....	86
	Publications	91
	Acknowledgements	91
	Lebenslauf / CV	92

Tables

Table 1: Circadian rhythmicity in skin physiology.....	12
Table 2, Abbreviations used to simplify description of conditions applied	26
Table 3, Conditions for Experiment 2.....	28
Table 4, New conditions used in Experiment 3.....	29
Table 5, All conditions for Experiment 3 summarized.....	30
Table 6, Preparation outline for the ELISA standard curve samples.....	36
Table 7, Effect of EtOH vehicle (1:1000 diluted in 1% BSA DMEM, vehicle control) vs non-EtOH-containing control in HaCaT Keratinocytes for BMAL1 (up) and Per2 (down).....	45
Table 8, Shapiro-Wilk test of normality for BMAL1 Δ Ct values in HaCaT Keratinocytes, Experiment 1A.....	49
Table 9, two-way repeated measures ANOVA for BMAL1 in HaCaT Δ Ct values, with UVB and D ₃ treatments as within-subjects factors and time as the between-subjects variable.....	49
Table 10, Between-Subjects Effects, BMAL1 Δ Ct values, Experiment 1A. HaCaT Keratinocytes.....	50
Table 13, Shapiro-Wilk test of normality for Per2 Δ Ct values, Experiment 1A. HaCaT Keratinocytes.....	51
Table 14. Two-way repeated measures ANOVA for Δ Ct values of Per2 in HaCaT keratinocytes.	52
Table 15. Tests of Between-Subjects Effects. Per2 Δ Ct values, Experiment 1A. HaCaT Keratinocytes.....	52
Table 16, Tests of simple main effects, Per2, Experiment 1A. Effects of D ₃ across the different levels of UVB. HaCaT Keratinocytes.....	54
Table 18 Experiment 1B, BMAL1 $-\Delta\Delta$ Ct values, Shapiro-Wilk normality test. Values for HaCaT, NHEK and SCL-1.....	55
Table 19, Experiment 1B, BMAL1 $-\Delta\Delta$ Ct values, two-way repeated measures ANOVA, Within-Subjects factor for UVB and D ₃ with cell type as the between-subjects factor. Within-Subjects effects.....	56
Table 20, Experiment 1B, BMAL1 $-\Delta\Delta$ Ct values, two-way repeated measures ANOVA, Within-Subjects factor for UVB and D ₃ with cell type as the between-subjects factor. Between-Subjects effects.....	56
Table 21, Experiment 1B, BMAL1 $-\Delta\Delta$ Ct values, post hoc Tukey HSD test for cell type.	57
Table 22, Experiment 1B, BMAL1 $-\Delta\Delta$ Ct values, HaCaT vs NHEK, two-way mixed ANOVA, with cell type and D ₃ as the between-subjects factors and UVB as the within-subjects factor.	59
Table 23, Experiment 1B, BMAL1 $-\Delta\Delta$ Ct values, HaCaT vs NHEK, two-way mixed ANOVA, with cell type and D ₃ as the between-subjects factors and UVB as the within-subjects factor.....	59
Table 24 Shapiro-Wilk test of normality of Per2 $-\Delta\Delta$ Ct. For HaCaT, NHEK and SCL-1.....	60
Table 25, Shapiro-Wilk normality test for all $-\Delta\Delta$ Ct values of Per2 gene expression. For HaCaT, NHEK and SCL-1.....	60
Table 26, Experiment 1B, Per2 $-\Delta\Delta$ Ct values, two-way repeated measures ANOVA. Within-Subjects Effects. For HaCaT, NHEK and SCL-1.....	61

Table 27, Experiment 1B, Per2 - $\Delta\Delta C_t$ values, two-way repeated measures ANOVA.	61
Table 28, Experiment 3, HaCaT CPDs, Normality Tests.	63
Table 29, Experiment 3, HaCaT CPDs, two-way repeated measures ANOVA,.....	63
Table 30 , Experiment 3, HaCaT CPDs, two-way repeated measures ANOVA. Between-Subjects effects.....	63
Table 31. Experiment 3, HaCaT 6-4PPs 3h after treatment. Two-way repeated measures ANOVA. ...	64
Table 32, Experiment 3, HaCaT Toxicity levels 24h after treatment.....	65
Table 33, Experiment 3, NHEK CPDs 1h after treatment.....	66
Table 34, Experiment 3, NHEK CPDs 1h after treatment.....	66
Table 35, Experiment 3, NHEK 6-4PPs 1h after treatment, two-way repeated measures ANOVA. Within-Subjects effects.....	67
Table 36, Experiment 3, NHEK 6-4PPs 1h after treatment, two-way repeated measures ANOVA. Between-Subjects effects.....	67

Figures' Table of contents

Figure 1: The core circadian clock transcriptional/translational feedback pathway (simplified).....	11
Figure 2 The steps of skin photocarcinogenesis..	13
Figure 3, Vitamin D ₃ synthesis and activation pathway (simplified).	15
Figure 4, Outline of the main interactions' network between the main researched variables.	19
Figure 5, Outline of Experiment 2 protocol design.	28
Figure 6, RT-qPCR Template for EtOH+50J condition as an example.	33
Figure 7, Example of an ELISA template for HaCaT CPDs 1h/24h.	36
Figure 8, Sample results of Dot Blot assays for «Experiment 2».....	37
Figure 9. BMAL1 and Per2 mean $-\Delta\Delta Ct$ values plotted over time for all 4 conditions with untreated 0h samples as the internal control.	46
Figure 10. Testing experiment, SCL-1 BMAL1 $-\Delta\Delta Ct$ values over 60h	48
Figure 11. Testing experiment, SCL-1 Per2 $-\Delta\Delta Ct$ values over 60h.	48
Figure 12. BMAL1 mean $-\Delta\Delta Ct$ values over 60h for HaCaT Keratinocytes with untreated 0h samples as the internal control.	51
Figure 13. Per2 mean $-\Delta\Delta Ct$ values for HaCaT Keratinocytes.	53
Figure 14, Experiment 1B, BMAL1 mean $2^{-\Delta\Delta Ct}$ values.	57
Figure 15 mean $2^{-\Delta\Delta Ct}$ values for BMAL1, Experiment 1B, HaCaT, NHEK, SCL-1	58
Figure 16, Experiment 1B, HaCaT vs NHEK, BMAL1 $-\Delta\Delta Ct$ plotted against UVB treatment.....	59
Figure 17, Experiment 1B, Per2 $2^{-\Delta\Delta Ct}$ values, untreated HaCaT as the internal control.	61
Figure 18, Experiment 1B, Per2 $2^{-\Delta\Delta Ct}$ values, normalized to each cell's control condition.	62
Figure 19, Experiment 3, HaCaT CPDs 1h/24h after treatment	64
Figure 20. Experiment 3, HaCaT mean 6-4PPs concentrations, 3h after treatment, between irradiated samples.....	65
Figure 21, Experiment 3, HaCaT Toxicity Levels 24h after treatment.	66
Figure 22, Experiment 3, NHEK CPDs 1h after treatment, D ₃ (-) vs D ₃ (+) samples.	67
Figure 23, Experiment 3, NHEK 6-4PPs 1h after treatment. UVB treatment plotted against D3 treatment (left) and all conditions together (right).....	68

Abbreviations:

6-4PPs	6-4 Photoproducts
7-DHC	7- dehydrocholesterol
ADSCs	Adipose-derived Stem Cells
AhR	Aryl hydrocarbon Receptor
ANOVA	Analysis of Variance
BMAL1	Brain and muscle ARNT-like 1
BSA	Bovine Serum Albumin
CC	Circadian Clock
CCGs	Circadian Clock Genes
cDNA	complementary - Deoxyribonucleic acid
CLOCK	circadian locomotor output cycles kaput
CPDs	Cyclobutane Pyrimidine Dimers
Cry1, Cry2	Cryptochromes 1, 2
DMEM	Dulbecco's Modified Eagle Medium
FCS	Fetal Calf Serum
FICZ	6-Formylindolo[3,2-b]carbazole
HaCaT	Human adult low Calcium high Temperature
LDH	Lactate Dehydrogenase
mRNA	messenger - Ribonucleic acid
NER	Nucleotide excision repair (system)
NHEK	Normal Human Epidermal Keratinocytes
PBS	Phosphate Buffer Saline
Per2	Period-2
ROR_{α, γ}	RAR related orphan gene receptor α , γ
RPMI	Roswell Park Memorial Institute
SCL-1	Squamous cell carcinoma Cell Lines
SCN	Suprachiasmatic Nucleus
TTFL	Transcriptional/Translational Feedback Loops
UVB	Ultraviolet B rays
VDR	Vitamin D Receptor

1. Introduction

1.1 Review of the literature

1.1.1 Overview of circadian clock physiology and its role in skin

From the first ever revolutionary documentation of genetic elements encoding biological timing in the common fruit fly by Ronald Konopka and Seymour Benzer in the 1970s¹, to the successful identification of the period (PER) gene in 1984² and the further illumination of its timekeeping properties³ by the teams of Jeffrey Hall, Michael Rosbash and Michael Young granting them the 2017 Nobel in Physiology and Medicine, research of the circadian clock has come a very long way. The term “circadian” originates from the latin words *circa* (“around”) and *diēm* (“day”), therefore the circadian rhythm represents a 24-hour circle of day-and-night and biological circadian clocks entail those processes through which our body responds to the constant rotation of the earth around its axis. The genes involved in the control of biologic timekeeping are thus called circadian clock genes (CCGs).⁴

Circadian clocks exist in almost all human cells and mediate their timekeeping properties through a complex system of autoregulatory Transcriptional/Translational Feedback Loops (TTFL), coordinated under a master pacemaker in the suprachiasmatic nucleus (SCN) of the hypothalamus. External stimuli called zeitgebers (=time cues) entrain the rhythm of the SCN which through a series of electrical and molecular circadian messages synchronizes subordinate peripheral clocks in other tissues.^{5,6} Light has been suggested as the most dominant zeitgeber, signaling the constant alterations of daily light-dark circles to the SCN through the retino-hypothalamic tract. Feeding-fasting circles have also been shown to be heavily involved in the synchronization of the central circadian clock and the circadian physiology of metabolism has recently become the center of research attention.⁷ However, the SCN is also capable of maintaining circadian rhythmicity even in the absence of external stimulation. Moreover, despite the strict hierarchical model of circadian clock synchronization having been popular for a long time, the discovery of peripheral clocks in multiple tissues, including the skin, which interact with time cues, like light, independently of the central clock, suggest a more complex system of clock organization.⁸

While tissue-specific differences exist between different clocks, a basic layout consisting of “core clock genes” and their respective interaction patterns with one another (as part of the TTFL) are common among all circadian oscillators. The genes that constitute the “core clock

genes” are brain and muscle ARNT-like 1 (*BMAL1*), circadian locomotor output cycles kaput (*CLOCK*), cryptochromes (*Cry1*, *Cry2*) and periods (*Per1*, *Per2*, *Per3*).^{7,8} *BMAL1* and *CLOCK* proteins bind in the cytoplasm forming a heterodimer that translocates to the cellular nucleus. There it binds to the E-box motif in the promoter region of “clock-controlled genes”, estimated to involve around 10% of the genome, and thereby fostering their expression. At the same time, transcription of the *PER* and *CRY* families of proteins is also stimulated. This second heterodimer inhibits the binding of *BMAL1* and *CLOCK* and *BMAL1/CLOCK*-mediated transcription, thereby obstructing their own formation and closing the feedback loop circle. Protein degradation allows the circle to repeat in approximately 24-hour-lasting intervals.^{8,9}

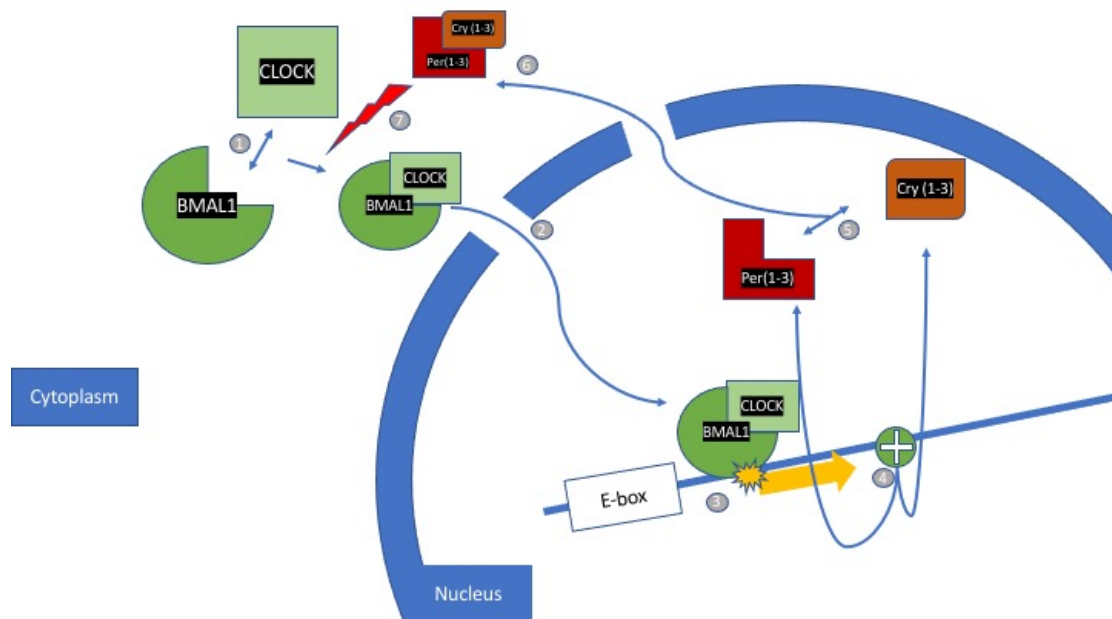


Figure 1: The core circadian clock transcriptional/translational feedback pathway (simplified). (1) *BMAL1* and *CLOCK* proteins form a heterodimer in the cytoplasm and (2) translocate to the nucleus, where they (3) bind to the E-box motif in the promoter region of “clock-controlled genes” inducing their transcription. At the same time (4) transcription of the *Per(1-3)* and *Cry(1-3)* family of genes is also stimulated. These proteins accumulate in the nucleus and then (5) form a second heterodimer and (6) translocate to the cytoplasm where they (7) inhibit the *BMAL1/CLOCK* heterodimerization and thereby also obstructing their own transcription.

The skin constitutes a very important model for studying the complexities of circadian clock systems. It involves multiple cell-types structured both across delimited compartments (epidermis-keratinocytes, dermis-fibroblasts, adipose tissue-fat cells) and with interconnected skin cells (melanocytes, hair follicles, sebaceous glands), immune cells (Langerhans cells, T-lymphocytes, mast cells) with distinct but probably coordinated circadian clocks. Moreover, several physiologic cutaneous processes, immune genes in skin and responses to environmental stress have been shown to be modulated by the circadian clock.^{5,6,9-13} Some examples of time-of-the-day dependent functions of skin physiology are listed in *Table 1* below.



 During the day	 During the night
↑ skin protection ↑ skin thickness ↑ sebum production ↑ pH ↓ cell proliferation	↑ DNA repair ↑ cell proliferation ↑ skin temperature ↑ barrier permeability ↑ skin penetration ↑ itching ↑ moisture loss ↑ skin blood flow ↓ barrier recovery rate

Table 1^{5,6}: Circadian rhythmicity in skin physiology. Left we see physiologic processes that are more active during the day and right the same thing for processes that are more active during the night. As a means of managing resources, cutaneous processes involved in protecting the skin from external stimulants (like UV-R and chemicals), are concentrated in those times of the 24h day, that are most often needed, whereas resting phases later in the day acquire less resources making the skin as a result more susceptible to environmental insults.

Notably, some skin cells are in contact with nerval endings, and therefore in probable communication with the SCN, while others don't. Trans- and intercellular regulation of clock synchronization further gains importance as a promising research field with accounts to the skin's direct proximity to external environment. Stimulation of cutaneous sensing mechanisms could explain alternative time-cue processing pathways, implying systematic modulatory effects of cutaneous clocks as part of the role of skin as an endocrine organ.⁶

1.1.2 The relevance of UV-R in cancer formation and its relationship with the circadian clock

Skin cancer is the most common form of cancer in humans from which the vast majority represent non-melanoma skin cancer, namely basal and squamous cell carcinomas (BCC and SCC respectively). Our skin is daily exposed to a number of environmental insults like pollutants and solar radiation. Solar ultraviolet (UV) radiation has been long known to play a major role in skin photocarcinogenesis, indicated also by the higher rates of skin cancer in outdoor compared to indoor workers.¹⁴ Non-melanoma skin cancer formation induced by UV radiation is characterized by a 3-step pathogenetic process: (1) Initiation, which involves the creation and collection of genetic mutations (photolesions) which affect by extension and alter signal transduction pathways. Failure to repair initiated damage can lead to (2) Promotion, which is characterized by clonal expansion of the cells involved and subsequently to (3) Progression, which refers to the malignant transformation of those cells.¹⁵ Solar UV radiation

(UV-R) is divided into 3 main subtypes: UVA (320-400nm), UVB (290-320nm) and UVC (200-290nm) but only UVA and UVB do in fact reach the surface of earth after partial absorption by the atmosphere. In spite of it accounting for only a minor part of UV reaching earth, UVB represents the major cause of photoaging and UV-induced skin cancer.¹⁴

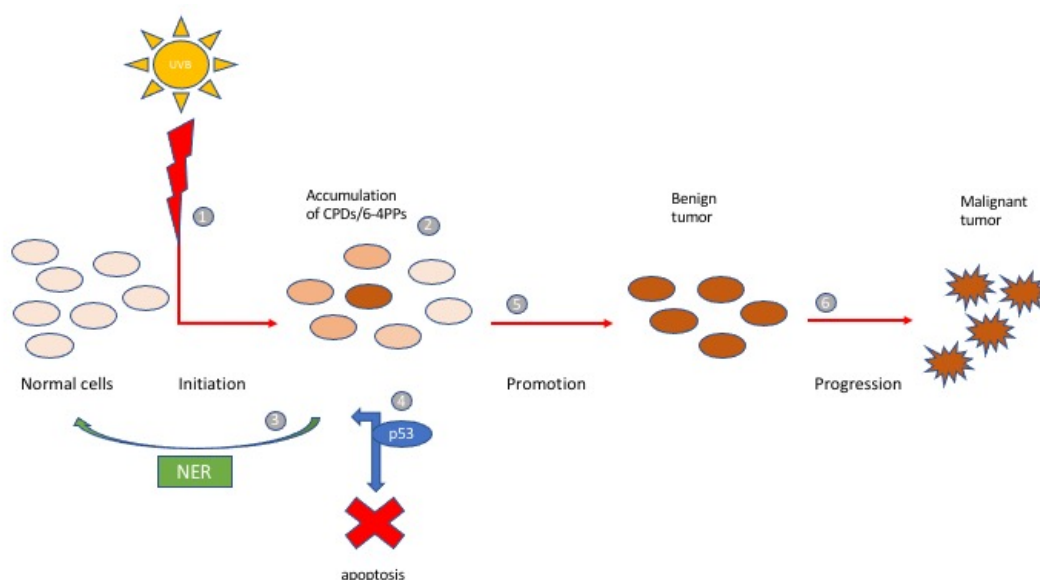


Figure 2 The steps of skin photocarcinogenesis: Normal skin cells are (1) exposed to UV-B radiation on a constant basis, resulting to (2) accumulation of DNA-damage in the form of photoproducts, especially CPD and 6-4PPs. The NER repair system (3) constitutes the sole repair mechanism in eucariotic organisms and is capable of reversing some of that damage. The p53 gene (4) can be of assistance in these processes either by halting cell cycle promoting repair when possible, or leading unrepairable damaged cells to their death. In cases where the reverse mechanisms fail to halt the process, this stage is followed by (5) Promotion, representing the clonal expansion- multiplication of - at that moment still- non-malignant cells. Further mutation within the benign tumor cells can lead to (6) progression, meaning their malignant transformation. From this point forward the lesion is described as skin cancer.

The two major photoproducts (photolesions) are cyclobutane pyrimidine dimers (CPDs) and 6-4 photoproducts (6-4PPs), both mediating mutagenic, cytotoxic and carcinogenic processes, with CPDs being the most abundant ones. Nevertheless, the cells have evolved certain protective and repair mechanisms to counteract those harmful effects of UV-R.¹⁶ The nucleotide excision repair system (NER) constitutes an enzymatic system capable of detection and removal of DNA damage. After detection of DNA damage in eucariotic organisms NER implements a dual incision peripheral to the damaged base, releasing it as a 24-32 nucleotide-long oligomers, while a polymerase replaces the formed oligomer gap and a ligase finally seals the repair patch. NER represents the sole repair system for CPD and 6-4PP in humans and mice.^{12,17}

Multiple evidence suggests a direct regulatory relationship between the body's UV-response mechanism and the circadian clock. The xeroderma pigmentosum group A (XPA), a vital part of the NER-mediated repair system whose mutation in humans results in xeroderma pigmentosum, a syndrome linked with a 5000-fold increase in skin cancer incidence in sun exposed body areas, has been recently found to be controlled by the circadian clock resulting in a time-dependency of the UV-mediated damaging effects and the respective repair mechanisms. Therefore, the NER system is indirectly regulated by the circadian clock.¹² Moreover, time of the day of UV-R exposure has been linked to sunburn apoptosis, inflammatory cytokine induction and erythema through time-dependent regulation of the p53 tumor suppressor gene.¹⁸ In essence, multiple sources of evidence indicate that evening radiation, when DNA replication is at its peak and DNA repair “rests”, finds the human skin at its most vulnerable state against the UV- radiation's damaging effects. This phenomenon has been directly linked to several core CCGs like BMAL1, CLOCK¹⁹⁻²¹ Cry2,^{22,23} Per2²⁰ etc. The link between shift-work and some forms of skin cancer (namely BCC and melanoma) indicate that researching further the mechanisms involving interactions between time and UV-R damage might be of increased clinical importance.²⁴

Interestingly, the relationship between UV-R damage and the circadian clock is bilateral; not only do CCGs modulate UV-radiation response mechanisms, but the UV-B -even in low doses- influences the expression of CCGs.²⁵, while recently a similar effect of UVA radiation was also shown in resetting circadian activity in *Drosophila*.^{26,27} Apart from complicating the understanding of the intertwined mechanisms between those two factors (circadian clock and UV-R damage), exploitation of these phenomena can be of clinical importance providing potentially new therapeutic options. Evidently, a group has already proposed a chemically-assisted photo-inducible modification of the circadian clock paving the way for a new field in medicine termed “chronopharmacology.”²⁸

1.1.3 Skin as an endocrine organ: the role of D₃

In spite of its photocarcinogenic influence UVB is essential for the cutaneous synthesis of Vitamin D₃ (D₃), a molecule with multiple important biologic functions. UVB-induced formation of pre-Vitamin D₃ from 7-dehydrocholesterol (7-DHC) takes place in epidermal keratinocytes and is thereafter thermally isomerized to D₃. Next, D₃ is hydroxylated to 25(OH)₂D₃ in the liver. Subsequently 25(OH)₂D₃, bound to transporter proteins in blood (mainly DBP – Vitamin D binding protein), is carried to the kidneys, where, after a final hydroxylation by CYP27B1 enzyme, 1,25α(OH)₂D₃ (calcitriol) is generated. This hormonally active form of D₃ mediates its numerous functions mainly by binding to the vitamin D receptors

(VDR) of VDR-positive target tissues.²⁹ It should nevertheless be noted, that keratinocytes unlike other cells (e.g. fibroblasts) are capable of fully synthesizing $1,25(\text{OH})_2\text{D}_3$ from 7-DHC.

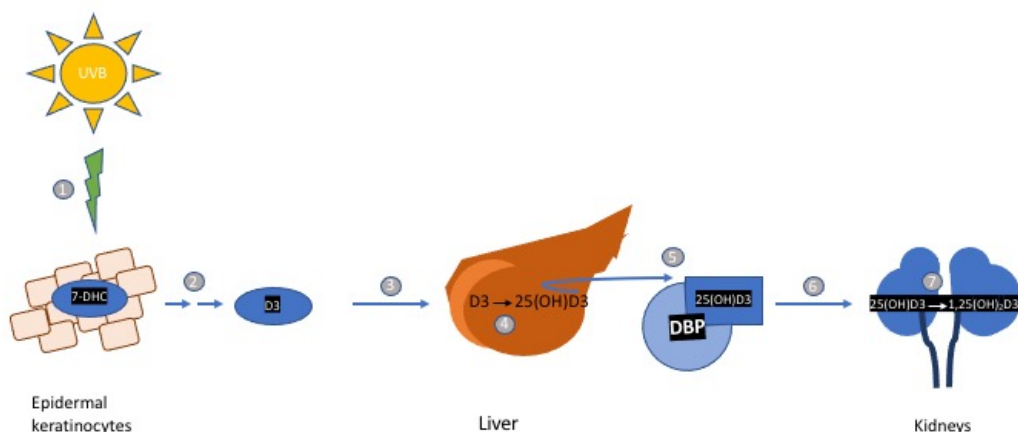


Figure 3, Vitamin D₃ synthesis and activation pathway (simplified): The process begins (1) in the skin cells, where 7-DHC is transformed to pre-Vitamin D₃ and then Vitamin D₃ through a UV-B-dependent non-enzymatic reaction. Vitamin D₃ is then transferred (3) to the liver where through a series of two enzymatic hydroxylations (4) the 25(OH)D₃ is produced. This, bound to DBP binding proteins (5) constitutes the most abundant form of circulating vitamin D₃ in the body. It is then transferred to (6) the kidneys, where it is further hydroxylated to (7) its active form, the 1,25(OH)₂D₃ (calcitriol), which mediates its actions mainly through its receptor - VDR. Calcitriol can either bind to VDR-receptors in the kidneys, or be transferred in other tissues and mediate its actions by binding to VDR-positive target tissues.

Interestingly calcitriol is characterised by several photoprotective properties. Despite not being an antioxidant, it has been shown to antagonize UV-induced oxidative stress. This effect is mediated by the reduction of UV-induced DNA-damage in skin cells, the increase of p53 levels in skin (a gene associated with skin DNA repair and reduction of reactive oxygen species-ROS), inhibition of stress activated kinases and the induction of metallothioneins.³⁰ Moreover, Vitamin D₃ decreases nitrosylation of repair mechanism enzymes by NO⁻ produced through UV irradiation. Other functions of Vitamin D₃ in favour of NER and the repair of DNA damage overall are nevertheless also suspected.³¹ Furthermore, calcitriol has exhibited anti-proliferative effect on BCC and SCC lines in human and mouse in vitro experiments, while its main target receptor (VDR) has been lately highlighted as a potential tumour suppressor in the skin, owing in part to the interaction between vitamin D₃ and p53 signaling pathways.^{29,32} In this regard the relationship between UVB, vitamin D₃ and skin cancer is of high interest.

Evidence of an effect of Vitamin D₃ in the regulation of the circadian clock has come recently also to light. In the experiments of Gutierrez-Morreal et al³³ in Adipose Derived Stem Cells

(ADSCs) it was indicated, that culturing cells with 1,25(OH)₂D₃ resulted in a significant synchronisation on the expression of central clock genes BMAL1 and Per2. This was evident both in continuous and spiked treatment with calcitriol. Moreover, Mengatto et al³⁴ found out, that in patients receiving dental implants differential expression between normal and vitamin D₃ deficient patients was most prominent for genes of the circadian clock pathway. Additionally, evidence suggests a regulatory role of the intestinal circadian system in skeletal bone homeostasis, with circadian CLOCK protein found to be interacting with VDR in a BMAL1-dependent way, thus enhancing its transcriptional activity in a rhythmic way.³⁵ suggests further a potential role of vitamin D in the regulation of the circadian clock. Nevertheless, targeted research of the effects of vitamin D₃ in skin cells and especially keratinocytes, a major anatomic site for D₃ physiology, both alone and in its interaction with UVB is significantly lacking from the literature.

1.1.4 UVB, p53 and vitamin D₃

The p53 gene regarded as “guardian of the genome” is critically involved in processes that govern DNA damage and acts as a major tumor suppressor gene in many cancers, including non-melanoma skin cancer. When DNA damage is recognized p53 - dependent on whether reparation of it is possible - can either arrest the cell cycle to encourage reparation, or alternatively induce apoptosis, thereby obstructing the accumulation of damage in cells and their mutagenesis.³⁶ Recently, evidence suggests the VDR also acting as a tumor suppressor, with the crosstalk between VDR -and therefore of 1,25(OH)₂D₃, its main ligand- and the p53 family of proteins (p53/p63/p73 proteins) has gained extra importance. Some of the effects exerted by the VDR/p53 interaction include increased skin pigmentation, reduction of CPDs and NO[•] products, regulation of murine double minute (MDM2) gene – a gene that negatively affects p53 expression- from vitamin D₃, while a direct influence of p53 proteins from VDR has also been recently suggested.^{29,37,38} With multiple evidence suggesting bilateral regulation of p53 and the CCGs^{20,39–43} it becomes evident that placing this network of interactive relationships under scrutiny could reveal both unexplored physiologic pathways and potential new ways of exploiting those interactions in a therapeutic setting.

1.1.5 The role of AhR in circadian clock physiology, UVB stress response and vitamin D₃ related pathways

The Aryl hydrocarbon Receptor (AhR) is a ligand activated transcriptional factor involved in the sensing and adaptive responses against environmental insults. The skin being the organ with the most direct and constant contact with external stimuli, underscores the importance of this

receptor for its physiology and disease. Indeed, the AhR has been recently shown to be involved in the regulation of skin pigmentation, photocarcinogenesis and skin inflammation.⁴⁴ AhR can be activated by either exogenous ligands (e.g. environmental chemicals, like arsenic), or by endogenous produced, like the UV-induced tryptophan derivatives FICZ mediating harmful processes on the living organisms.⁴⁵ Especially regarding skin cancers, AhR has been evidenced as a susceptibility gene for SCC and a prognostic factor for melanoma and Merkel cell carcinoma, being majorly involved in the regulation of UV-induced DNA-damage response mechanisms⁴⁶, being evidently shown to repress NER repair system and contribute to photocarcinogenesis.⁴⁷ Moreover, the AhR is majorly involved in the regulation of drug metabolizing enzymes, like those of the cryptochrome P450 family (CYP1A1, CYP1A2, CYP1B1).⁴⁸

Ligation of AhR drives its translocation from the cytosol to the nucleus and forms a heterodimer complex with ARNT (Aryl hydrocarbon Receptor Nuclear Translocator). Formation of the AhR/ARNT complex induces expression of drug-metabolizing and detoxifying enzymes. At the same time activation of Aryl hydrocarbon repressor gene (AHRR) provides negative feedback, which additionally to the ubiquitination of AhR after the protein is exported again to the nucleus, balances out this system of insult response. Not surprisingly, AhR has been shown to modulate several endocrine, metabolic and immunological functions both systemic and cutaneous.⁴⁹

AhR notably showed circadian rhythmicity in its expression, time-dependent sensitivity to activation by ligands and its heterodimer partner ARNT structurally resemblances BMAL1 (for this reason also called ARNTL; ARNT-like protein), one of the core CCGs, had raised suspicions regarding its relationship with the circadian clock since many years.^{45,49} Indeed, AhR activation desynchronizes CCG expression and suppresses their rhythms. At the same time, disrupted circadian clocks have been shown to alter AhR-signaling and desensitize activation of AhR and its target genes from AhR-agonists.⁵⁰ The ligand-dependency and the AhR's modulatory role in metabolism are therefore both factors that should be taken into account while researching circadian clock modifying therapeutics.

The relationship between vitamin D₃ analogs and AhR constitutes a research field with high potential for both shedding light on complex physiologic phenomena and translationally provide with new therapeutic options. Calcitriol indicated suppressive effect on AhR in human T-cells,⁵¹ while CYP1A1, a prime AhR target gene, was found to be induced by calcitriol, the main VDR agonist, in the presence of AhR agonist benzo[α]pyrene (BaP) in U937 macrophages, suggesting an interesting crosstalk between VDR and AhR pathways.⁵² Another

important finding was the discovery of novel non-calcemic vitamin D₃ analog 20,23(OH)₂D₃, for which the AhR represents its top target receptor with proven activation of the AhR-pathway through induction of downstream AhR-target genes CYP1A1 and CYP1B1 by the substance.⁵³ While these substances were artificially constructed, their discovery highlights the importance of further researching the complex relationship between vitamin D₃ analogs. They represent an example of potential in function (relating to their being an effective ligand for AhR), while negating the common vitamin D₃'s main disadvantage as a therapeutic (meaning the calcium related side effects, that are missing from these novel substances.) Interestingly these novel secosteroid have been identified as inverse agonists or antagonists of both ROR_α and ROR_γ receptors^{54,55} two orphan nuclear receptors long known to play important roles in the expression of core clock gene BMAL1,⁵⁶ thereby further involving the circadian clock into this complex interaction network.

1.2 Goals of research

The role of CCGs in UVB-induced photocarcinogenicity and the interplay with Vitamin D are the prime focus of this study. We selected epidermal keratinocytes as our research subject due to both their heavy involvement in D₃ synthesis and the long established relevance of UV-B radiation in keratinocyte carcinogenicity. Through this study model we aim to answer the following main questions:

1. Is there evidence of circadian activity in human keratinocytes?
2. Are there differences in circadian activity in keratinocytes during different stages of skin photocarcinogenicity?
3. Does UVB and/or 1,25(OH)₂D₃ synchronize or modulate CCG activity in human epidermal keratinocytes?
4. Does UVB and/or 1,25(OH)₂D₃ have different effects in keratinocytes during different stages of skin photocarcinogenicity?
5. How are VDR- and AhR-pathways involved in the above processes?

To our knowledge we are the first to be researching the interplay of CCGs, UVB/D₃ and cancer status in keratinocytes. Our research focus, compared to the established body of research in the literature is illustrated in *Figure 4*.

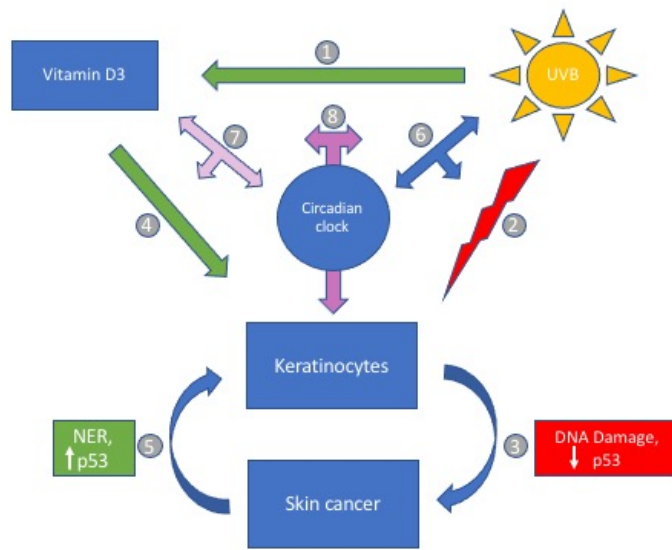


Figure 4, Outline of the main interactions' network between the main researched variables. (1) vitamin D₃ is dependent on UVB-radiation to be synthesized and activated. (2) UVB mediates damaging effects on epidermal keratinocytes, being majorly involved in the stimulation of photocarcinogenesis. Accumulation of DNA-damage and a disrupted expression of p53 (3) are skin cancer-inducing effects, whereas vitamin D₃ has been shown to (4) mediate anti-skin cancer effects which together with (5) a normal p53 expression and NER activity halt work halting and even reversing cancer formation. Between UVB-effects and the CCGs exist a recently much researched bilateral relationship, with both CCGs modulating UVB-effects and the UVB influencing CCG expression. The part of UVB influencing CCG expression is however also underexplored and investigating it is also a goal of this project. Our research is more heavily focused on the pink (7) and purple (8) arrows of this diagram, representing respectively the bilateral relationships of vitamin D₃ and the Circadian Clock and of the combined effects UVB and Vitamin D₃.

2. Methods and Materials

2.1 Basic Laboratory Principles

During all experiments, nitrile medical examination gloves (ABENA©) were used to minimize contamination with pathogens and/or RNase/DNases. Especially during cell culture processes, gloves would be immediately either changed or lightly sprayed with 70% Isopropylalcohol (Hedinger; Ch. B.: 05364) after touching objects outside the sterile bench (HA 2448 GS; Heraeus LaminAir®). Between processes samples would be temporarily stored on ice, produced by a Flake Line ice machine (Wessemat GmbH). For pipetting we used VWR Signature™ ergonomic high-performance pipettes and Biosphere® Filter Tips (Sarstedt). To ensure good mixture all samples and solutions used would be thoroughly vortexed with a REAX 2000 (Heidolph) vortexer before use. The RNA/DNA/RNase/DNase free 1.5ml collection tubes (Sarstedt) used in most of our protocols would come in bulk in plastic bags and would then be transferred in simple glass jars covered with aluminum foil and autoclaved in a VX-75 (Systec) autoclaving machine and then be placed in a Heraeus Laboratory oven at 100°C for 4 hours to ensure complete sterilization. A similar process would be followed for the autoclavation of our PBS-Bottles used in sterile conditions during our cell culture processes. The 500 ml bottles (Duran®; DWK Life Sciences) would be filled with Phosphate Buffered Saline- PBS-buffer at pH 7,2-7,4 (Pharmacy of the University Clinic of Saarland) and placed inside the autoclavation machine without fully closing the lid during the autoclavation process. Used bottles would be washed in a bottle wash machine (Beko; DFN 6632.5) and then let to air dry. Long 230mm glass Pasteur pipettes (VWR; Cat. No.: 612-1702) used in our cell culture processes would be heat-sterilized at 200°C for 4 hours.

2.2 Cell culture

Eucariotic cell lines used and their purpose

2.2.1 HaCaT Keratinocytes

Human adult low calcium temperature (HaCaT) Keratinocytes used in these experiments were bought from the CLS Cell Lines Service® (Cat. No.: 300493). HaCaT keratinocytes are a spontaneous in vitro transformed cell line used in basic science experiments as an excellent model to study skin physiology, due to many of their practical advantages like low cost, and high growth potential (immortalized cell line; maintain normal degree of morphologic differentiation even in high passage numbers). They are regarded as a great subject to study the

process of malignant transformation of human epithelial cells⁵⁷ and they have been recently proven to have a functional cell autonomous circadian clock⁵⁸ we found them as an excellent candidate for our project. Additionally they present a mutated p53 status⁵⁹, therefore in regards to p53 status we would be using them as a model for the precancerous actinic keratosis.

2.2.2 SCL-1 cells

In our experiments we used SCL-1 cells from the Center of Cancer Research (Deutsches Krebsforschungszentrum – DKFZ) in Heidelberg. SCL-1 cells represent a poorly differentiated form of cutaneous squamous cell carcinoma, also maintaining their morphological stability over a high number of passages. Cutaneous SCC cell lines are often presenting a null p53 phenotype due to multiple mutations on the tumor suppressor gene.⁶⁰ Interestingly a recent study indicated a potential prognostic value in p53 overexpression in cSCC.⁶¹ For our study we would be using this subject as an experimental model for SCC.

2.2.3 NHEK Cells

In our experiments we used pooled juvenile NHEK cells bought from Promocell (Cat. No.: 12007) We used 2 sets of pooled cells (Lot. No.: 459Z009 and 466Z002) each coming from 3 different donors, which were then further pooled together. Overall our cultures were thereby coming from a total of 6 different donors. Using more donors, we aimed to decrease possible variations in cell phenotype and behavior due to the different genetic background of donors. Primary keratinocytes were obviously used as a model for normal keratinocytes.

NHEK cells were transported as proliferated cells in 50ml culture flasks. Immediately upon receipt, flasks were placed inside the incubator (APT.line™ C150 E2; Binder) for 3 hours at 37°C and humidified with 5% CO₂, in order to recover from the transportation shock. Then the culture flasks were carefully opened under a sterile bench and the inner side of the lid rinsed with 70% EtOH diluted in deionized water and let to air dry. After that, transport medium was aspirated through a glass Pasteur pipette (Hirschmann®) and a fresh 10ml medium was added with a serologic pipette (Corning® Costar® Stripette®; Merck) controlled by an RF3000™ Li-Ion Battery Pipet Controller (Heathrow Scientific®.) Cell density and quality were then checked under microscope (DM IL LED; Leica®.) Afterwards a trypsination and transfer to petri dishes (1 vessel distributed to 2 petri dishes) followed, as detailed described in 2.5.

2.3 Defrosting Cells

HaCaT and SCL-1 cells used were stored inside a liquid nitrogen tank (Apollo®; Cryotherm) in cryovessels (Cryopreserved cells). The vessels were first let to thaw at room temperature for

15 minutes and then their cellular content was collected through resuspension using 5ml of the respective medium (described below) with a serological pipette and a pipette controller, under a sterile bench. This was further distributed to labeled 100 x 20 mm petri dishes (Cellstar®, Greiner Bio-One) already containing medium to a final medium volume of 5ml. From each vessel a respective petri dish was produced, which was then placed inside the incubator at 37°C with 5% CO₂.

2.4 Culturing Cells

Cell culture of HaCaT Keratinocytes, SCL-1 and NHEK cells was always conducted under a sterile bench. All cells were cultivated in 100 x 20mm labeled petri dishes. For HaCaT Keratinocytes and SCL-1 cells we used Gibco® Dulbecco's Modified Eagle Medium - DMEM- (ThermoFisher Scientific, Cat. No.: 41966-029) and Gibco® Roswell Park Memorial Institute - RPMI 1640 (ThermoFisher Scientific; Cat. No.: 21875-034) medium respectively, both supplemented with 10% Gibco® Fetal Bovine Serum - FBS (ThermoFisher Scientific®, Cat. No.: 11573337) and 1% L-Glutamine (ThermoFisher Scientific, Cat. No.: 11514426). For NHEK cells we used Keratinocyte Growth Medium 2 (Cat. No.: 20011) supplemented with 10% (50ml) SupplementMix (Cat. No.: C-39015) and 0,01% (60µL) CaCl₂ Solution (Cat. No.: C-34005). Change of medium for all cells was performed every 3-4 days. This was done by simply vacuuming the old medium with a sterile glass Pasteur pipette and replacing it with 5ml of the respective fresh medium.

2.5 Subculturing / Passaging of Cells

All cells were regularly inspected under microscope for cell density and splitted/subcultivated after reaching a confluence of >70%. Subcultivation protocol for HaCaT Keratinocytes and SCL-1 cells began with aspiration of the existing medium with a sterile glass Pasteur pipette under sterile bench. Cells were then washed twice with ~5ml Phosphate Buffered Saline- PBS- buffer at pH 7,2-7,4 (Pharmacy of the University Clinic of Saarland) which was then also aspirated before applying 750µL of 0,25%-Trypsin EDTA (ThermoFisher Scientific®, Cat. No.: 2520056) and ensuring complete coverage across the petri dish's surface. The double wash with PBS before trypsinization was performed to more thoroughly rid the cells of the trypsin-neutralising FBS included in the respective mediums of both HaCaT and SCL-1 cells. Cells were then placed back into the incubator for about 5 minutes. After ensuring detachment of the majority of the cells from the ground of the petri dish, by lightly tapping them on the side and inspecting their movement under microscope, petri dishes were transferred again under the sterile bench. Using a pipette controller and a 10ml serological pipette, we pipetted 5ml of the

respective medium thus neutralising trypsin and collecting cells in a 50ml tube (Cellstar®; Greiner Bio-One) For every 4-5 petri dishes we would use a fresh 5ml of medium. The same process was repeated once more, to ensure that the maximum amount of detached cells would be eventually collected. After successful collection of the cells in the tubes those would be sealed and centrifuged at 1200 rpm/min (Megafuge® 1.0R; Heraeus) for 3 minutes, while old petri dishes were discarded. Centrifuged tubes were transferred back to the sterile bench, where overlying medium would be aspirated using a Pasteur glass pipette, while carefully maintaining the integrity of the underlying cell pellet. Then a fresh amount of medium (relative to the amount of cells collected inside the tube/number of petri dishes to which the content would be aliquoted; concept explained with more details below) would be immediately added and resuspended with the serologic pipette until homogeneity. In cases, where collected cells were distributed across 2 or more tubes, these would be mixed into one, then the remaining tube would be washed once with the respective medium in order to collect cell residues before the old tube being eventually discarded. From this point forward, the next step was decided according to whether the subcultivated cells would be used for an experiment the following day, or if they were just being passaged for an experiment later down the line. For simple passaging, we would produce 3-4 new petri dishes from each of the former dishes. For each of the labeled new petri dishes a total volume of 5ml cell-containing medium would be pipetted. To achieve that, we would add fresh medium inside the 50ml tube containing the collected cells until reaching an amount of (petri dishes to be produced) x 5ml + 5ml buffer and then the solution would be mixed by resuspending with the serological pipette. Any leftover cells would be equally distributed among the new petri dishes. In this step small differences in the amount of cells per new petri dishes were of lesser importance, since these would be further redistributed down the line, before they would be used in any experiment. But with cells that would be tested in an experiment the following day, precision in the amount of cells distributed was of much higher importance. In this case after collecting cells in a 50ml tube and lightly vortexing them, a 100µL sample would be collected inside a 1.5ml collection tube (Sarstedt®.) That would be further vortexed before measuring its cellular concentration with a Scepter™ 2.0 Handheld Automated Cell Counter (Merck) using 60 µm Scepter™ Sensors (Merck) strips. Then the amount containing 500.000 cells would be calculated accordingly. New petri dishes would be properly labeled and filled with 5ml of the respective fresh medium. Then the previously calculated amount of the cell-containing-medium per petri dish would be pipetted, after another round of vortexing to ensure homogeneity. Petri dishes would be then placed in the incubator to rest and stabilize/attach to the bottom of the petri dishes for around 24 hours. After each trypsinization the passage number was updated.

Our subcultivation protocol for NHEK was conducted with the help of the DetachKit (Promocell; Cat. No.: C-41220). We would first transfer the petri dishes (or culture vessels after receipt) under the sterile bench and aspirate the medium content with a glass Pasteur pipette. Then we would add 2ml of Hepes Solution and move the petri dish (or vessel) back and forth to ensure coverage of the whole cell containing surface. Then after about 15'' we would aspirate it back and add 2ml of Trypsin Solution. This time incubation with trypsin was performed at room temperature and with constant inspection of the cells under the microscope to ensure effective detachment, whilst avoiding a prolonged stress inducing action of trypsin to the overly sensible NHEK cells. After about 3-4' and having ensured that the majority of the cells were detached from the bottom of the petri dish, we would neutralize trypsin by adding 2ml of Trypsin Neutralizing Solution - TNS. Since our culture was performed completely serum free, neutralization of trypsin with the medium was in this case not an option. Afterwards, 3ml medium were used to collect the detached cells from the petri dishes to a 50ml tube similarly to how it was also conducted in HaCaT and SCL-1 cells. This process was performed at least twice. Since NHEK cells were both slower growing and much more expensive than our other 2 cell lines, we were much more thorough in trying to effectively collect as many cells as possible during passaging. In the occasion that a noticeable amount of cells remained attached to the old petri dish we would either attempt a second round of trypsinization or in some occasions add fresh 5ml medium in the old petri dish and continue to cultivate them, thus producing two different passage numbers (old / new). After collecting cells in 50ml tubes, these would be sealed and centrifuged at 800 rpm/min for 3 minutes, a slower pace due to primary cells being much more sensible to stress than those coming from cell lines. We would then transfer the tubes back under the sterile bench and carefully aspirate the overflow, leaving only the underlying cell pellet. Then fresh medium would be added and all contents would be transferred and mixed into one 50ml tube. Distribution in the new petri dishes as part of either a simple subcultivation protocol, or preparation for an upcoming experiment in the following day would follow the same lines as described for HaCaT and SCL-1 cells. As Promocell company guarantees that NHEKs would not differentiate for up to 5-6 trypsinization cycles we avoided to use in our experiments cells that exceeded this limit. For HaCaT and SCL-1 cells no such restrictions were taken into account (as already discussed above.)

Cells would be regularly inspected for bacterial contamination under the microscope and all suspected specimens would be immediately discarded. Moreover, cell quality was also regularly checked, especially for the more susceptible NHEK cells. In some cases, NHEK cells would take a strange spherical shape, similar to that after trypsinization, and partly failing to be attached to the bottom of the petri dishes, indicating that cells were situated under some undefined form of stress. In some of those cases, cells would come back to their previews

normal state after some weeks, while only undergoing medium change in the meantime. At the end, all cells used in our experiments came from those subpopulations which at no time during their culture did experience any such sort of incongruence. But, because of facing multiple failed attempts at growing enough cells, as well as experiencing some major contaminations we were, at the end, unable to provide the necessary 3 biologic replicates for one of our experiments, for which reason, as discussed in “statistical analysis” despite performing statistical analysis on those samples, interpretation of the final results should be conducted with caution.

2.6 Methodology of cell treatment

2.6.1 General Principles

In all experiments we used medium supplemented with 1% Bovine Serum Albumine (Sigma Aldrich; Cat. No.: 9048468) The exact amount of BSA was measured with a precision scale (VWR®; Sartorius) and then applied to the respective medium (DMEM for HaCaT, RPMI for SCL-1 and KGM2 for NHEK) in non-sterile conditions. Medium was then transferred under a sterile bench. A 45mm Steriltop® filter (Millipore Express) was placed upon a sterile autoclaved 500ml glass bottle (Duran®; DWK Life Sciences) and the suction pump (VWR) from the sterile bank, was attached on the filter to create negative pressure and therefore vacuum the medium through the filtration membrane into the bottle. This way the 1% BSA supplemented medium was now sterile and ready to be used for experiments. As all used treatment substances (described below) were dissolved in alcohol, we used in all cases a vehicle control, containing absolute EtOH (Emsure®; Sigma Aldrich; Cat. No.: 64175) in the same concentration as that of our tested substances. For conditions involving irradiation, the medium was first aspirated under the sterile bench and then the petri dishes were placed (3 at a time) inside a UVB-irradiator (UVP-Crosslinker CL-1000M; Analytik Jena) and be instantly irradiated at 50 J/m^2 with an open lid. The lid would then be immediately closed again and the petri dishes would be transferred back under the sterile bench for further treatment. For conditions involving $1,25(\text{OH})_2\text{D}_3$ (calcitriol) we used, as already described an EtOH dissolved form of the substance (Sigma Aldrich®; Cat. No.: 3222063) coming at 10^{-2} M dilution in EtOH, which we further diluted 1:100 with 100% EtOH to a final concentration of 10^{-4} M . This was then added to the respective medium with 1% BSA in an analogy of 1:1000, resulting to a solution with a final concentration of 10^{-7} M . To simplify explanation of our experimental protocols we would be using the abbreviations depicted in *Table 2* to describe the respective conditions.

Abbreviation		Detailed explanation of the condition
1	BSA	5 ml of medium respective to the cell type used, supplemented with 1% BSA
2	EtOH	Like (1), with added 100% EtOH in 1:1000 dilution
3	BSA + 50 J/m² UV-B	Irradiated as described above and then (1) added
4	EtOH + 50 J /m² UV-B	Irradiated as described above and then (2) added
5	D₃	Like (1), with added 1,25(OH) ₂ D ₃ in 10 ⁻⁷ M final concentration
6	D₃ + 50 J/m² UV-B	Irradiated as described above and then (5) added

Table 2, Abbreviations used to simplify description of conditions applied. BSA and EtOH and represent control conditions (with or without addition of EtOH in 10⁻⁷ M concentration, respectively) and BSA+50 J/m² UVB and EtOH+50 J/m² UVB represent the irradiated samples (with or without EtOH in 1:1000 dillution) The BSA and BSA+50 J/m² conditions were only used to show that EtOH in the applied concentration was not significantly influencing results, as discussed below. Therefore, for the rest of our experiments and comparisons we only used EtOH and EtOH+50 J/m² UVB, referred to as “control” or “vehicle control.” For simplicity we used: EtOH= Control, EtOH+50 J/m² UVB, D₃+50 J/m²= UVB+D₃.

2.6.2 Experiment 1A

For this part of the experiment we used HaCaT keratinocytes. Time of treatment was established as our reference time point 0h. We used all 6 conditions depicted in Table 2, working in sterile conditions under a sterile bench, following a specific order of treating cells, which was also followed during the harvesting stage as to minimize time irregularities resulting from delays related to the actual technical execution of the experiments. A different petri dish, each containing 500.000 cells, as described above, was prepared the day before and treated for each condition and each time point (t=0h.) After treatment, cells were being harvested in 6-hour intervals starting from time 0h (immediately after treatment) and over a span of 60h for a total 11 time points/samples per condition. Treatment of cells for the 0h time point was conducted independently, exactly after the treatment of other conditions, to ensure that harvesting would be achieved as close to the treatment as possible. All other specimens were treated at the same time. Despite our system of maintaining a specific order of treating and harvesting cells, the fact that we would at a time treat 42 different cells, in what would last for almost 1-hour start-to-finish, can indicate that small time irregularities between conditions would be practically unavoidable and suggest a possible limitation of our study. Harvesting protocol is described with detail in 2.7. The experiment was replicated 3 times with independent experiments, each containing cells of different passage.

As part of our preparatory experiments, we repeated the same protocol design using SCL-1 cells (RPMI 164 instead of DMEM Medium). We only replicated this experiment once, having as a main goal to design a second part of the experiment in which we would research differences

between different cells, while avoiding repeating the same, arguably very time and fund consuming protocol. And we thus introduced SCL-1 experiments through one-time sampling in Experiment 1B. Nevertheless, the overall results of this one replicate are also included for reference in 3.7.

2.6.3 Experiment 1B

In this experiment we aimed to test differences between different types of cells and the effect of the researched conditions to absolute expression of genes without the element of time related variability. In this experiment we tested HaCaT, SCL-1 and NHEK, testing the conditions: Control (vehicle control), UVB (vehicle control irradiated with 50 J/m²), D₃ and UVB + D₃ as described in the legend of *Table 2*. Harvesting was performed once 12h after treatment. Because we already had the respective samples from experiment 1A for all 3 replicates of HaCaT and one replicate for SCL-1, we used these same samples for our further measurements. The rest of the replicates were produced through a series of independent experiments, so in the end we had 3 biologic replicates for each of the 4 conditions, for each of the 3 cell types.

2.6.4 Experiment 2

For our 2nd experiment we wanted to test whether time of the day influenced the actual DNA-damage development and reparation in cell cultures. Unfortunately, due to practical problems regarding culturing and collecting of samples we had to forgo this experiment after its first repetition and exclude its results from the rest of our work. We nevertheless document the methodology used for reference. For this experiment we only used HaCaT Keratinocytes. For all treated cells, even those undergoing some form of pretreatment, time of irradiation was established as the time point 0h. We divided the cells into 2 groups of treatment: those irradiated at 18:00 and those 6 hours later at 00:00 at the same day. In both groups there existed one condition in which irradiated cells had to be pretreated with 1,25(OH)₂D₃. Both of those cell populations were pretreated with 1% BSA DMEM Medium containing 10⁻⁷M 1,25(OH)₂D₃ at 12:00, in essence pretreatment 6 and 12 hours before irradiation respectively at 18:00 and 00:00 of the same day. For those cells, that were pretreated with 1,25(OH)₂D₃, medium was aspirated before irradiation and then fresh medium which did not contain 1,25(OH)₂D₃ was added and left for the whole duration up until sampling. Moreover, one condition per time group involved irradiation with addition of 1,25(OH)₂D₃-containing medium immediately after; in this case the 1,25(OH)₂D₃-containing medium remained until time of harvesting. The remaining condition was an irradiated control, in which BSA 1%, with 1:1000 EtOH medium was added after irradiation. In all cases, samples were harvested at time points 0h, 1h, 2h, 4h, 6h and 12h after irradiation as described in 2.7. In *Table 3* abbreviations for the aforementioned conditions are summarized, *Figure 5* further illustrates a schema of the treatment and harvesting plan.

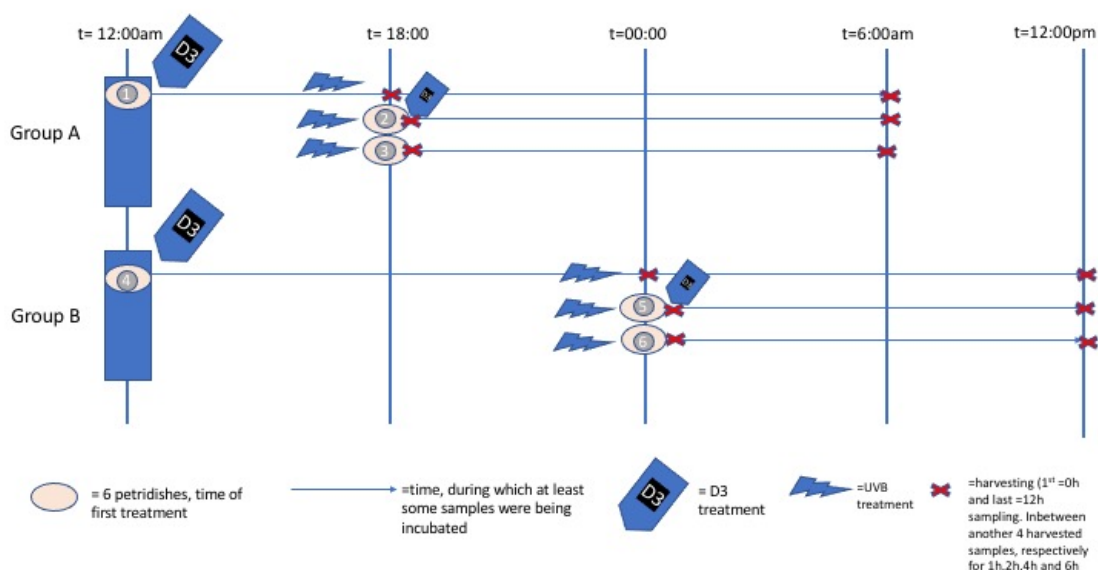


Figure 5, Outline of Experiment 2 protocol design. The numbers represent the conditions detailed described in Table 3 below.

Abbreviation	Condition in details
1 D ₃ ->UVB (18:00)	Pretreatment with BSA 1% in DMEM with 10 ⁻⁷ M 1,25(OH) ₂ D ₃ at 12:00, then aspiration of medium and irradiation at 18:00, then addition of BSA 1% DMEM medium without 1,25(OH) ₂ D ₃
2 D ₃ +UVB (18:00)	Irradiation at 18:00 as described above and then addition of BSA 1% in DMEM with 10 ⁻⁷ M 1,25(OH) ₂ D ₃
3 UVB (18:00)	Irradiation at 18:00 as described above and then addition of BSA 1% in DMEM Medium with 1:1000 EtOH
4 D ₃ ->UVB (00:00)	Pretreatment with BSA 1% in DMEM with 10 ⁻⁷ M 1,25(OH) ₂ D ₃ at 12:00, then aspiration of medium and irradiation at 00:00, then addition of BSA 1% DMEM medium without 1,25(OH) ₂ D ₃
5 D ₃ +UVB (00:00)	Irradiation at 00:00 as described above and then addition of BSA 1% in DMEM with 10 ⁻⁷ M 1,25(OH) ₂ D ₃
6 UVB (00:00)	Irradiation at 00:00 as described above and then addition of BSA 1% in DMEM Medium with 1:1000 EtOH

Table 3, Conditions for Experiment 2. Our initial goal was to test the effect of time outside of the influence of CCG circuit's influence. We only replicated this experiment once and excluded its results due to practical constraints.

2.6.5 Experiment 3

For this experiment we used combinations of the already described conditions with two further substances, the 2-methyl-2H-pyrazole-3-carboxylic acid (2-methyl-4-o-tolylazo-phenyl)-amide (CH-223191) AhR antagonist (Sigma Aldrich®; Cat. No.: 301326227) and the VDR-

inhibitor Calcifediol (Sigma Aldrich®; Cat. No.: 19356-17-3). Both substances were diluted with EtOH to a final concentration of 10^{-4} M and then dissolved in the respective BSA containing medium 1:1000 to a final concentration of 10^{-7} M, matching the one of $1,25(\text{OH})_2\text{D}_3$. CH-223191 has been described as a potent AhR antagonist,⁶² as well as calcifediol as a potent VDR inhibitor^{1*,63,64}. The exact concentrations used were from the experience of other research projects in the field in our laboratory. These specific concentrations also provided the benefit of matching the concentration of $1,25(\text{OH})_2\text{D}_3$ used, therefore making it easier to account for a control with the same vehicle concentration parameters.

The tested conditions are summarized in *Table 4*. Abbreviations summarized in *Table 2* are also used for simplicity.

Abbreviations		Conditions in detail
1	AhR-i	AhR antagonist (CH-223191) in a final concentration of 10^{-7} M in the respective medium
2	VDR-i	VDR inhibitor (Calcifediol) in a final concentration of 10^{-7} M in the respective medium
3	A+V	(1) and (2) added into the same medium

Table 4, New conditions used in Experiment 3. The ones summarized in Table 2 were also combined.

All treatments took place at the same time, in a specific order, which was also followed during the time of harvesting as to minimize time irregularities between conditions resulting from delays during experiment's execution. Time of treatment was established as reference time point 0h. Treatment conditions were divided into 4 basic groups of intervention, exactly emulating those in experiment 1 and involved a non-irradiated vehicle control, an irradiated (50 J/m^2) vehicle control, a non-irradiated group treated with 10^{-7} M $1,25(\text{OH})_2\text{D}_3$ medium and an irradiated group treated with 10^{-7} M $1,25(\text{OH})_2\text{D}_3$ medium immediately after irradiation. For each of those a total 4 subgroups of interventions were added accounting for a further vehicle control (addition of EtOH at a 1:1000 dilution), CH-223191 at 10^{-4} M dissolved in the medium at 1:1000 to a final concentration of 10^{-7} M, Calcifediol at 10^{-4} M dissolved in the medium at 1:1000 to a final concentration of 10^{-7} M and addition of both CH-223191 and Calcifediol both at a final concentration of 10^{-7} M. In essence we would test for this experiment 16 conditions, summarized in *Table 5*.

Conditions tested			
Control	+ VDR-i	+ AhR-i	+ A+V
+UVB	+ VDR-i + UVB	+ AhR-i + UVB	+A+V + UVB

¹ * Calcifediol as a potent VDR inhibitor: <https://www.medchemexpress.com/Calcifediol.html>

D₃	D₃ + VDR-i	D₃ + AhR-i	D₃ +A+V
UVB + D₃	UVB + D₃ + VDR-i	UVB + D₃ + AhR-i	UVB + D₃ +A+V

Table 5, All conditions for Experiment 3 summarized

Following treatment, samples were harvested after 1h, 3h and 24h for HaCaT Keratinocytes and after 1h for NHEK cells, as described in 2.7. For HaCaT, additionally to the cells harvested at 24h we also sampled medium to be tested for LDH-Assays at the Institute of Experimental Neurology. Protocol for harvesting samples for LDH-Assays is described in detail in 2.15. For each of the HaCaT Keratinocyte petri dishes, a total 500.000 cells were passaged the day before. For NHEKs we passaged 2 petri dishes for each of the 16 different conditions, one containing 500.000 and one containing 1.000.000 cells. These were both treated at the same time and pooled together during the harvesting stage, for a total of 1.500.000 cells per sample. We opted for such a high amount of NHEKs per condition, since NHEK are in our experience often unable to produce an acceptable amount of gDNA after DNA-isolation and since for each sample we were aiming to conduct at least 2 measurements with ELISA, we decided to prepare a higher amount to avoid such technical complications. At the same time, we did not want to passage all 1.500.000 cells per condition into one petri dish, as that would involve the risk of losing a higher percentage of the cells due to overcrowding.

2.7 Harvesting of cells and Storage of samples

Harvesting protocol was same for all cell types used, for all experiments and was conducted manually under non-sterile conditions. The medium would be first aspirated with a glass Pasteur pipette, followed by a wash with ~2 ml PBS Puffer. After that was also aspirated, a second 2ml amount of PBS was pipetted with the serological pipette and the cells were scrapped with a disposable cell scraper (Greiner Bio-One®). Scrapped cells were then transferred inside a 15 ml tube (Cellstar®, Griener Bio-One), while multiple washes with PBS would ensure maximum efficiency of the sample harvesting process. Tubes were then centrifuged (Megafuge® 1.0R; Heraeus®), at 1200 rpm/min for 3 minutes for HaCaT and SCL-1 and at 800 rpm/min for 3 minutes for NHEKs. Overlying PBS was then aspirated with a glass Pasteur pipette and the labeled samples were put on ice for up to 20 minutes before being transferred into the freezer (Platinum 550; Angelantoni®), where it would be conserved at -70°C until further use. In the case of the 24h samples that would be also tested in LDH-Assays, the harvesting of the medium as discussed in 2.15 and would precede this protocol. Other than that, harvesting in those cases would follow the exact same principles.

2.8 Isolation of mRNA

Isolation of mRNA was performed with RNeasy Mini Kit (Qiagen; Cat. No.: 74106) and QIAshredder Kit (Qiagen; Cat. No.: 79656.) Samples were let to thaw on ice for 15-20' before isolation began. We first added 600 μ L of a 1:100 β -mercapto-EtOH (Sigma Aldrich; Cat.: 60242) to RPL Buffer solution and mixed well by pipetting. The lysate was then applied inside a QIAshredder Mini Spin Column and centrifuged at 13.000 rpm/min for 2 minutes. The top of the column was then discarded, leaving the underlying collection tube. A 600 μ L of a 70% EtOH to deionized water (Sigma Aldrich; Cat. No.: 7732185) solution was added and mixed well by pipetting, then a final volume of 600 μ L of the mixture was placed inside an RNeasy Mini Spin Column and centrifuged for 15'' at 10.000 rpm/min in a Z216-MK microcentrifuge (Hermle). The same process was repeated for the remaining part of the mixture and then empty collection tubes were discarded. After both of these steps, flow-through in the collection tube was emptied after centrifuge. In the next step a 350 μ L amount of RW 1 Buffer was added and the mixture was further centrifuged for 15'' at 10.000 rpm/min and then flow-through was once again discarded. A total volume of 80 μ L of a DNAase/DNAase Buffer Solution [10 μ L RNase free DNAase + 7 μ L DNAase Buffer 10X (Promega; Cat. No.: M6101) + 63 μ L of RNAase free water) was pipetted and incubated at room temperature for 15 minutes. Then a total 350 μ L RW 1 Buffer was added, followed by centrifuging the mixture at 10.000 rpm/min for 15''. After discarding flow-through in the collection tube, we pipetted 500 μ L of RPE Buffer and centrifuged again at 10.000 rpm/min for 15''. Collection tube was then discarded and replaced with a new one. Another 500 μ L were once again pipetted and centrifuged, this time, for a total of 2 minutes, then flow-through discarded and a round of 1-minute centrifuge at 13.000 rpm/min. The tops of the columns were then placed in 1.5ml collection tubes and the collection vessels were discarded. We then pipetted 32 μ L of RNAase free water inside the column centrally to its membrane and centrifuged at 10.000 rpm for 15'', then pipetted the flow-through again inside the column and repeated a cycle of 10.000 rpm/min centrifuge for another 15''. Concentrations of isolated mRNA samples were measured using a spectrophotometer (GE Nanovue UV-sensitive Spectrophotometer, GE Life Sciences) and then stored at -70°C until further use.

2.9 Reverse Transcription of mRNA to cDNA

For the reverse transcription of mRNA to cDNA we used the OmniScript Kit (Qiagen, Cat. No. 205111). We first diluted our isolated 1 μ g of mRNA per sample with RNAase free water to a total of 12,2 μ L in 1.5ml autoclaved RNAase free collection tubes. Then we prepared a master mix solution containing the following ingredients per sample:

- i. 2 μ L of 10X RT Buffer
- ii. 2 μ L of dNTP's (5mM each)
- iii. 1.8 μ L of Random Primer (Promega; Cat.No.: C1181) (diluted 1:10 with RNAase free water to a final concentration of 50 μ g/ml)
- iv. 1 μ L of RNase Inhibitor (10 units/ μ L)*
- v. 1 μ L of Omniscript

**Preparation of RNase Inhibitor (10 U/ μ L) was performed by adding 10 μ L of RNAsin® (Promega; Cat. No.: N2515), 3 μ L of RT Buffer 10X and 27 μ L of RNAase free water.*

Then a 7.8 μ L of the above master mix solution was pipetted to each diluted sample and mixed well. Then the mixture was placed inside a circulator bath (model: 118A-E; Huber) and let to incubate at 37°C for 90 minutes. Afterwards samples were placed in dry block heater (model: QBD2; Grant Instruments) for 10 minutes at 93°C to be inactivated. Concentration of the cDNA samples were measured with a spectrophotometer and then stored at -20°C until further use.

2.10 Measurement of Gene Expression with RT-qPCR

Measurement of gene expression was in all cases performed with Real-Time /quantitative Polymerase Chain Reaction (RT-qPCR). RT-PCR is a common method of measuring gene expression, that has been established since its invention in 1984.⁶⁵ We would be using relative quantification, meaning our results would not express absolute expression of the respective genes, but rather relative expression to one of the reference genes, as described below. All pipetting and plate preparations took place in a room and with equipment dedicated only to conducting RT-qPCR as to minimize risk of RNase contamination. Moreover, all pipetting was performed using one-use filtered tips that were discarded and replaced after each use.

For our measurements we used the QuantiTect SYBR Green® PCR Kit (Qiagen, Cat. No.: 204145). We further used premade primers (QuantiTech®; Qiagen) for BMAL1/ARNTL (Cat. No.: QT00011844), PER2 (Cat. No.: QT00011207), GADPH (Cat. No.: QT00079247) and ACT- β (Cat. No.: QT00095431). Primer mixture was prepared by adding 1.1ml TE Puffer (see 2.14 for preparation protocol) in the vessels and after thorough mixing by vortex, it was aliquoted into multiple 1.5ml collection tubes and stored at -20°C until use.

We firstly diluted a total amount of 1 μ g of cDNA with RNase free water to a final volume of 3 μ L. We prepared the total amount needed per sample for each plate run, with a 25% additional amount as buffer, in one 1.5ml collection tube. For example, for a sample to be pipetted in 8

plate wells we would prepare 30µL of diluted cDNA containing a total amount of 10µg of the respective cDNA. We would then prepare one primer master mix for each of the target and house-keeping genes. This would include, per well to be pipetted, 10µL of SYBR Green PCR Buffer, 5µL of the respective primer solution and 2 µL of ROX dye. For our experiments we used 96-well MicroAmp™ Fast Optical 96 Reactionplates from Applied Biosystems. We first pipetted 3µL of cDNA solution to each well (or RNase-free water for the negative controls) and then added 17µL per well from the respective Primer Master Mix while resuspending to ensure good mixture of the solution. Before each pipetting, solutions would always be thoroughly vortexed. All samples with the exception of the negative controls were assayed in technical duplicates. A pipetting template example, showcasing both sample and primer placement inside the plate is depicted below:

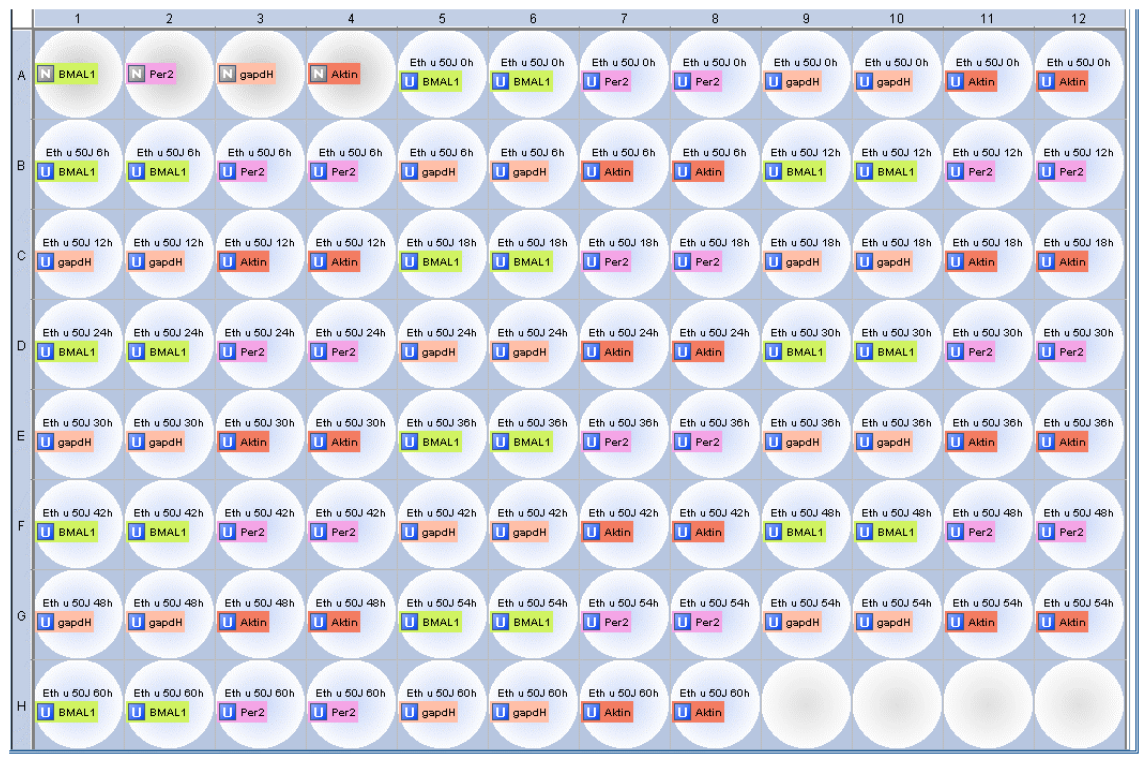


Figure 6, RT-qPCR Template for EtOH+50J condition as an example.

After pipetting was complete, the plate was sealed with a MicroAmp™ Adhesive film (Applied Biosystems) and centrifuged for ~6'' up to 1000 rpm/min to ensure that all contents were resting at the bottom of each well. The plate was then applied inside the StepOnePlus RealTimePCR-Systems PCR machine (Applied Biosystems) and the run was immediately launched. Inbetween runs, pipetted plates would occasionally be stored at 4.5°C for up to 20' before the machine would be available for the next launch. Each run lasted 1:17 hours.

2.11 Isolation of DNA

Isolation of DNA was performed with the NucleoSpin® Tissue Kit (Macherey-Nagel; Cat. No.: 740952.250). Samples were thawed on ice for 15-20'. Then 200µL of T1 Lysis Buffer was pipetted and resuspended to homogeneity. The mixture was then transferred in an autoclaved 1.5ml collection tube. A solution of 25µL Proteinase K and 200µL of Buffer B3 were added and the mixture, vortexed well and then let to incubate on a dry heat blocker at 70°C for about 10-15min. An amount of 210µL of EtOH 100% was added and the mixture was vigorously vortexed for 3-4". For each sample one NucleoSpin® Tissue column was placed into a Collection Tube. The sample was then applied inside the column and centrifuged at 11.000 rpm/min for 1 minute. Afterwards the collection tube was discarded and replaced with a new one. A further 500µL of Buffer BW was added and the mixture was centrifuged again at 11,000 rpm/min for 1 minute, after which the residues in the collection tube was discarded. A 2nd wash of the silica membrane followed, through the addition of 600µL of Buffer B5 into the column and another round of centrifuge at 11,000 rpm/min for 1 minute. After discarding the flow-through from the collection tube, a second centrifuge followed again at 11.000 rpm/min for 1 minute. The collection tube was then discarded and the column was placed inside a 1.5ml collection tube. A 50µL of Buffer BE warmed up at 70°C was added and left to incubate for 2' at room temperature. This last step was then repeated and after another 2' of incubation at room temperature the mixture was centrifuged at 11.000 rpm/min for one minute. Samples of gDNA were then stored at -70°C until time of measurement.

2.12 Dot Blot Assays

We used 0,5µg of gDNA from each sample according to the measured concentrations and diluted it with RN/DNase free water (leftovers from Omniscript cDNA reverse transcription Kit; Qiagen) to a final volume of 10µl. Each drop of 10µl solution was pipetted centrally on a GeneScreenTM Hybridization Transfer Membrane (Biotechnology Systems NEN Research Products; Cat. Nr.: NEF-983), accounting 1,5cm x 1,5cm space for each sample droplet. After all samples were pipetted, the membrane was let to dry at 80°C for 15' in a preheated oven. The dried membrane was later immersed in a solution of 5% skimmed milk (Sucofin®) in PBS on an orbital shaker (Edmunf Bühler GmbH; KL 1) for 2 hours (blocking) at room temperature. The membrane was then transferred into a simple autoclaved plastic membrane transformed into an envelope through heating of its edges with a heat sealer (Polystar® 242; Rische and Herfurth GMBH) and adding 3ml of anti-Thymine Dimer mouse antibody (Sigma Aldrich, Cat. Nr.: T1192) in a 1:500 concentration in the above-described blocking solution. After carefully making sure that no bubbles were left inside the envelope, its edges were finally sealed with

the heat sealer and it was left overnight on an orbital shaker inside the fridge at a 4°C temperature. The next day the envelope was cut open and the membrane was washed 3 times in PBS for 10 minutes each. For this, the membrane was first transferred into a 50ml tube with ~20ml PBS and then left for 10 minutes on followed by changing to fresh PBS and repeating the process as described. Then the membrane was transferred into a 15ml tube, in which a secondary goat anti-mouse antibody (Sigma Aldrich, Cat. No.: A3682) on a 1:1000 final concentration in the blocking solution was added and was left on the coulter mixer (The Coulter Mixer; Denley Instruments) for 2 hours. Then a second round of washing the membrane, 3 times for 10 minutes each, followed as already described above. The membrane was then transferred into a light-isolating cassette (Curix™ Screens Blue 200 HC Systems; AGFA) and 2ml of a 1:1 mixture of Detection Reagents 1 and 2 (Pierce™ ECL Western Blotting Substrate; ThermoFisher Scientific; Cat. No.: 32106) was carefully pipetted across the whole membrane surface and was let to incubate at the dark for 5' at room temperature. The membrane containing cassette was then transferred in a dark room, in the absence of UV light sources. An X-Ray film (Amersham Hyperfilm™ ECL; GE Healthcare Limited; Cat. No.: 28906838) was placed in front of the membrane covering all placed samples and then the cassette was sealed for 10-20 minutes. The film was then submerged into a developer solution [200ml from developer concentrate (Adefo Chemie GmbH; Cat. No.:00045) to 1L of deionized water], then submerged into tap water and finally submerged into a fixing solution [250ml of fixier concentrate (Adefo Chemie GmbH; Cat. No.: 00045) to 1L of deionized water]. Films were then washed with tap water and photographed with an iPad 9.7' Camera and image was edited using Procreate® Application for iOS. The stage of X-Ray film incubation and development was repeated for several different time spans, in order to produce an image with the most defined Dots and the least background noise, as that would better represent the results and allow for a better analysis of them.

2.13 ELISA

All ELISA measurements were performed using the OxiSelect™ UV-Induced Damage ELISA Kits (Cat.Nr.: STA-322 for CPD Quantification, STA-323 for 6-4PP Quantification and STA-322-C for CPD/6-4PP Quantification.) Upon receipt and until use, Reduced DNA, CPD-DNA and 6-4PP-DNA were stored at -20°C, while the rest of the Kit components were kept at 4°C until use. In order to convert them to single-stranded DNA, DNA Samples, Reduced DNA, CPD-DNA (and/or according to the measurement) 6-4PP DNA were left for 15' to thaw on ice and then placed into a dry heat blocker and let to incubate for 10 minutes at 95°C before rapidly chilling them down on ice for a further 10 minutes. Denatured DNA samples were diluted to 10µg/mL in cold TE Buffer (*methodology of preparation of TE Buffer described below*) Despite

the recommended sample concentration in the Kit being 4 µg/mL we found after testing that in our experiments the CPD and 6-4PP would fall on the very low end of the standard curve had we used such a low concentration, for which reason we opted for the higher sample concentration, while still using the recommended dilution (4 µg/mL) for our standard curve samples. To prepare our standard curve samples we first diluted both the Reduced DNA and CPD- (or 6-4PP) DNA to 4µg/mL in 1.5ml collection tubes. Then we prepared 8 Standard tubes according to the *Table 6* below.

Standard Tubes	4 µg/mL Denatured CPD (or 6-4PP) DNA (µL)	4 µg/mL Denatured Reduced DNA (µL)	CPD-DNA (or 6-4PP-DNA) (ng/mL)
1	10	390	100
2	200 of tube #1	200	50
3	200 of tube #2	200	25
4	200 of tube #3	200	12.5
5	200 of tube #4	200	6.25
6	200 of tube #5	200	3.13
7	200 of tube #6	200	1.56
8	0	200	0

Table 6, Preparation outline for the ELISA standard curve samples.

Before starting pipetting we extracted -each time- stripes of the DNA High-Binding plate that we would not need for that measurement and store them at 4°C for later use. We pipetted a volume of 50µL pro well in the DNA High Binding plate using technical duplicates for both our standard and test samples. An example (for HaCaT CPDs 1h and 24h after treatment) layout is depicted in *Figure 7* below.

	1	2	3	4	5	6	7	8	9	10	11	12
A	ST1	ST1	A1.1h	A1.1h	B1.1h	B1.1h	C1.1h	C1.1h	D1.1h	D1.1h		
B	ST2	ST2	A2.1h	A2.1h	B2.1h	B2.1h	C2.1h	C2.1h	D2.1h	D2.1h		
C	ST3	ST3	A3.1h	A3.1h	B3.1h	B3.1h	C3.1h	C3.1h	D3.1h	D3.1h		
D	ST4	ST4	A4.1h	A4.1h	B4.1h	B4.1h	C4.1h	C4.1h	D4.1h	D4.1h		
E	ST5	ST5	A1.24h	A1.24h	B1.24h	B1.24h	C1.24h	C1.24h	D1.24h	D1.24h		
F	ST6	ST6	A2.24h	A2.24h	B2.24h	B2.24h	C2.24h	C2.24h	D2.24h	D2.24h		
G	ST7	ST7	A3.24h	A3.24h	B3.24h	B3.24h	C3.24h	C3.24h	D3.24h	D3.24h		
H	ST8	ST8	A4.24h	A4.24h	B4.24h	B4.24h	C4.24h	C4.24h	D4.24h	D4.24h		

Figure 7, Example of an ELISA template for HaCaT CPDs 1h/24h. For explanation of the symbols and their corresponding conditions, see below:

ST= Standard Curve, numbers according to the respective tube numbers, as described in Table 6.

A: Control, B: VDR- inhibitor, C: AhR-inhibitor, D: VDR- + AhR- inhibitor

1: Control, 2: UVB treated, 3: D₃ treated, 4: UVB + D₃ treated

1h: sampling 1h after treatment, 24h: sampling 24h after treatment

We added 50µL of DNA Binding Solution to each well and mixed well with pipetting, then let the plate overnight on an orbital shaker. On the next day we removed all samples from the plate and washed twice with PBS by adding 250µL of PBS per well with a Multipipette® Plus (Eppendorf) and Combotips advanced® (Eppendorf) and then blotting the plate on paper towels to remove fluid residues. We then added 200µL of Assay Diluent to each well and blocked for 1 hour at room temperature. After removing the Assay Diluent, we blotted the plate again on paper towels to remove excess fluid. We, then, added 100µL of diluted (1:1000 to Assay Diluent) anti-CPD (or anti-6-4PP) Antibody to all wells and let incubate further for 1 hour at room temperature on an orbital shaker. After that we washed 5 times with 250µL of Wash Buffer solution (Wash Buffer 10X diluted 1:10 to deionized water) per well and at the last wash, wells were emptied and blotted on paper towels to remove excess fluid. After that we added 100 µL of secondary Antibody-HRP Conjugate to all wells and incubated for 1 hour at room temperature on an orbital shaker. We then washed the strip wells 5 times with Wash Buffer solution as described above. Substrate Solution was let to reach room temperature during this time and was then added in a volume of 100µL per microwell including the blank wells. Incubation of 2-30 minutes was again performed on an orbital shaker at room temperature. Actual incubation time was subjectively estimated according to the color of the standard and test samples, in order to ensure that samples would fall within the values of the standard curve. The enzyme reaction was then stopped using a 100µL of Stop Solution to each well. The plate was directly measured in an Infinite® 200 PRO Configurations plate reader (Tecan) using 450nm as the primary wave length and the Reduced DNA Standard as an absorbance blank. Analysis of the Results were automatically performed by the Tecan software according to the known above-described concentrations of the standard curve.

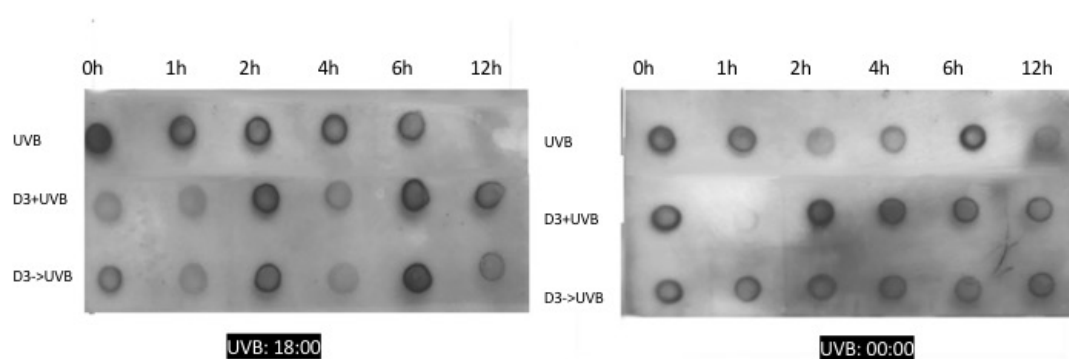


Figure 8, Sample results of Dot Blot assays for «Experiment 2» as described above in HaCaT keratinocytes treated with UVB (50 J/m²), or treatment with 1,25(OH)₂D₃ (10⁻⁷ M) either immediately before irradiation or 6h and 12h before irradiation and sampling in 0, 1, 2, 4, 6 and 12h following administration of UVB. As we lacked equipment to scan images and transform the dots into numerical values we could only subjectively compare our data. ELISA providing us with numbers we could directly use for statistics was for this reason the assay of choice for our DNA-damage measuring experiments.

Between the Dot Blot and ELISA assay we opted for the ELISA, as we lacked sufficient equipment needed to scan and analyze the images assayed in Dot Blots in order to produce

numerical values we could use for statistics. In this instance ELISA -providing results in form of numbers- offered a more systematic and objective method of analyzing our data.

2.14 Preparation of TE-Buffer

We would start by adding 0,121 g of TRIS (Pufferan®; Roth; Cat. No.: 4855.2) per 100 ml deionized water. We would first only pour half of the amount of water and slowly add the rest, while at the same time pipetting small amounts of HCL acid (Pharmacy of the University of Saarland) in order to bring the final pH of the solution to pH 8. Levels of pH were tested in real time, with a pH – meter (pHenomenal® pH 1100L; VWR), while the solution was being mixed with a magnetic stir bar on a stirrer (VMS-C7 Stirrer; VWR). Finally, we would add 0,023 g EDTA (Sigma Aldrich; Cat. No.: E-5134) per 100 ml of TRIS/water solution and steer until good mixture was achieved.

2.15 Preparation of samples for LDH-Assays of cellular toxicity

Medium from cells treated as described at 2.2 and which were to be harvested 24h was resuspended with a 1000µL pipette to mix well and then a 1.5ml volume was placed in a 1.5ml autoclaved collection tube and then stored at 4°C until the time of transportation to the Center for Experimental Neurology of the University of Saarland as to perform the LDH-Assays. As a standard an extra petri dish containing untreated cells at the same confluence as the others was treated with Triton-X Solution (Merck Millipore; kindly gifted from the Institute of Experimental Neurology) diluted down to 1% in DMEM Medium containing 1% BSA. Medium was suctioned from the petri dish and a final volume of 5ml DMEM Medium containing 1% Triton-X and 1% BSA was added. The sample was then placed on an incubator for 15' and then medium was received and stored as described above.

Principally this assay focuses on measuring activity of medium lactate hydrogonase (LDH) enzyme, in treated vs untreated cells. This enzyme is normaly located in the cellular cytosol, but in cases of destabilized membrane permeability, -as in cases of increased cellular damage and toxicity- it can be rapidly released in the free medium. Therefore LDH-activity measured in free medium of treated cells, is directly proportional to the level of toxicity underwent by the cells under their respective treatment.⁶⁶

2.16 Statistical Analysis

All statistical analysis was done using SPSS® v26 (IBM). Preparation of data was performed in Microsoft Excel Spreadsheets 2016. For the RT-qPCR experiments, the Ct values were

imported into Excel, where ΔCt values were calculated by subtracting the Ct of the respective House Keeping Gene (GADPH or ACT-B) from the Ct of the gene of interest (BMAL1 or PER2):

$$\Delta Ct = Ct_{(\text{gene of interest})} - Ct_{(\text{reference gene})}$$

Then $\Delta\Delta Ct$ Values were calculated by subtracting ΔCt of the control condition (most times vehicle control, 1:1000 EtOH diluted in 1% BSA Medium or time point 0h for the experiments with multiple time associated measurements) from the condition of interest.

$$\Delta\Delta Ct = \Delta Ct_{(\text{intervention condition})} - \Delta Ct_{(\text{control condition})}$$

Then the $2^{-\Delta\Delta Ct}$ values were further calculated, representing the relative expression (double fold change) of the respective genes to that of the control condition. For statistical analysis we either used ΔCt or $\Delta\Delta Ct$ values, as explained in *Results (3)*.

All Experiments were performed with technical duplicates between which standard deviation was calculated and those pairs of values exceeding our threshold of 0,5 were marked. For the Experiment 1A, RT-qPCR runs were performed for each set of samples twice, in order to account for the smallest possible technical error. Runs which involved bigger standard deviations even between single pairs of data were excluded, so in the end only whole unaffected sets of data were included in the further steps of the analysis. From these, mean Ct between the technical replicates were calculated which were further used to calculate ΔCt and $\Delta\Delta Ct$ values as previously discussed.

We wanted to select the best of the two reference genes (GADPH and ACT- β) in order to normalize the target gene expression values for our first experiment (Experiment 1A), but also to select the one we would use for the Experiment 1B, as for that Experiment we wanted to place all conditions of each replicate in one RT-qPCR plate, in order to avoid interplate variance as a result of multiplate measurements. We therefore averaged all Ct values from all time-points and conditions and calculated the standard deviation (SD) for each of the two genes. We found:

$$SD_{GADPH} = 1,68838068$$

$$SD_{Act-\beta} = 1,98222544$$

As stable expression between measured conditions is the single most important characteristic of a suitable reference gene, the lower SD of the GAPDH Ct values (and by a significant 17,4%) we chose this for our statistical analysis and as the measured reference gene for Experiment 1B

For experiment 1B the same steps were followed until the calculation of the respective $2^{-\Delta\Delta Ct}$ values for each of the tested conditions. In this instance, having already established GAPDH as the most suitable House Keeping Gene, in terms of stable expression throughout the tested conditions and time differences compared to Act- β it was decided for it to be the only House Keeping Gene for this experiment. This way we were able to test all samples of each biological replicate for all 3 tested cell lines at the same run, thus eliminating the inter-plate variance that would exist when testing samples between multiple RT-qPCR runs.

We used untreated HaCaT keratinocytes as internal control, thus being able to compare expression values of the same conditions between different cell lines and therefore research differential gene expression between cells. Additionally, we tested the untreated samples (control) of each of the 3 cell lines, meaning SCL-1 control for SCL-1 conditions, NHEK control for NHEK conditions and HaCaT control for HaCaT conditions. This way we were able to both test the effect of the conditions within the cells in question, but also how those effects differed in magnitude and quality between the cells.

For the ELISA experiments we also assayed all samples, both standard and tested, in duplicates. Mean CPD-/6-4PP concentrations were automatically calculated from Tecan® software according to the known concentrations of the standard curve, as described above. Due to technical difficulties regarding the measurement of 6-4PPs in HaCaT Keratinocytes 1h after treatment, meaning high variance between technical replicates, and inconsistent results despite repetitions of measurement, we opted to exclude those measurements from further analysis, thereby only including results for the 3h respective samples.

Detailed explanation of the analysis and tests used for each of the above experiments follows in the *Results (3)*.

General practices regarding statistical analysis:

For the first experiment we aimed to research the effects of time, UVB and D₃ treatment, but also the different combinations of probable interaction effects. Having more than 2 different groups of interventions (conditions) we would have to choose between one of the different types of Analysis Of Variance (ANOVA) for our statistical analysis. In ANOVA we have to

differentiate between the within-subjects factors and the between-subjects factors, their difference being whether the respective conditions were performed upon the same experiment unit or not. An example of that from the clinical research, to explain the difference between those two factors would be the following: We want to test if therapy A lowers blood pressure over the span of 48h. We would divide our testing subjects (volunteers) into a control group (receiving a placebo) and an intervention group (receiving the therapy A). We would then be measuring their blood-pressure levels, for example, after 12h, 24h and 48h. The tested outcome in this instance is of course the blood-pressure levels and the two variables are Therapy A (having two levels: Therapy vs Placebo) and time (having 3 levels: 12h, 24h and 48h). In this instance the control group and the intervention group involve different people and therefore the variable of “Therapy” in this instance is a between-subjects factor. The recurrent timed measurements of blood-pressure were, however, conducted on the same person and are therefore subjected to a subject-dependency. In this case the “Time” variable represents a within-subjects factor. The therapy measurements are “unpaired”, whereas the recurrent timed measurements are “paired” because of their dependency to the subject. If we handled both of those variables as independent, we would be unnecessarily sacrificing statistical power, since even a smaller change between the recurrent values of an individual subject, is more valuable than a similar change between different subjects, as the latter could also be attributed to personal differences between the subjects. With basic science experiments, some different rules might apply. Due to each biological replicate coming from a single passage of cells, each petri dish of each repetition of the experiment represents a clone of one another. Therefore, even if we are testing different petri dishes, in essence the subject-units are dependent to one another, due to their genetic similarity and the extremely controlled conditions under which they are prepared for experimenting. We would therefore be making our analysis as if each petri dish were the same person. In that regard, all tested conditions would be considered as “within-subject” factors. However, in regards to our first experiment, where a total of 11 different time-points were selected we would still be treating the time-variable as a “between-subjects factor”. That is because in fact cells, opposite to human subjects, grow exponentially with time, which could very well be influencing our results, especially since this variable in our case would have so many levels. In experiments involving different cells, we would of course be treating the variable of “cell type” also as a between-subjects factor. Not taking into account such dependencies between testing groups, is a common mistake in the statistical analysis of basic science experiments’ results, which unnecessarily deprives analysis of power.⁶⁷

Testing with ANOVA requires that some assumptions be fulfilled⁶⁸. First, the populations which the samples are taken from should be normally distributed. This can be tested with normality tests like the Shapiro-Wilk test, with the null hypothesis being that samples in each

testing group are normally distributed. A significant p-value (i.e. $p < 0,05$) suggests a rejection of the null hypothesis and therefore a violation of normality. In such cases non-parametric alternatives to the ANOVA should be used, like the Kruskal-Wallis test. Nevertheless, in basic science experiments sample sizes are usually significantly limited and proving normal distribution can be challenging. Empirically, ΔCt and $\Delta\Delta Ct$ values are analyzed using parametric tests as long the other assumptions are met. A second assumption of between-subjects ANOVA is the homogeneity of variance, also known as homoscedasticity. This means that the variance between the tested groups should be approximately equal. The Levene's test of equality of variances is commonly used in order to test this assumption, having as the null hypothesis that the error variances between the groups are equal. A significant p-value ($p < 0,05$) rejects the null hypothesis, proving a violation of homogeneity of variance; the samples are in that case heteroscedastic (\neq homoscedastic). Testing heteroscedastic samples of unequal sample sizes with ANOVA results in falsely increased testing significance (type 1 errors; Falsely rejecting the null hypothesis). However, ANOVA should in practice be quite robust against mild or even moderate deviations from these assumptions. Especially regarding the homogeneity of variance between equal sized samples, like in our experiments, ANOVA can be robust against heteroscedasticity as long as the ratio of the highest/lowest variance of the groups tested is smaller than 4.*² Regarding homogeneity of variance, we would therefore be using Levene's test as a preliminary test of homoscedasticity and if a violation was found we would be calculating the ratio of variances as described. In repeated-measures ANOVAs instead of homoscedasticity, a sphericity assumption is needed. This means the variances of the differences (and not of the values themselves as with homoscedasticity) between all combinations of levels (e.g. D₃ treatment vs UVB treatment) are equal. Mauchly's test is commonly used to assess if a violation of sphericity is present. For violations of sphericity an adjustment of the significance levels is needed to avoid type 1 errors. These adjustments can be performed with the use of some correction values called "Epsilon values", the most common ones are Huyn-Feldt and Greenhouse-Geisser. Lower-bound epsilon values represent the absolute most conservative significance adjustment Epsilon and are rarely used. In all cases of violation of sphericity, we will be using the more conservative Greenhouse-Geisser Epsilon for significance adjustment. In cases of mixed ANOVAs, meaning ANOVAs containing both within- and between-subjects factors, both the assumption of homogeneity of variance and that of sphericity (additionally to that of normality) need to be fulfilled. Homoscedasticity, is obviously assumed in paired samples.

*²Howell, D. C. (2013). *Statistical Methods for Psychology*. Belmont, CA: Wadsworth Cengage Learning (page 213).

2.17 Kit Components:

2.17.1 RNeasy RNA Isolation Kit and QIAshredder Kit

RNeasy Mini Kit
RNeasy Mini Spin Columns (pink)
Collection Tubes (1.5 ml)
Collection Tubes (2 ml)
Buffer RLT
Buffer RW1
Buffer RPE (concentrate)
RNase-Free Water

QIAshredder
QIAshredder Mini Spin Columns
Collection Tubes (2 ml)

2.17.2 Omniscript Kit for cDNA reverse transcription

Omniscript RT Kit
Omniscript Reverse Transcriptase
Buffer RT, 10X
dNTP Mix, 5mM
RNase-Free Water

2.17.3 SYBR Green RT-qPCR Kit

QuantiTect SYBR Green PCR Kit
HotStartTaq DNA Polymerase
QuantiTect SYBR Green PCR Buffer
dNTP mix
SYBR Green I dye
ROX dye

2.17.4 NucleoSpin Tissue DNA Isolation Kit

NucleoSpin Tissue DNA Isolation Kit
Lysis Buffer T1
Lysis Buffer B3
Wash Buffer BW
Wash Buffer B5 (Concentrate)*
Elution Buffer BE*
Proteinase K (lyophilized)
Proteinase Buffer PB
NucleoSpin® Tissue Columns (light green rings)
Collection Tubes (2 mL)

* Composition of Elution Buffer BE: 5 mM Tris/HCl, pH 8.5

2.17.5 OxiSelect™ UV-Induced Damage ELISA Kits

OxiSelect™ UV-Induced Damage ELISA Kit
1. DNA High-Binding Plate (Part No. 232404): One 96-well strip plate.
2. DNA Binding Solution (Part No. 232405): One 6 mL bottle.
3. Anti-6-4PP Antibody (Part No. 232301) or Anti-CPD Antibody (Part No. 232202): One 20 µL vial.
4. Secondary Antibody, HRP Conjugate (Part No. 10902): One 50 µL vial.
5. Assay Diluent (Part No. 310804): One 50 mL bottle.
6. 10X Wash Buffer (Part No. 310806): One 100 mL bottle.
7. Substrate Solution (Part No. 310807): One 12 mL amber bottle.
8. Stop Solution (Part. No. 310808): One 12 mL bottle.
9. 6-4PP-DNA Standard (Part No. 232302): One 100 µL vial of 25 µg/mL 6-4PP-DNA in 1X TE Buffer.
10. Reduced DNA Standard (Part No. 232207): One 100 µL vial of 0.2 mg/mL reduced DNA in TE Buffer.

3. Results

3.1 Preexaminations

3.1.1 EtOH (diluted 1:1000) has no significant effect on expression of circadian clock genes in cultured HaCaT keratinocytes.

As discussed in “*Methods*”, compounds to be tested for their effects on expression of CCGs [1,25(OH)₂D₃, AhR- and VDR-antagonists] were diluted in EtOH before they were added to the medium (DMEM medium containing 1% BSA). Therefore, it was important to investigate at the beginning of our study whether EtOH itself has an effect on expression of CCGs. To test whether EtOH, even in those very small concentrations, has an effect on expression of our target genes, two-way repeated measures ANOVA was performed, demonstrating that EtOH (1:1000) has no significant effect on expression of circadian clock genes in cultured HaCaT keratinocytes. As demonstrated in *Table 7*, no significant effect of neither the EtOH alone, nor in interaction with UVB, nor of time was found for any one of our target genes (results are depicted with the p-values assuming sphericity as this is the most liberal value of significance).

Tests of Within-Subjects Effects

BMAL1 - vehicle vs normal control: MEASURE_1

Source		Type III Sum of Squares	df	Mean Square	F	Sig.	Partial Eta Squared
Ethanol_Vehicle	Sphericity Assumed	.040	1	.040	.005	.946	.001
Ethanol_Vehicle * UVB	Sphericity Assumed	14.872	1	14.872	1.964	.234	.329
time * UVB	Sphericity Assumed	8.510	10	.851	.791	.638	.165
Ethanol_Vehicle * time	Sphericity Assumed	2.799	10	.280	.888	.552	.182
Ethanol_Vehicle * time * UVB	Sphericity Assumed	3.219	10	.322	1.021	.444	.203

Tests of Within-Subjects Effects

Per2 - vehicle vs normal control: MEASURE_1

Source		Type III Sum of Squares	df	Mean Square	F	Sig.	Partial Eta Squared
Ethanol_Vehicle	Sphericity Assumed	1.514	1	1.514	.277	.627	.065
Ethanol_Vehicle * UVB	Sphericity Assumed	6.075	1	6.075	1.111	.351	.217
time * UVB	Sphericity Assumed	7.419	10	.742	1.074	.404	.212
Ethanol_Vehicle * time	Sphericity Assumed	1.976	10	.198	1.351	.238	.252
Ethanol_Vehicle * time * UVB	Sphericity Assumed	.598	10	.060	.409	.934	.093

Table 7, Effect of EtOH vehicle (1:1000 diluted in 1% BSA DMEM, vehicle control) vs non-EtOH-containing control in HaCaT Keratinocytes for BMAL1 (up) and Per2 (down). Two-way repeated measures ANOVA for EtOH (2 levels; treated vs untreated) and time (11 levels for each time point) and with UVB as between-subjects factor for BMAL1 (up) and Per2 (down genes). Effect of time alone was removed for simplicity. No significant effect of EtOH, nor any interaction effect of it with neither UVB nor time was found. Therefore, “vehicle control” and “normal control” can be regarded as equal.

(influence of time alone, was obviously significant ($p < 0.001$) but was excluded from the graph, as this characteristic would be important to discuss later in the experimental results.)

Taking the above into account, we can safely use the vehicle control as our control condition for the rest of our analysis. Effects found could be safely attributed to the respective condition and not the vehicle. From now on as “control” we regard the vehicle control (EtOH 1:1000 diluted in 1% BSA DMEM medium.)

3.2 Expression of core CCGs BMAL1 and Per2 shows circadian rhythmicity in HaCaT keratinocytes.

By plotting expression values for both of our researched CCGs over time, we clearly see a pattern involving positive and negative expression «peaks» over 24h intervals for both BMAL1 and Per2 in HaCaT keratinocytes. This is also evident for untreated («control» in *Figure 9*) samples suggesting that HaCaT keratinocytes used in this study possess functional circadian circuitries. As explained in Introduction, BMAL1 and Per2 expression patterns have opposite phases, with BMAL1 being the positive and Per2 the negative «arm» of the circadian circuitry. This phenomenon appears as well between our subjects as evidenced in «Control» HaCaT, in which BMAL1 positive peaks are mainly positioned against the Per2 negative peaks.

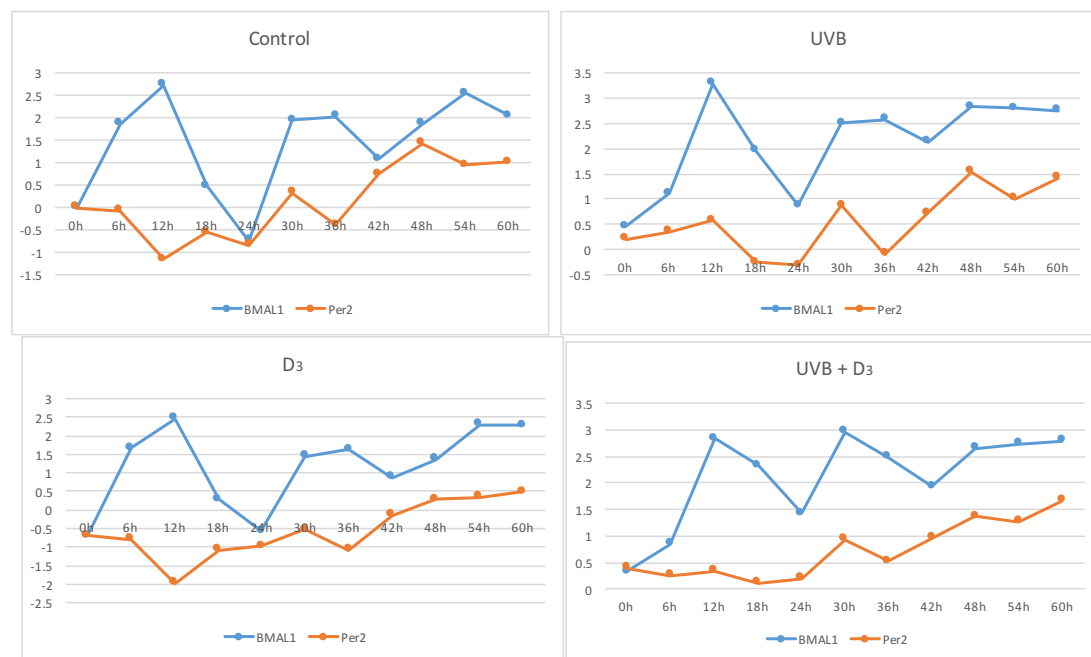


Figure 9. *BMAL1 and Per2 mean $-\Delta\Delta C_t$ values plotted over time for all 4 conditions with untreated 0h samples as the internal control. We notice an interchange of positive and negative “peaks” every ~24h in untreated samples, indicating functional circadian rhythmicity. BMAL1 and Per2 show a phase-difference, as expected, with BMAL1’s positive peaks positioned against Per2’s negative peaks. For Per2 a relative phase-difference can be suggested between non-irradiated and irradiated samples, although no clear conclusions can be drawn from these diagrams and with important SD between measurements..*

As we see, expression patterns of BMAL1 remain pretty much stable between all 4 conditions, with no relative change in period-length, nor in the position of positive and negative peaks. While, the high standard deviations between the replicates would make it difficult to draw conclusions regarding periodicity and characterizing patterns just from the means, it should be noted that Per2 expression patterns show signs of a phase change, for irradiated samples both irrespective of D₃ treatment, while other elements of CC activity like period-length, remain largely unchanged. This could potentially signify a synchronization / rhythm influencing of Per2 due to UVB irradiation, while a lack of a similar effect from D₃ treatment can be safely assumed owing to the great similarity between the respective expression pattern diagrams.

3.3 Circadian activity of core CCGs BMAL1 and Per2 may differ between normal (HaCaT) and cancerous (SCL-1) keratinocytes. A reference test-run.

Comparisons between treatment conditions indicate the most interesting differences: Expression of BMAL1 is overall suppressed after treatment with UVB, D₃ or UVB+D₃, while in Per2 the combination of UVB+D₃ «cancels» pattern changes of individual UVB or D₃ treatment.

As described in 2.6.1 before designing Experiment 1B, we replicated Experiment 1A with SCL-1 for n=1 replicates, before deciding to only focus on one time point (t=12h), as already explained. By plotting those results, we can see for BMAL1 a noticeable suppressive effect of both UVB and D₃ conditions on its expression (*Figure 10*; left) while no obvious oscillation is noticed in the control, opposite to what is seen in the UVB and D₃ conditions (*Figure 10*; right). With Per2 the oscillatory expression is very obvious, the period seems to change both after UVB and after D₃ in an identical manner (*Figure 11*; right), whereas combined these conditions seem to mediate a self-canceling effect (*Figure 11*; left), where expression of control seems almost identical to that of UVB + D₃, whereas expression of D₃ seems almost identical to that of UVB. These are of course only for reference and with n=1 replicates no safe conclusions can be drawn. Comparing untreated BMAL1 expression of untreated HaCaT (*Figure 9*) with that of untreated SCL-1 (*Figure 10*) we notice a strong difference in circadian activity, with SCL-1 indicating oscillatory activity only after treatment with either UVB, D₃ or a combination.

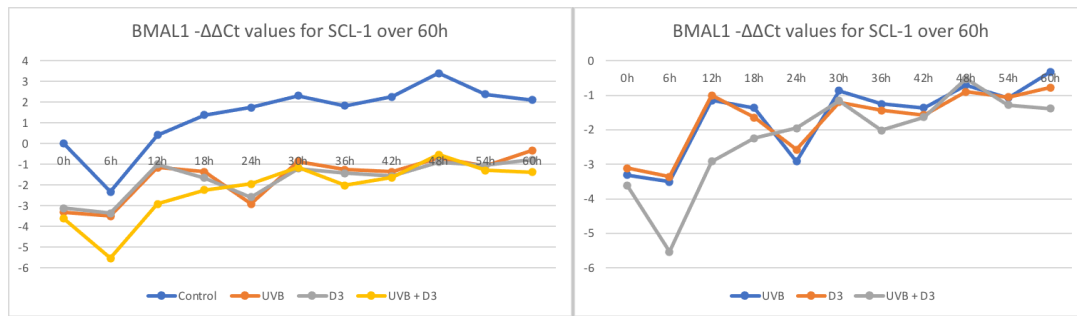


Figure 10. Testing experiment, SCL-1 BMAL1 -ΔΔCt values over 60h

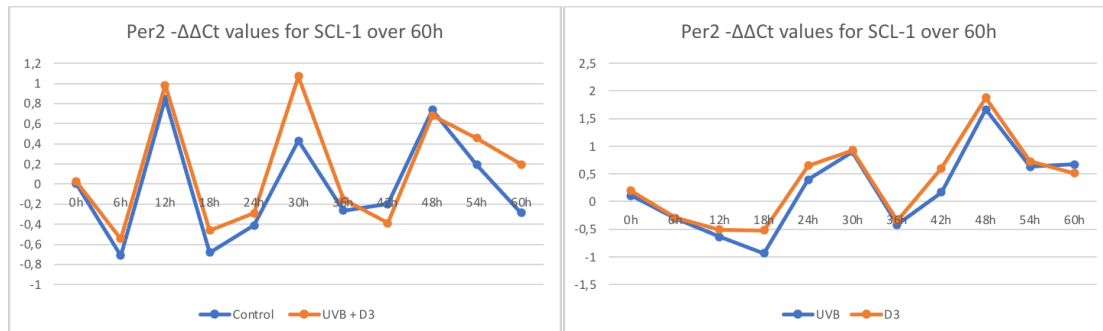


Figure 11. Testing experiment, SCL-1 Per2 -ΔΔCt values over 60h. n=1 replicate.

The potential effects of applied conditions (UVB, D₃ and UVB+D₃) offered some very interesting prospects. To delve deeper into the roles of these treatments in gene expression of CCGs we selected an important time point (t=12h; ½ of a period’s length) and focused on comparisons between conditions and different cells (HaCaT, SCL-1 and NHEK.) Nevertheless, further researching and comparison of expression patterns of core CCGs between untreated HaCaT and untreated SCL-1 would be an interesting topic for future endeavors.

3.4 UVB radiation significantly upregulates both BMAL1 and Per2 in HaCaT keratinocytes, while 1,25(OH)₂D₃ only mediated a marginal downregulation effect in Per2 and only between non-irradiated samples.

3.4.1 BMAL1

For simplicity we would be using “Control” to describe vehicle control samples, “UVB” to describe samples irradiated with 50 J/m² at reference time 0h, “D₃” for samples treated with DMEM -containing 1% BSA and 1,25(OH)₂D₃ (10⁻⁷ M) at time 0h and “UVB + D₃” for samples irradiated with 50 J/m² and then immediately treated with DMEM containing 1% BSA and 1,25(OH)₂D₃ (10⁻⁷ M) at time 0h.

The 4 researched populations were therefore (1) Control, (2) only UVB treatment, (3) only D₃ treatment, (4) UVB + D₃ treatment. As explained in “statistical analysis” in Methods, we had to test the normality assumption with the Shapiro-Wilk test of normality (Table 8), which indicated no violation in any of those groups.

	Shapiro-Wilk		
	Statistic	df	Sig.
Control	.943	33	.081
UVB	.949	33	.122
D3	.946	33	.102
UVB+D3	.961	33	.268

Table 8, Shapiro-Wilk test of normality for BMAL1 ΔCt values in HaCaT Keratinocytes, Experiment 1A. No significant violation of normality was found.

Levene’s test of equality of error variances showed no violation of homogeneity of variance and while Mauchly’s test showed a violation of sphericity we decided to correct our significance values according to the most conservative Lower-Bound estimates.

Our null hypothesis was that the means of the ΔCt values for BMAL1 (under all 3 conditions= time, UVB and D₃) were equal and the alternative hypothesis (H_a) was that at least one of those means differed from the others.

$$H_0: \mu_1 = \mu_2 = \dots = \mu_v$$

H_a: at least one of those means differs with the others

The respective Within- and Between-Subjects Effects for the two-way repeated measures ANOVA are depicted in Tables 9 and 10 (see “Sig.” for significance/ p-values.)

BMAL1 for HaCaT keratinocytes		∴ MEASURE_1				
Source		Type III Sum of Squares	df	Mean Square	F	Sig.
UVB_radiation	Lower-bound	21.402	1.000	21.402	18.784	<.001
UVB_radiation * time	Lower-bound	15.086	10.000	1.509	1.324	.278
D3_treatment	Lower-bound	.512	1.000	.512	.250	.622
D3_treatment * time	Lower-bound	1.762	10.000	.176	.086	1.000
UVB_radiation * D3_treatment	Lower-bound	.554	1.000	.554	.434	.517
UVB_radiation * D3_treatment * time	Lower-bound	.978	10.000	.098	.077	1.000

Table 9, two-way repeated measures ANOVA for BMAL1 in HaCaT ΔCt values, with UVB and D₃ treatments as within-subjects factors and time as the between-subjects variable. We found a significant effect of UVB radiation (p<0,001.) No other factor or interaction effect was noted.

Tests of Between-Subjects Effects

HaCaT BMAL1 Experiment 1A: MEASURE_1

Transformed Variable: Average

Source	Type III Sum of Squares	df	Mean Square	F	Sig.	Partial Eta Squared
Intercept	3996.600	1	3996.600	1471.451	.000	.985
time	103.585	10	10.358	3.814	.004	.634

Table 10, Between-Subjects Effects, BMAL1 Δ Ct values, Experiment 1A. HaCaT Keratinocytes. Significant effect of time ($p=0,004$) as expected, since our genes as CCGs are known for their expression being time-dependent.

A significant effect of time ($p < 0,05$) is found, as was expected since the genes we are researching are in fact circadian clock genes and therefore their expression is in constant periodical alteration. The second –and most interesting- finding is the significant effect of UVB radiation in BMAL1 expression ($p < 0,001$).

In *Figure 12* we are seeing the expression of BMAL1 over 60h across all 4 conditions. Expression values are represented as $-\Delta\Delta$ Ct values with untreated 0h samples posing as the internal control. It should be mentioned that Δ Ct and $\Delta\Delta$ Ct represent a counter analog gene expression, meaning that the lower they are, the higher is the relative expression. To avoid confusion and for better illustration of our results we chose to present values as $-\Delta\Delta$ Ct rather than $+\Delta\Delta$ Ct. It should further be noted that standard deviations between the individual time-points/conditions were quite big, for which reason we avoided including error bars in our graphs of expression plotted against time, as this would not offer any further understanding of the results, while making the interpretation of it more confusing. However, high variance is of course counted in the statistical analysis tests for significance calculation, as represented by the p-values noted.

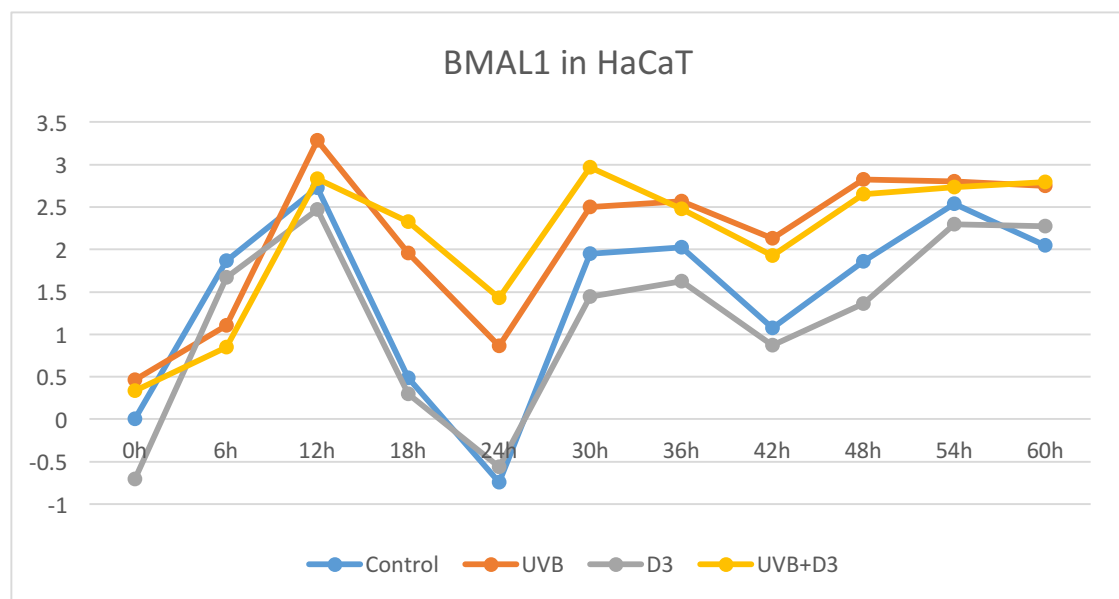


Figure 12. BMAL1 mean $-\Delta\Delta Ct$ values over 60h for HaCaT Keratinocytes with untreated 0h samples as the internal control. As evident in the statistical analysis UVB radiation significantly influences BMAL1 expression, irrespective of D_3 treatment. As illustrated above UVB upregulates BMAL1 expression, as BMAL1 activity is increased in the majority of time points beginning 12h post-treatment. D_3 treatment shows neither an effect on BMAL1 activity nor influences BMAL1's response to UVB treatment.

From the graphical illustration and in accordance we results from the statistical analysis as described above, we conclude that UVB significantly upregulates BMAL1 expression in HaCaT keratinocytes over 60h following treatment, with no effect (simple or interaction) from D_3 .

While it is obvious that magnitude of UVB's effect differed between the different time-points we wanted to quantify the average increase in BMAL1 expression across all time points. Ratio was calculated irrespective of D_3 treatment, as proven earlier that D_3 did not intervene or influence BMAL1 expression in anyway. To calculate ratio we first calculated average ΔCt value of non-radiated samples ($\Delta Ct_{\text{non-radiated}} \sim 5,9$) and subtracted it from all (non-radiated and irradiated) ΔCt values to form $\Delta\Delta Ct$ values which were then used to calculate fold-change using the $2^{-\Delta\Delta Ct}$ form. Geometric means were then calculated in Excel (=GEOMEAN):

Non-radiated samples ratio: 1 (SD: 1.807857504)

Irradiated samples ratio: 1.747540386 (SD: 1.780692155)

In conclusion:

UVB significantly upregulated BMAL1 expression by an average of 74,8%, while D_3 showed no significant effect (main or interaction.)

3.4.2 Per2

We then followed the same principles testing again with Per2 (ΔCt values of Per2 normalized to GADPH) expression, by conducting a mixed ANOVA using D_3 and UVB as the within-subjects factors and time as the between-subjects factor.

Tests of Normality - Per2			
	Shapiro-Wilk		
	Statistic	df	Sig.
Control	.962	33	.291
UVB	.955	33	.184
D_3	.949	33	.126
UVB+ D_3	.956	33	.195

We performed again the Shapiro-Wilk test of normality (Table 13) and the Mauchly's test of Sphericity. In regards to normality and sphericity no violations were found.

Table 11, Shapiro-Wilk test of normality for Per2 ΔCt values, Experiment 1A. HaCaT Keratinocytes. No violation of normality indicated.

However, the Levene’s test of equality of variances indicated a mild violation of the assumption of homogeneity of variance ($p < 0,05$) for the UVB and UVB+D₃ groups. As explained under “statistical analysis” in Methods, we would be calculating the ratio of highest/lowest variances, as our groups had equal sample sizes. We first calculated the respective variances of the 4 test groups using Excel (=VAR):

$$\sigma^2_{\text{Control}}: 1,423$$

$$\sigma^2_{\text{UVB}}: 0,663$$

$$\sigma^2_{\text{D}_3}: 2,591$$

$$\sigma^2_{\text{UVB} + \text{D}_3}: 0,954$$

$$\text{Ratio: } \sigma^2_{\text{D}_3} / \sigma^2_{\text{UVB}} = 2,591 / 0,663 = 3,907 < 4.$$

Therefore the degree of deviation from homogeneity of variance in our case should not be impacting the validity of our results. We would therefore be safely applying the mixed ANOVA.

We found the following results:

Per2 for HaCaT keratinocytes		MEASURE_1				
Source		Type III Sum of Squares	df	Mean Square	F	Sig.
UVB	Lower-bound	24.197	1.000	24.197	29.503	<.001
UVB * time	Lower-bound	5.307	10.000	.531	.647	.759
D3	Lower-bound	2.161	1.000	2.161	1.039	.319
D3 * time	Lower-bound	1.707	10.000	.171	.082	1.000
UVB * D3	Lower-bound	6.215	1.000	6.215	7.125	.014
UVB * D3 * time	Lower-bound	.344	10.000	.034	.039	1.000

Table 12. Two-way repeated measures ANOVA for ΔC_t values of Per2 in HaCaT keratinocytes. Significant effects for UVB ($p < 0,001$) and the two-way interaction of D₃*UVB ($p = 0,014$).

HaCaT Per2 Experiment 1A: MEASURE_1						
Transformed Variable: Average						
Source	Type III Sum of Squares	df	Mean Square	F	Sig.	Partial Eta Squared
Intercept	2931.569	1	2931.569	1753.762	.000	.988
time	50.963	10	5.096	3.049	.014	.581
Error	36.775	22	1.672			

Table 13. Tests of Between-Subjects Effects. Per2 ΔC_t values, Experiment 1A. HaCaT Keratinocytes. Significant effect of time ($p = 0,014$). As to be expected, since Per2 is a known CCG.

As with BMAL1, we find here once again a significant influence of time ($p = 0,014$) and a significant effect of UVB ($p < 0,001$), while we also observe a significant UVB*D₃ interaction effect ($p = 0,014$).

An interaction effect between two variables means that the effects of (at least) one of the variables changes across the different levels of the other variable, meaning that either/both UVB affects Per2 expression differently based on whether cells would be treated with D₃ following their irradiation, or/and D₃ mediates an effect differently based on whether the cells that would be subjected to D₃ were first irradiated or not. For this we have to take the graphical illustration of gene expression into account.

Below the expression diagrams for Per2 under all 4 conditions over 60h.

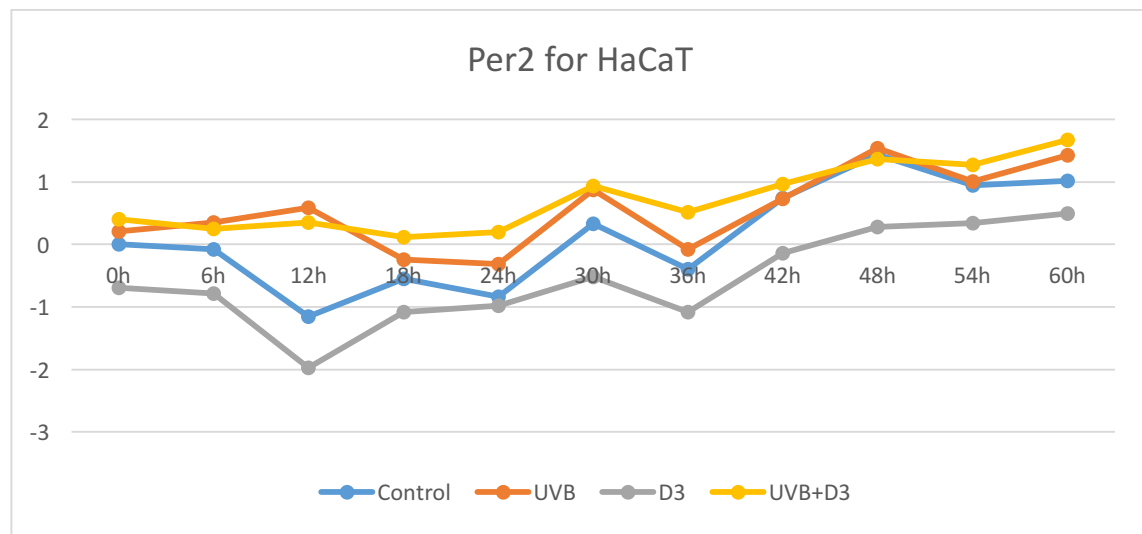


Figure 13. Per2 mean -ΔΔCt values for HaCaT Keratinocytes. Once again UVB-radiation results in an increase in gene activity, irrespective of D₃ treatment. Moreover D₃-treated samples indicated downregulated Per2 expression compared to control.

Since diagrams of UVB and UVB+D₃ are majorly intercepting one another, whereas D₃ expression pattern is majorly illustrated to be below that of the control's diagram, we can assume that, while UVB affects Per2 irrespective of D₃ treatment, there is a probably different effect of D₃ based on whether HaCaT keratinocytes were irradiated previous to D₃ treatment. To test this hypothesis we would have to be testing D₃'s effects between the 2 different levels of UVB (non-irradiated vs irradiated.)

We would be therefore performing 2 more mixed ANOVAs:

1. Within-subjects factor: D₃ treatment (for UVB= no UVB treatment)
2. Within-subjects factor: D₃ treatment (for UVB= treatment with 50 J/m²)

For all the above conditions, time (11 different time points) would serve as a between-subjects factor. Each time a statistical test is performed, there exists the chance of type 1 errors, meaning a result indicating significance even if there is none (Falsely rejecting the null hypothesis.) Our acceptance threshold was set at the beginning at $\alpha = 0,05$. This means we accept at most a 5% of type 1 error. Since we would be performing this part of our analysis 2 times, we would need

to adjust our acceptance interval accordingly. Therefore, for this part of the analysis our acceptance interval is set at $\alpha = 0,05/2 = 0,025$. This adjustment is called Bonferroni correction. We would be considering p-values as indicating statistical significance if they are lower than that. ($p < 0,025$)

For the effects of D_3 across the different levels of UVB we found the following results:

Tests of Within-Subjects Effects^a

Per2 in non-irradiated HaCaT keratinocytes .: MEASURE_1

Source		Type III Sum of Squares	df	Mean Square	F	Sig.
D3_treatment	Lower-bound	20.410	1.000	20.410	14.829	<.001
D3_treatment * time	Lower-bound	4.186	10.000	.419	.304	.972

a. UVB_50J = no UVB

Tests of Within-Subjects Effects^a

Per2 in irradiated HaCaT keratinocytes .: MEASURE_1

Source		Type III Sum of Squares	df	Mean Square	F	Sig.
D3_treatment	Lower-bound	5.948	1.000	5.948	3.904	.061
D3_treatment * time	Lower-bound	2.828	10.000	.283	.186	.996

a. UVB_50J = UVB

Table 14, Tests of simple main effects, Per2, Experiment 1A. Effects of D_3 across the different levels of UVB. HaCaT Keratinocytes. We found a significant effect of D_3 in non-irradiated samples ($p = 0,001$), but not between irradiated samples ($p = 0,061$).

Therefore, for Per2 expression we conclude that: D_3 has a significant effect on Per2 expression between non-irradiated samples ($p = 0,001$), but not between the irradiated ones ($p = 0,061$).

To calculate upregulation of Per2 by UVB radiation irrespective of D_3 treatment (as no effect was observed between UVB and UVB+ D_3), we calculated the ratio similar to how we did it for BMAL1, resulting in:

Ratio of non-irradiated HaCaT: 1 ($SD_{\text{non-irradiated}}$: 1.266650499)

Ratio of irradiated HaCaT: 1.810380344 ($SD_{\text{irradiated}}$: 1.6301282)

And similarly for the downregulation effect of D_3 between non-irradiated HaCaT:

Ratio of untreated HaCaT: 1 ($SD_{\text{untreated}}$: 0.943216837)

Ratio of D_3 treated HaCaT: 0.619902308 ($SD_{D_3 \text{ treated}}$: 1.043883393)

- UVB significantly upregulated Per2 by an average of 81% in HaCaT keratinocytes irrespective of D_3 treatment.
- D_3 treatment indicated an average of 38% decrease in Per2 expression in non-irradiated, but not in irradiated HaCaT keratinocytes.

3.5 Cancerous SCL-1 cells show an overall decreased expression of BMAL1 and a further suppression following UVB radiation as opposed to an upregulation observed in HaCaT and even more strongly in NHEK keratinocytes, while no such cell-specific differences were observed for Per2.

3.5.1 BMAL1

Cell type, UVB and their interaction significantly influence BMAL1 expression.

In the 2nd part of our first experiment, we aimed to research effects of UVB and D₃ in accordance with cell type on the circadian clock, leaving in this instance outside the variable of time. We chose to test these effects between 3 cells with different p53 status, which also model 3 different steps across the carcinogenic process: NHEK (p53 wild type; models normal keratinocytes), HaCaT Keratinocytes (mutated p53; models acanthotic keratosis) and SCL-1 (lack of p53 expression; models Squamous Cell Carcinoma cells.)

Expression Ct values were normalized to the GADPH reference gene and then subsequent Δ Ct values were further normalized to untreated HaCaT samples (arbitrarily chosen in order to represent a reference point, so that other expression values can be relatively quantified.) These $\Delta\Delta$ Ct values [-log(fold change) data] were further used for statistical analysis, specifically a mixed ANOVA with “cell type” (*HaCaT*, *NHEK*, *SCL-1*) as the between-subjects factor, while UVB and D₃ (+/-) were the within-subjects factors.

Tests of Normality

	Shapiro-Wilk		
	Statistic	df	Sig.
Control	.938	9	.566
only UVB	.910	9	.319
only D3	.976	9	.940
UVB + D3	.915	9	.351

Table 15 Experiment 1B, BMAL1 - $\Delta\Delta$ Ct values, Shapiro-Wilk normality test. Values for HaCaT, NHEK and SCL-1. No violation found

Since we were going to compare gene expression between different cells we conducted a Shapiro-Wilk normality test (*Table 15*) for all our values combined, which again indicated no violation ($p > 0,05$) of the assumption.

Levene’s test indicated no violation of the assumption of homogeneity of variance ($p < 0,05$) and Mauchly’s Test showed no violation of sphericity. Therefore, no significance correction would be needed.

In Table 16 and 17 we can see the results of the two-way repeated measures ANOVA for the within- and between subject factors respectively.

Tests of Within-Subjects Effects

BMAL1 Experiment 1B: MEASURE_1

Source		Type III Sum of Squares	df	Mean Square	F	Sig.	Partial Eta Squared
D3	Sphericity Assumed	.053	1	.053	.709	.432	.106
D3 * cell_type	Sphericity Assumed	.118	2	.059	.787	.497	.208
UVB	Sphericity Assumed	1.839	1	1.839	9.383	.022	.610
UVB * cell_type	Sphericity Assumed	5.321	2	2.661	13.574	.006	.819
D3 * UVB	Sphericity Assumed	.175	1	.175	3.651	.105	.378
D3 * UVB * cell_type	Sphericity Assumed	.338	2	.169	3.525	.097	.540

Table 16, Experiment 1B, BMAL1 - $\Delta\Delta C_t$ values, two-way repeated measures ANOVA, Within-Subjects factor for UVB and D₃ with cell type as the between-subjects factor. Within-Subjects effects. We find significant effects of UVB ($p < 0,05$) and an interaction effect UVB*cell type ($p = 0,006$).

Tests of Between-Subjects Effects

Experiment 1B - BMAL1: MEASURE_1

Transformed Variable: Average

Source	Type III Sum of Squares	df	Mean Square	F	Sig.	Partial Eta Squared
Intercept	3.096	1	3.096	1.151	.325	.161
Cell_type	90.329	2	45.164	16.794	.003	.848
Error	16.136	6	2.689			

Table 17, Experiment 1B, BMAL1 - $\Delta\Delta C_t$ values, two-way repeated measures ANOVA, Within-Subjects factor for UVB and D₃ with cell type as the between-subjects factor. Between-Subjects effects. We see a significant effect of cell type ($p = 0,003$).

Our analysis indicates a significant effect of UVB radiation ($p=0,02$), of cell type ($p=0,003$) and an interaction effect of cell type*UVB.

A significant difference in expression based on cell type means that at least one of the different cells differs with the others, in relation to its BMAL1 expression. To further test how cell type influences BMAL1 expression we performed a post hoc Tukey HSD test for cell type:

Multiple Comparisons

Experiment 1B - BMAL1: MEASURE_1
Tukey HSD

(I) Cell_type	(J) Cell_type	Mean Difference (I-J)	Std. Error	Sig.	95% Confidence Interval	
					Lower Bound	Upper Bound
HaCaT	NHEK	-.8082542	.66949153	.492	-2.8624381	1.2459296
	SCL-1	2.8823788*	.66949153	.012	.8281950	4.9365627
NHEK	HaCaT	.8082542	.66949153	.492	-1.2459296	2.8624381
	SCL-1	3.6906331*	.66949153	.004	1.6364492	5.7448169
SCL-1	HaCaT	-2.8823788*	.66949153	.012	-4.9365627	-.8281950
	NHEK	-3.6906331*	.66949153	.004	-5.7448169	-1.6364492

Based on observed means.

The error term is Mean Square(Error) = .672.

*. The mean difference is significant at the .05 level.

Table 18, Experiment 1B, BMAL1 - $\Delta\Delta C_t$ values, post hoc Tukey HSD test for cell type. No significant difference between NHEK and HaCaT ($p=0,492$), whereas significant difference between HaCaT/NHEK and SCL-1 ($p=0,012-0,004$)

From that we can conclude that NHEK and HaCaT Keratinocytes do not indicate significant differences in relation to BMAL1 expression ($p=0,49$), while they both significantly differ from SCL-1 ($p=0,004$ and $0,012$ respectively).

This difference based on cell type can be better understood by looking at Figure 14, where all values for expression under all conditions for each cell type are illustrated. All $\Delta\Delta C_t$ values are normalized to the untreated HaCaT keratinocytes as a reference point.

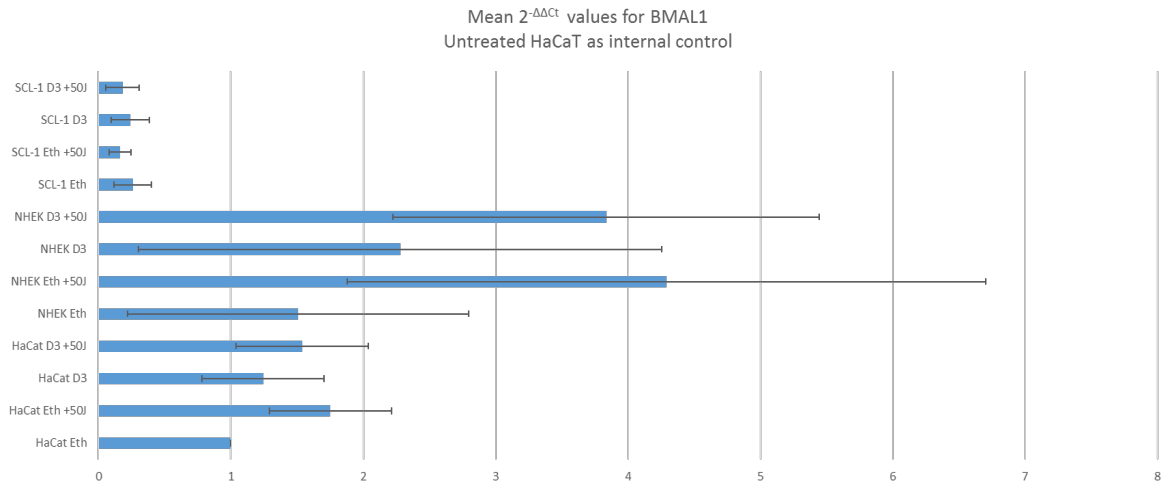


Figure 14, Experiment 1B, BMAL1 mean $2^{-\Delta\Delta C_t}$ values, NHEK and HaCaT show a significantly higher BMAL1 expression compared to SCL-1.

As it becomes obvious from the diagram, BMAL1 expression is significantly lower for SCL-1 in all conditions.

In order to better comprehend the other two found differences (UVB and UVB*cell type), we used a different set of diagrams. This time we normalized each set of ΔCt values to the respective control of each different cell type. Example for NHEK, D₃ treated, below:

$$\Delta\Delta Ct_{NHEK(D3)} = \Delta Ct_{NHEK(D3)} - \Delta Ct_{NHEK(Control)}$$

In relation to the cell type*UVB interaction effect it is prominent from the *Figure 15* below, that while UVB irradiation has a significant influence in BMAL1 of all 3 researched cells, in SCL-1 the effect is suppressive, while in NHEK and HaCaT it is activating. Therefore at least in part this can be explained from this pattern.

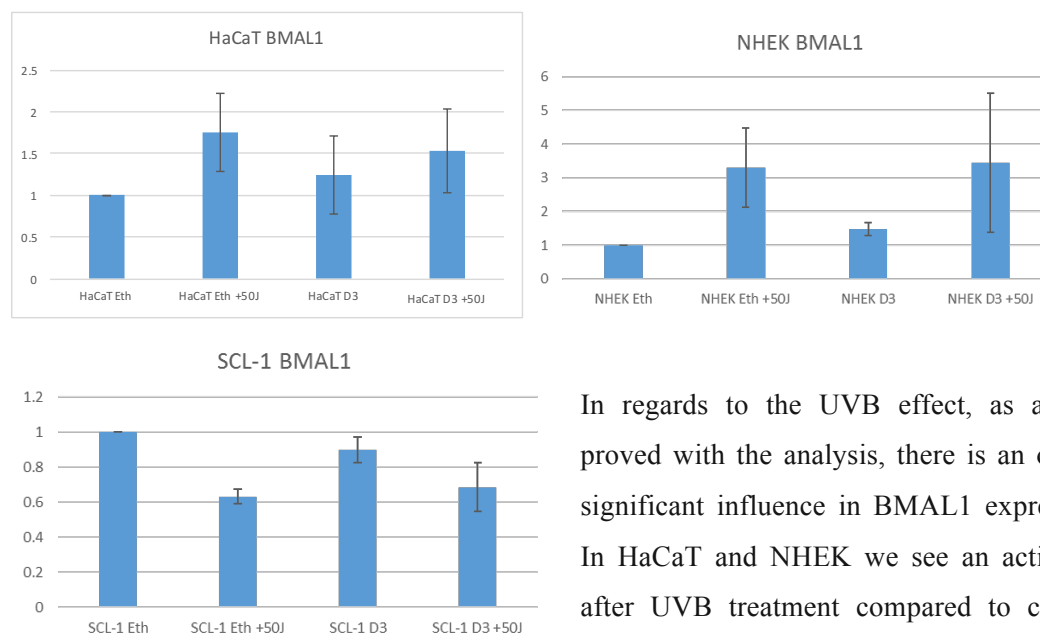


Figure 15 mean $2^{-\Delta\Delta Ct}$ values for *BMAL1*, Experiment 1B, HaCaT, NHEK, SCL-1

In regards to the UVB effect, as already proved with the analysis, there is an overall significant influence in BMAL1 expression. In HaCaT and NHEK we see an activation after UVB treatment compared to control, whereas in SCL-1 we observe a significant suppression. This explains in part the UVB*cell type interaction effect, meaning

that the reaction of BMAL1 against UVB treatment differs between cells and the difference exists at least between NHEK/HaCaT and SCL-1 (as in both cases we have a significant effect of UVB, albeit activation on the one side and suppression on the other.) The remaining question is whether such a difference also exists between NHEK and HaCaT keratinocytes.

In order to test whether UVB radiation has a different effect between HaCaT and NHEK (UVB*cell type for HaCaT vs NHEK) we performed a two-way (mixed) ANOVA between HaCaT Keratinocytes and NHEK with UVB as the within-subjects factor and cell type (and D₃) as the between subject factors. Sphericity was, as proven before, not violated. The results are shown in *Table 19* and *20*:

Tests of Within-Subjects Effects

BMAL1 HaCaT vs NHEK: MEASURE_1

Source		Type III Sum of Squares	df	Mean Square	F	Sig.	Partial Eta Squared
UVB	Sphericity Assumed	5.353	1	5.353	31.031	.001	.795
UVB * cell_type	Sphericity Assumed	.956	1	.956	5.540	.046	.409
UVB * D3	Sphericity Assumed	.450	1	.450	2.608	.145	.246
UVB * cell_type * D3	Sphericity Assumed	.014	1	.014	.081	.783	.010

Table 19, Experiment 1B, BMAL1 - $\Delta\Delta$ Ct values, HaCaT vs NHEK, two-way mixed ANOVA, with cell type and D₃ as the between-subjects factors and UVB as the within-subjects factor. Significant differences for UVB corroborate the previews results. A significant UVB*cell type is also observed meaning that HaCaT and NHEK indeed differ in relations to their reaction against UVB treatment.

Tests of Between-Subjects Effects

BMAL1 HaCaT vs NHEK: MEASURE_1

Transformed Variable: Average

Source	Type III Sum of Squares	df	Mean Square	F	Sig.	Partial Eta Squared
Intercept	15.447	1	15.447	14.233	.005	.640
cell_type	3.920	1	3.920	3.612	.094	.311
D3	.102	1	.102	.094	.767	.012
cell_type * D3	.066	1	.066	.061	.811	.008
Error	8.682	8	1.085			

Table 20, Experiment 1B, BMAL1 - $\Delta\Delta$ Ct values, HaCaT vs NHEK, two-way mixed ANOVA, with cell type and D₃ as the between-subjects factors and UVB as the within-subjects factor. No significant difference for cell type, as already found in previews testing.

This corroborates the results of the preview analysis (that cell type and D₃ treatment alone, have no significant interaction), but further proves that UVB*cell type is also significant (even if only marginally accepted p-value) between NHEK and HaCaT (p=0,046). Taking together the findings from the diagram, we can conclude that UVB has a significantly stronger activating effect in NHEK compared to HaCaT regarding BMAL1 expression, or that NHEK are more susceptible to UVB-induced activation of BMAL1. This is further illustrated in *Figure 16*.

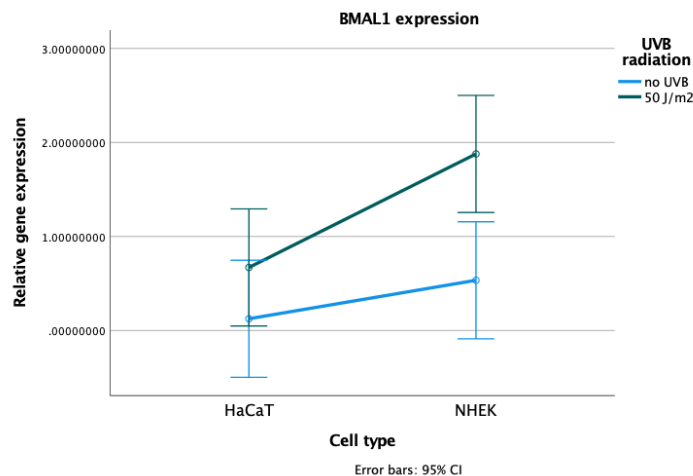


Figure 16, Experiment 1B, HaCaT vs NHEK, BMAL1 - $\Delta\Delta$ Ct plotted against UVB treatment. Expression in irradiated NHEK is significantly higher than that of irradiated HaCaT.

3.5.2 Per2

*While UVB influences Per2 expression, neither an indication of a significant cell-specific effect nor of a UVB*cell-type interaction effect were evidenced.*

We normalized ΔCt values to untreated HaCaT, like before, and then conducted statistical analysis on the log(fold change) data ($-\Delta\Delta Ct$ values). We tested our data for normality with Shapiro-Wilk test (*Table 21*) and found only a marginal violation of normality for UVB ($p=0,047$). Owing to the small sample size, normality tests are very sensitive even to smaller differences in normal distribution. Conducting the test for the whole Per2 expression values (*Table 22*) indicated further no violation of normality. ANOVA should nevertheless be quite robust against small or even moderate violations of normality, even if that is the case with our data set.

Tests of Normality

	Shapiro-Wilk		
	Statistic	df	Sig.
Control	.929	9	.475
only UVB	.832	9	.047
only D3	.874	9	.135
UVB + D3	.941	9	.595

Table 21 Shapiro-Wilk test of normality of Per2 $-\Delta\Delta Ct$. For HaCaT, NHEK and SCL-1. Marginal violation of normality for UVB ($p=0,047$). The small sample size should be taken into account.

Tests of Normality

	Shapiro-Wilk		
	Statistic	df	Sig.
Per2_expression	.948	36	.089

Table 22, Shapiro-Wilk normality test for all $-\Delta\Delta Ct$ values of Per2 gene expression. For HaCaT, NHEK and SCL-1. No violation of normality indicated.

We performed once again a mixed ANOVA with UVB and D₃ as the within-subjects factors and cell type as the between-subjects factor. Levene's and Mauchly's tests indicated no significant violation of the assumptions of homoscedasticity and sphericity respectively indicated no violation of sphericity for UVB, D₃ and UVB*D₃, therefore p-values can be calculated assuming sphericity.

Results are depicted in *Tables 23* (Within-Subjects Effects) and *24* (Between-Subjects Effects).

Tests of Within-Subjects Effects

Per2 Experiment 1B: MEASURE_1

Source		Type III Sum of Squares	df	Mean Square	F	Sig.	Partial Eta Squared
UVB	Sphericity Assumed	27.863	1	27.863	110.979	.000	.949
	Greenhouse-Geisser	27.863	1.000	27.863	110.979	.000	.949
UVB * Cell_Type	Sphericity Assumed	1.475	2	.738	2.938	.129	.495
	Greenhouse-Geisser	1.475	2.000	.738	2.938	.129	.495
D3	Sphericity Assumed	.406	1	.406	3.419	.114	.363
	Greenhouse-Geisser	.406	1.000	.406	3.419	.114	.363
D3 * Cell_Type	Sphericity Assumed	.273	2	.137	1.149	.378	.277
	Greenhouse-Geisser	.273	2.000	.137	1.149	.378	.277
UVB * D3	Sphericity Assumed	.008	1	.008	.081	.785	.013
	Greenhouse-Geisser	.008	1.000	.008	.081	.785	.013
UVB * D3 * Cell_Type	Sphericity Assumed	.003	2	.001	.015	.985	.005
	Greenhouse-Geisser	.003	2.000	.001	.015	.985	.005

Table 23, Experiment 1B, Per2 - $\Delta\Delta C_t$ values, two-way repeated measures ANOVA. Within-Subjects Effects. For HaCaT, NHEK and SCL-1. We see a significant effect of UVB ($p < 0,001$), otherwise no significant differences.

We see a significant effect of UVB ($p < 0,001$) in all cells and unlike with BMAL1, no UVB*cell type interaction effect ($p = 0,129$) is noted.

Tests of Between-Subjects Effects

Per2 Experiment 1B: MEASURE_1

Transformed Variable: Average

Source	Type III Sum of Squares	df	Mean Square	F	Sig.	Partial Eta Squared
Intercept	28.313	1	28.313	25.213	.002	.808
Cell_Type	1.633	2	.817	.727	.521	.195
Error	6.738	6	1.123			

Table 24, Experiment 1B, Per2 - $\Delta\Delta C_t$ values, two-way repeated measures ANOVA. Between-Subjects Effects. No significant effect of cell type in the expression of Per2.

At the same time no significant effect of cell type is found, therefore Per2 expression and reaction against UVB treatment are similar between HaCaT, NHEK and SCL-1, unlike with BMAL1 for the same cells. This is better illustrated in *Figure 17* below.

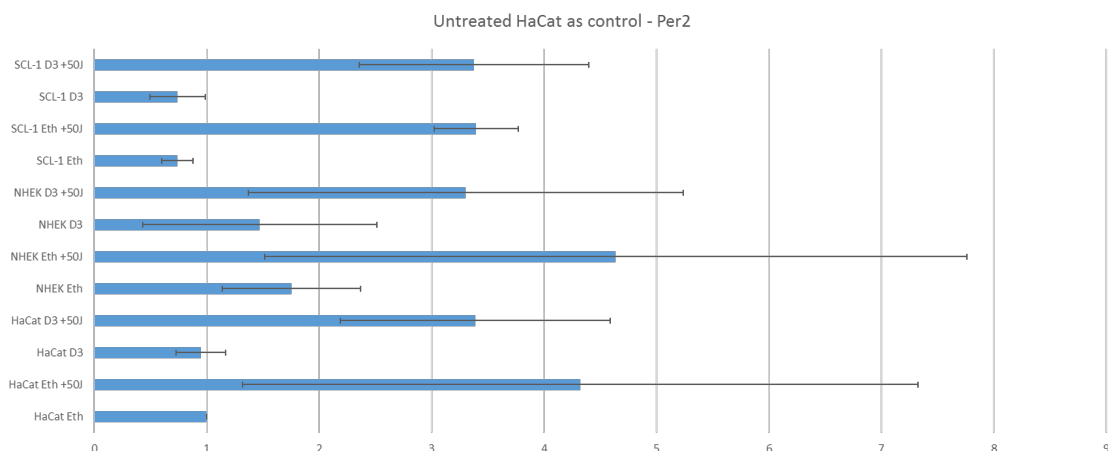


Figure 17, Experiment 1B, Per2 $2^{-\Delta\Delta C_t}$ values, untreated HaCaT as the internal control. While the difference between non-irradiated and irradiated samples is prominent between all 3 cell types, the

relative differences in expression under the same conditions seem quite similar between all 3 cells, corroborating the results of our statistical analysis.

We can see that cell types, between the different conditions, do not seem to significantly differ with one another, even if differences between conditions differ strongly. To inspect closely the effects of conditions upon the different cell subjects, we normalized their ΔC_t values to their respective $\Delta C_{t\text{Control}}$. From these we calculated the $2^{-\Delta\Delta C_t}$ values which are illustrated in Figure 21, below. These effects of different conditions are also notable in diagram, where each untreated condition from the respective cell acts as the internal control:

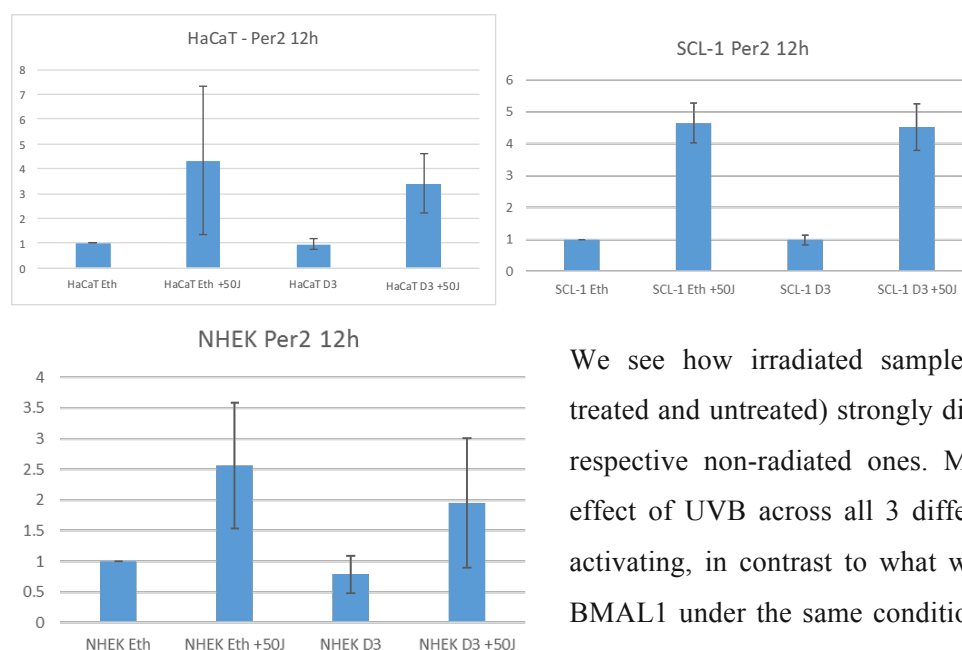


Figure 18, Experiment 1B, Per2 $2^{-\Delta\Delta C_t}$ values, normalized to each cell's control condition.

We see how irradiated samples (both D3-treated and untreated) strongly differ from the respective non-irradiated ones. Moreover, the effect of UVB across all 3 different cells, is activating, in contrast to what was noted for BMAL1 under the same conditions, in which UVB posed an activating effect on BMAL1 expression of NHEK and HaCaT (with a significantly stronger effect in NHEK) and a suppressing role in SCL-1.

- 3.6 No significant effect was noticed after administration of AhR and VDR antagonists in HaCaT and NHEK cells regarding UVB-induced DNA damage, reparation and LDH-toxicity.

1,25(OH)₂D₃, UVB, AhR- and VDR- antagonism indicate neither a significant effect on production and repair of CPD and 6-4PP photoproducts, nor on the toxicity levels for HaCaT Keratinocytes, with the exception of UVB significantly raising cellular toxicity in HaCaT Keratinocytes.

3.6.1 HaCaT CPDs

For this experiment average DNA damage concentration was calculated as described in “Methods and Materials” earlier. For HaCaT keratinocytes we analyzed both CPDs 1h and 24h

after UVB radiation using a two-way repeated measurements ANOVA for time (two levels; 1h and 24h) and D3 treatment (2 levels) as within-subject effects and AhR- and VDR-inhibitors as between-subject effects. Levene's and Mauchly's tests indicated no violation of homogeneity of variances and sphericity respectively. Shapiro-Wilk test showed only a marginal violation of normality ($p=0,049$), due to the small sample size we will not be taking that into account.

Tests of Normality

	Kolmogorov-Smirnov ^a			Shapiro-Wilk		
	Statistic	df	Sig.	Statistic	df	Sig.
Control 1h	.237	12	.061	.860	12	.049
D3 1h	.229	12	.083	.876	12	.079
Control 24h	.180	12	.200 [*]	.938	12	.473
D3 24h	.214	12	.136	.873	12	.072

*. This is a lower bound of the true significance.

a. Lilliefors Significance Correction

Table 25, Experiment 3, HaCaT CPDs, Normality Tests. Marginally significant difference in Shapiro-Wilk test for Control 1h. Nevertheless, ANOVA should be quite robust against small normality violations

Having satisfied the assumptions for ANOVA, we conducted the analysis, in which –outside of the expected DNA-repair associated- effect of time ($p<0,001$), no other significant effect was found (Tables 26 and 27).

Tests of Within-Subjects Effects

HaCaT CPDs 1h and 24h after UVB: MEASURE_1

Source		Type III Sum of Squares	df	Mean Square	F	Sig.	Partial Eta Squared
time	Sphericity Assumed	138.899	1	138.899	33.205	.000	.806
time * AhR	Sphericity Assumed	3.335	1	3.335	.797	.398	.091
time * VDR	Sphericity Assumed	.260	1	.260	.062	.810	.008
time * AhR * VDR	Sphericity Assumed	.643	1	.643	.154	.705	.019
D3	Sphericity Assumed	4.737	1	4.737	3.031	.120	.275
D3 * AhR	Sphericity Assumed	.157	1	.157	.100	.759	.012
D3 * VDR	Sphericity Assumed	.150	1	.150	.096	.765	.012
D3 * AhR * VDR	Sphericity Assumed	.458	1	.458	.293	.603	.035
time * D3	Sphericity Assumed	6.292	1	6.292	2.967	.123	.271
time * D3 * AhR	Sphericity Assumed	.084	1	.084	.040	.847	.005
time * D3 * VDR	Sphericity Assumed	1.353	1	1.353	.638	.448	.074
time * D3 * AhR * VDR	Sphericity Assumed	.007	1	.007	.004	.954	.000

Table 26, Experiment 3, HaCaT CPDs, two-way repeated measures ANOVA, Significant effect of time, due to DNA-damage repair, otherwise no significant effect found.

Tests of Between-Subjects Effects

Experiment 3, HaCaT CPDs 1h/24h: MEASURE_1

Transformed Variable: Average

Source	Type III Sum of Squares	df	Mean Square	F	Sig.	Partial Eta Squared
Intercept	507.977	1	507.977	72.318	.000	.900
VDR	.962	1	.962	.137	.721	.017
AhR	4.776	1	4.776	.680	.433	.078
VDR * AhR	.015	1	.015	.002	.964	.000

Table 27, Experiment 3, HaCaT CPDs, two-way repeated measures ANOVA. Between-Subjects effects. No significant effect found.

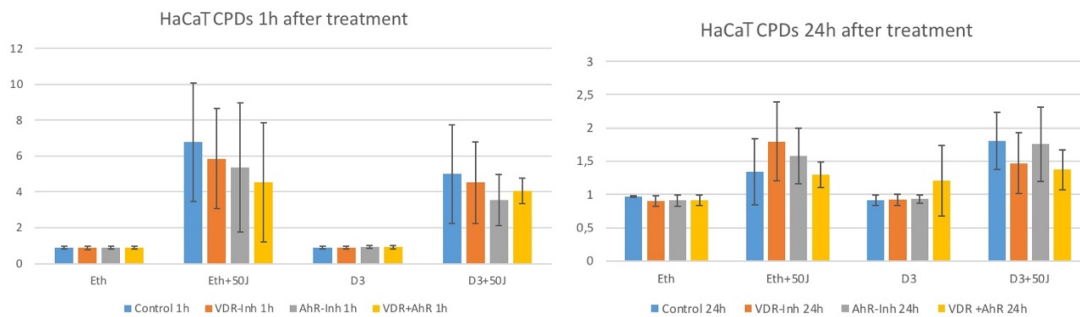


Figure 19, Experiment 3, HaCaT CPDs 1h/24h after treatment. Irradiated samples present, obviously reduced DNA-damage values compared to non-irradiated as expected and 24h irradiated samples present reduced DNA-damage levels compared to 1h after UVB treatment. A tendency of a $1,25(OH)_2D_3$ protective effect can also be noticed, however this was not supported by our statistical analysis ($p=0,120$).

3.6.2 HaCaT 6-4PPs

The results of our 6-4PPs concentrations 1h after radiation for HaCaT were unfortunately inconsistent and with massive variability between replicates. After repeating them for a total of 3 times, having found significant inconsistencies within the measurement of the same samples, we had to discard them and only use the 3h values for further analysis. We analyzed only irradiated samples with one another, since 6-4PPs values for non-irradiated samples stand very close to the lower part of the standard curve and were therefore flagged, as the assay is not sensitive enough to be detecting such small differences in values. We conducted once again a two-way repeated measurement ANOVA with D_3 and AhR-inhibition as within-subjects factors and VDR-inhibitor as the between-subject factor for 6-4PPs concentrations 3h after UVB irradiation. The results are depicted in *Table 28*.

Tests of Within-Subjects Effects							
HaCaT Keratinocytes, 6-4PPs 3h after radiation: MEASURE_1							
Source		Type III Sum of Squares	df	Mean Square	F	Sig.	Partial Eta Squared
D3	Sphericity Assumed	105.494	1	105.494	3.103	.153	.437
D3 * VDR	Sphericity Assumed	.343	1	.343	.010	.925	.003
AhR	Sphericity Assumed	75.213	1	75.213	7.085	.056	.639
AhR * VDR	Sphericity Assumed	.810	1	.810	.076	.796	.019
D3 * AhR	Sphericity Assumed	1.973	1	1.973	.180	.693	.043
D3 * AhR * VDR	Sphericity Assumed	12.842	1	12.842	1.172	.340	.227

Table 28. Experiment 3, HaCaT 6-4PPs 3h after treatment. Two-way repeated measures ANOVA. No significant difference, outside of a marginally rejected effect of UVB + AhR-inhibition ($p=0,056$)

No significant differences were found, albeit the AhR- inhibition presented a marginally rejected p-value ($p=0,056$). The plotted graph (*Figure 20*) further illustrates the results:

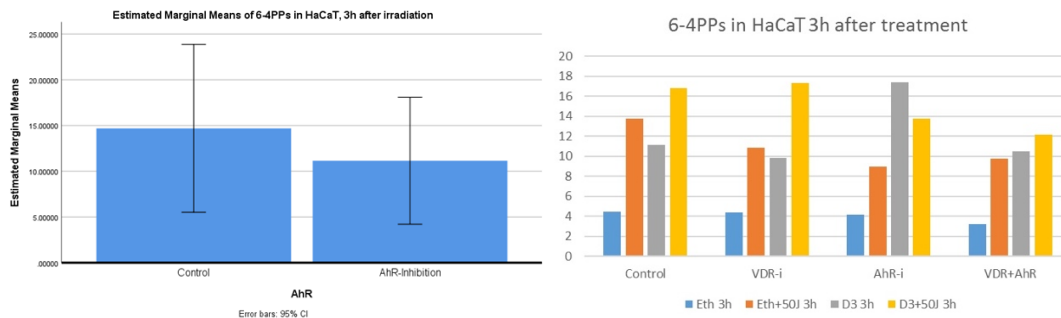


Figure 20. Experiment 3, HaCaT mean 6-4PPs concentrations, 3h after treatment, between irradiated samples. Despite the marginal rejection of the significant of the difference between AhR-i(+) and AhR-i(-) treated samples, we see a relative reduction of the DNA-damage under AhR inhibition compared to control.

3.6.3 LDH-Toxicity Assays

Lastly, we performed LDH- Toxicity Assays on medium collected from HaCaT Keratinocytes 24h after treatment. We performed 4-way paired (repeated-measures) ANOVA, for UVB, D3, AhR- and VDR- inhibition as within-subjects factors, the Mauchly's test indicating no violation of sphericity, with the following results:

Tests of Within-Subjects Effects

HaCaT 24h Toxicity levels: MEASURE_1

Source		Type III Sum of Squares	df	Mean Square	F	Sig.	Partial Eta Squared
UVB	Sphericity Assumed	3.669	1	3.669	39.984	0.024	0.952
D3	Sphericity Assumed	0.380	1	0.380	7.928	0.106	0.799
AhR	Sphericity Assumed	0.228	1	0.228	3.541	0.201	0.639
VDR	Sphericity Assumed	0.000	1	0.000	0.002	0.969	0.001
UVB * D3	Sphericity Assumed	0.798	1	0.798	13.393	0.067	0.870
UVB * AhR	Sphericity Assumed	0.162	1	0.162	1.380	0.361	0.408
D3 * AhR	Sphericity Assumed	0.045	1	0.045	0.169	0.721	0.078
UVB * D3 * AhR	Sphericity Assumed	0.088	1	0.088	2.483	0.256	0.554
UVB * VDR	Sphericity Assumed	0.373	1	0.373	3.110	0.220	0.609
D3 * VDR	Sphericity Assumed	1.207	1	1.207	3.231	0.214	0.618
UVB * D3 * VDR	Sphericity Assumed	0.008	1	0.008	0.185	0.709	0.085
AhR * VDR	Sphericity Assumed	0.574	1	0.574	10.185	0.086	0.836
UVB * AhR * VDR	Sphericity Assumed	0.037	1	0.037	0.135	0.748	0.063
D3 * AhR * VDR	Sphericity Assumed	0.394	1	0.394	2.258	0.272	0.530
UVB * D3 * AhR * VDR	Sphericity Assumed	0.013	1	0.013	0.137	0.747	0.064

Table 29, Experiment 3, HaCaT Toxicity levels 24h after treatment. Significant effect of UVB radiation ($p= 0,024$), otherwise no significant effect found.

We found a significant effect of UVB ($p= 0,024$), indicating an increase in cellular toxicity following 24h after treatment. The results are further illustrated in *Figure 21*.

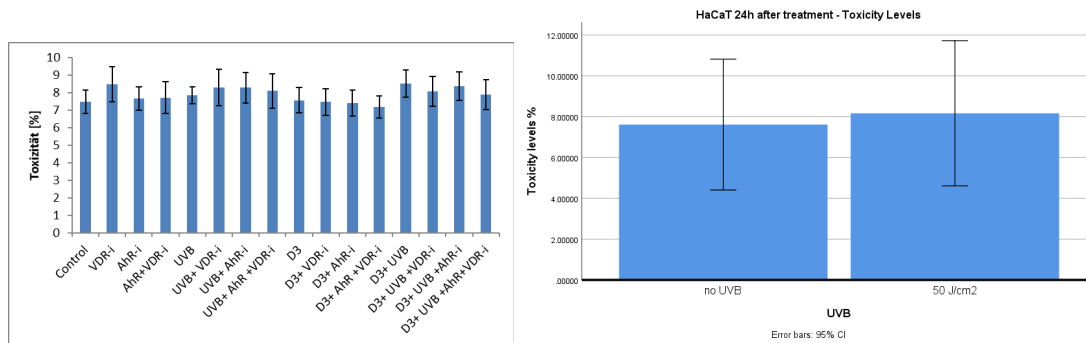


Figure 21, Experiment 3, HaCaT Toxicity Levels 24h after treatment. UVB radiation shows a moderate increase in cell toxicity, 24h after treatment. Otherwise no significant effects were observed.

1,25(OH)₂D₃ has both a DNA-damaging and photoprotective effect on NHEK cells, with a difference regarding the CPD and 6-4PP damaging process.

3.6.4 NHEK CPDs

Despite having only n=2 replicates, we performed two-way repeated measures ANOVA for NHEK for CPDs 1h after treatment only between irradiated [UVB(+)] samples, as well (D₃ and AhR as the within-subject factors and VDR-inhibitor as the between-subjects factor) and getting the following results (sphericity not violated):

Tests of Within-Subjects Effects^a

NHEK CPDs 1h after UVB: MEASURE_1

Source		Type III Sum of Squares	df	Mean Square	F	Sig.	Partial Eta Squared
D3	Sphericity Assumed	1090.346	1	1090.346	213.425	.005	.991
D3 * VDR	Sphericity Assumed	8.328	1	8.328	1.630	.330	.449
AhR	Sphericity Assumed	43.471	1	43.471	1.314	.370	.397
AhR * VDR	Sphericity Assumed	9.979	1	9.979	.302	.638	.131
D3 * AhR	Sphericity Assumed	.269	1	.269	.089	.793	.043
D3 * AhR * VDR	Sphericity Assumed	25.654	1	25.654	8.512	.100	.810

a. Cell_type = NHEK

Table 30, Experiment 3, NHEK CPDs 1h after treatment. Significant effect of D₃ (p= 0,005). Number of biologic replicates n=2.

Tests of Between-Subjects Effects

Experiment 3, NHEK CPDs 1h after treatment: MEASURE_1

Transformed Variable: Average

Source	Type III Sum of Squares	df	Mean Square	F	Sig.
Intercept	4238.480	1	4238.480	307.877	.003
VDR	46.925	1	46.925	3.409	.206

Table 31, Experiment 3, NHEK CPDs 1h after treatment. No significant effects.

And as illustrated in *Figure 22*, there is a potential for a damaging effect of D₃ in NHEK cells.

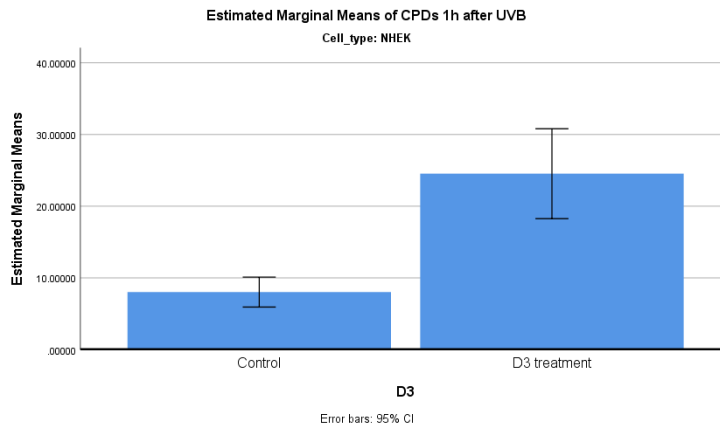


Figure 22, Experiment 3, NHEK CPDs 1h after treatment, D₃ (-) vs D₃ (+) samples. D₃ (+) samples present obviously higher CPD-levels. Number of biologic replicates n=2.

3.6.5 NHEK 6-4PPs

We further analyzed the 6-4PP values of NHEK for the 2 available biological replicates, using a two-way repeated measures ANOVA with factors of D₃ and UVB treatment and between-subject factors the AhR- and VDR- inhibition, with the following results:

Tests of Within-Subjects Effects

NHEK 6-4pp 1h after UVB: MEASURE_1

Source		Type III Sum of Squares	df	Mean Square	F	Sig.	Partial Eta Squared
D3	Sphericity Assumed	28.565	1	28.565	22.105	.009	.847
D3 * VDR	Sphericity Assumed	.001	1	.001	.001	.983	.000
D3 * AhR	Sphericity Assumed	.053	1	.053	.041	.849	.010
D3 * VDR * AhR	Sphericity Assumed	2.295	1	2.295	1.776	.254	.307
UVB	Sphericity Assumed	54.925	1	54.925	144.364	.000	.973
UVB * VDR	Sphericity Assumed	.009	1	.009	.025	.882	.006
UVB * AhR	Sphericity Assumed	.019	1	.019	.051	.833	.013
UVB * VDR * AhR	Sphericity Assumed	.655	1	.655	1.723	.260	.301
D3 * UVB	Sphericity Assumed	88.551	1	88.551	68.885	.001	.945
D3 * UVB * VDR	Sphericity Assumed	2.378	1	2.378	1.850	.245	.316
D3 * UVB * AhR	Sphericity Assumed	.160	1	.160	.125	.742	.030
D3 * UVB * VDR * AhR	Sphericity Assumed	.432	1	.432	.336	.593	.078

Table 32, Experiment 3, NHEK 6-4PPs 1h after treatment, two-way repeated measures ANOVA. Within-Subjects effects. Significant differences found for D₃ (p= 0,009), UVB (p< 0,001), UVB*D₃ (p= 0,001).

Tests of Between-Subjects Effects

NHEK 6-4pp 1h after UVB: MEASURE_1

Transformed Variable: Average

Source	Type III Sum of Squares	df	Mean Square	F	Sig.	Partial Eta Squared
Intercept	2841.791	1	2841.791	2879.899	.000	.999
VDR	4.023	1	4.023	4.077	.114	.505
AhR	1.249	1	1.249	1.266	.323	.240
VDR * AhR	.326	1	.326	.331	.596	.076
Error	3.947	4	.987			

Table 33, Experiment 3, NHEK 6-4PPs 1h after treatment, two-way repeated measures ANOVA. Between-Subjects effects. No significant difference found.

The results indicated a significant effect of D₃ (p=0,009), UVB (p<0.001) and a two-way interaction effect of UVB*D₃ (p=0,001).

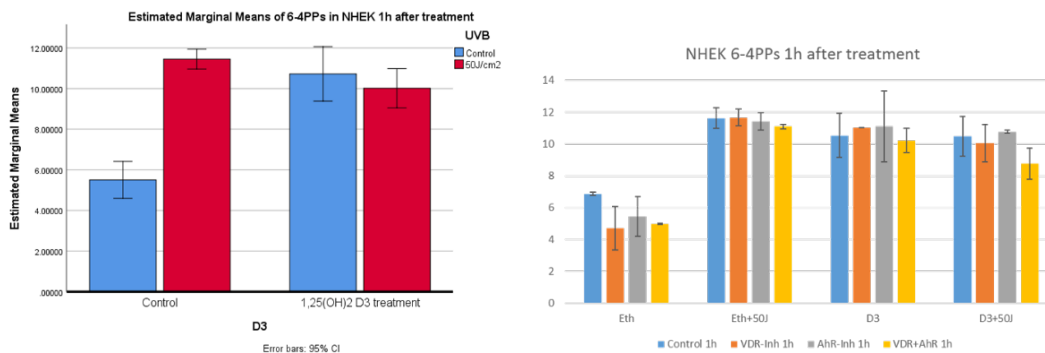


Figure 23, Experiment 3, NHEK 6-4PPs 1h after treatment. UVB treatment plotted against D₃ treatment (left) and all conditions together (right). We see the obvious increase in DNA-damage 1h after UVB, compared to non-irradiated samples. Interestingly we also notice an obvious increase in 6-4PP concentration 1h after D₃ treatment compared to control in non-irradiated samples. At the same time we see that between irradiated samples D₃ (+) samples present a lower 6-4PP concentration compared to their D₃ (-) counterparts, explaining the UVB*D₃ interaction effect noted in the statistical analysis.

Interestingly we see a damaging effect of D₃ treatment compared to control, an obvious damaging effect of UVB (increase of 6-4PP photoproducts after treatment), but their combined action seems to present a protective effect (6-4PPs concentrations in D₃(+) irradiated samples is lower than in D₃ (-) irradiated samples), which can probably be attributed to a D₃-mediated effect.

4. Discussion

Low-dosed UVB radiation upregulates CCGs in HaCaT keratinocytes and increases cellular toxicity.

While the regulatory role of circadian genes on the cutaneous and systemic response against UVB-radiation has centered the attention of several research groups, there is a serious gap of knowledge regarding the effects of UVB-radiation on CCG expression. In fact, since the study of Kawara et al in 2002²⁵, only one *in vitro*⁶⁹ and one *in vivo*⁷⁰ study have specifically investigated effects of UVB on CCGs in keratinocytes and not vice versa. In both of those cases primary human keratinocytes (NHEK) were used and mRNA of several CCGs, different to the ones used in our experimental model, were measured. There existed both results of short-term suppression of CCGs and of relative upregulation following UVB radiation in standard doses. In our case we notice a strong upregulation effect of UVB for both BMAL1 and Per2 ($p < 0,001$), which begins after a short $< 12\text{h}$ period following radiation. The effects are less clear immediately after treatment and 6h thereafter, which makes it possible that short-term suppression or dysregulation could be happening before the increase in gene expression activity follows. This corroborates the findings of Kawara et al²⁵, who similarly found a restoring of the initial suppression between the first 12-20h following treatment. It therefore seems that UVB radiation takes time to manifest its effects in CCG expression.

Unfortunately, most studies investigating effects on CCG expression follow the classic experimental design of testing a control condition against an intervention, drawing general conclusions regarding the up- or downregulation of tested genes from only limited time points. An example of such a study model is the -above mentioned- *in vivo* investigation of Cry1 and Cry2 regulation in dermis, epidermis and adipose tissue after UVB radiation, in which samples were only taken once 24h after treatment.⁷⁰ Other studies only conduct repeated measurements over a very short span (most frequently over a total 24h; example of stress affecting BMAL1 expression in neonatal rats⁷¹), which is also subject to limitations, as indicated by studies proving an altering effect of conditions (e.g. UVB) on circadian clock between the first 24h and thereafter a reversal of this effect.²⁵ Of course providing several different time points would both increase the cost and time investment needed for the experiments, but also pose several practical problems, since frequent sampling over a span of 48-72 hours would necessitate presence in the laboratory outside of the normal working hours. Despite the high variance between our biologic replicates, we believe our approach overcomes those limitations by testing

the investigated conditions over a span of 60h or approximately 2.5 period lengths. We believe we have thus succeeded in painting a representative picture of the interactions tested against the circadian clock in a more holistic way.

A second important limitation of other studies researching effects on circadian rhythms are their lack of studying alterations on period length and phase changes, but solely focusing on qualitative differences of relative expression. However, investigating properties outside of the increase or decrease of relative gene expression, would require more frequent sampling. In our case we observed no significant alterations of phase or rhythm properties, in what can also be attributed to the high variance between the replicates and the comparatively infrequent measurements we performed. The more frequent the sampling over at least one period length, the more sensitive it becomes to period length alterations or phase changes. These characteristics are especially important for studies regarding aging and cancer formation. Senescent (aged) cells have indicated prolonged circadian periods and phase changes in the form of delayed peak-times⁷², while several systemic conditions have also been linked to lengthening of circadian period like idiopathic insomnia⁷³ and an inverse correlation with HbA1c in diabetic patients⁷⁴. Owing to an increased Cry1/Cry2 ratio found in epidermal/dermal samples 24h after UVB radiation, Nikkola et al (2019)⁷⁰ further hypothesized a potential extension of the circadian period. In the same regard, our finding of UVB treatment significantly increasing cellular toxicity in HaCaT keratinocytes ($p < 0,05$), suggests that the upregulation of core CCGs BMAL1 and Per2 in those same cell-subjects characterizes another damaging effect, potentially through an acceleration of cellular senescence. It becomes evident that the full scope of UVB's damaging properties needs to be further illuminated, extending further from the already established model of UVB initiating direct DNA damage.

The skin provides great opportunities to test such properties; until now an established method using dermal fibroblasts, was used to test individual circadian rhythms and period length. Fibroblasts would be isolated from biopsies and transfected with luciferase-carrying viral vectors targeting promoter regions of known core CCGs, emitting bioluminescence based on gene expression which would be measured with a special microscope. Thereby gene expression and oscillation were quantified in real time.⁷⁵ Lately, a new less invasive method was proposed, which used instead of biopsied skin, hair follicles to measure BMAL1, Per2 and Per3 individual rhythmic activity.⁷⁶ Both cases utilized the same concept with viral vectors. The advantage of such methods, compared to simply taking frequent repetitive samples and measuring CCG expression in them with RT-PCR, is that assessment of gene expression is done real-time (no in-between time points are therefore omitted), requiring only one sample session. Especially the minimal intervention needed to assess individual circadian rhythms even in in/ex vivo

experiments makes this of great clinical relevance, opening new ways of therapeutics based on exploitation or even modulation of circadian rhythms. Exploitation of biologic clock properties to administer effective cancer therapy has gained attention in recent years and is being termed as “cancer chronotherapy”.⁷⁷

Results from the second part of Experiment 1 (Experiment 1B) further corroborated those results, both for HaCaT as well as for NHEK in which post-radiation gene activation for BMAL1 was also significantly stronger than for HaCaT. While extending this finding from the one time-point tested in NHEK to an overall conclusion would have its limitations, one has to note that HaCaT keratinocytes despite their differences with NHEK, are very regularly used in their place as the more convenient testing subject while sharing many aspects of normal keratinocyte physiology, including a functional circadian clock.⁵⁸ Regarding the two studies researching UVB radiation effect on CCG activity, one has to notice that in both studies investigating post-UVB circadian clock regulation in NHEK, cell culture was performed with serum, especially the study of Park et al⁶⁹ involved serum shock (50% FBS used for 2h before irradiating the cells) a known cell cycle synchronizing practice⁷⁸ prior to the administration of UVB treatment. Our experiments in NHEK cells were, contrariwise, conducted serum free. Serum shock has been shown to synchronize circadian clocks of adipose derived stem cells (ADSCs), similarly to how 1,25(OH)₂D₃ (D₃) treatment was supposed to affect their expression.³³ However, when combined they showed no amplifying effect. As discussed later in more detail, despite HaCaT and NHEK showcasing no significant differences regarding their overall expression ($p=0,49$), when compared with each other in regards to their CCG’s reaction against UVB, NHEKs were found to be significantly more strongly activated than HaCaT (*UVB*cell type; p=0,046*) To our knowledge, no studies exist researching the effects of UVB on CCGs of HaCaT keratinocytes, therefore while them being a solid model for keratinocyte circadian clock and them showing no difference to normal keratinocytes regarding their overall expression, drawing conclusions from them and directly linking them to studies involving NHEKs shall only be done with caution.

Another common practice of synchronizing circadian clocks in cell cultures involves Dexamethasone treatment.⁷⁹ The premise is that in cell cultures individual cells lack a common circadian rhythm due to the absence of a central pacemaker providing them with the necessary rhythmic signals. By using dexamethasone or serum shock treatments one tries to emulate how individual dependent clocks are constantly under the regulation of the dominant ones. Part of our extending hypothesis was that D₃ acts as such a signal of circadian clock synchronization, since it is an abundant circulating substance, whose levels are dependent on a known time cue stimulus (UVB / sun light). Since our investigation involved researching those mechanisms of

synchronization, we had to experiment in absence of such intervening strategies to avoid having any of the tested effects masked because of that. We nevertheless used a lower concentration of FBS (10% as described in Methodology) in our HaCaT cultures, as culturing the cells completely serum-free for the longer periods needed in our experimental setting could impact gene expression for reasons related to survivability and therefore outside of the scope of our research, while serum-starvation itself –similar to serum-shock- has also been described as a potent cell cycle synchronizing tactic.⁷⁸

There can be many mechanistic explanations attributed to post-UVB induction of CCGs. Firstly, as already explained DNA is more susceptible to damage in periods of high replication, which also explains why radiation in the evening is more damaging than in the morning, when DNA replication is at its lowest and its repair is at its highest.¹² Circadian genes are constantly expressed, albeit with altering time-dependent levels of expression. Therefore, CCGs would be susceptible to DNA damage whereby affecting their initiation sequences and therefore pushing them to overexpression, the magnitude of which could be directly linked to their phase at the time of radiation. Despite only using low-dosed UVB radiation, our LDH-Assays indicated a statistically significant ($p=0,024$) increase in cellular toxicity following 24h after treatment. Due to CCG's direct link to the cell cycle and cell senescence⁷² it is possible that these effects observed on CCG expression reflect the cellular toxicity from the damaging effects of UVB. At the same time, increased cellular toxicity could be part of the cellular coping mechanisms in riding the organism off damaged –with dysregulated circadian rhythms- cells. In other words, overexpression of CCGs could either result in earlier cellular death due to a disruption of the cell cycle, or be an indirect effect of the cellular mechanisms to prevent uncontrollable multiplication of cells with dysregulated cell cycles. The physiologic links between the cell cycle and the circadian rhythms explaining these phenomena are several. Cell cycle and circadian clocks share the same frequency of oscillation, with CCGs supervising cell cycle check points, like the c-Myc mediated regulation of G0/G1 transition by the BMAL1/CLOCK complex, the inverse relation of BMAL1 with cell cycle inhibitor p21 and of course the regulation of p53 DNA damage checkpoint from Per2.^{80,81} In that regard, CCGs are possibly implicated in halting the cell cycle, within the p53 pathway or independent of it, to assist repair of UVB-induced damage while avoiding its progression in the human genome. The role of p53 is more thoroughly discussed later.

1,25(OH)₂D₃ shows no effect in BMAL1 expression but is significantly implicated in the downregulation of Per2 between non-irradiated HaCaT keratinocytes.

An important theory we wanted to test was whether the observed UVB effects were at least in part mediated by D₃ synthesized in keratinocytes following UVB treatment potentially through a VDR-dependent mechanism. In that regard, D₃ supplementation in the absence of irradiation should at least in part emulate the observed effects of UVB. On the contrary, D₃ either showed no influence in gene expression (in BMAL1) or only an effect opposite to that of UVB (Per2 downregulation in non-irradiated samples.) And while the UVB*D₃ interaction effect, of D₃ only showcasing an influence on Per2 expression in the absence of UVB suggests a potential interplay of the two heavily connected factors, it is highly unlikely that our initial theory connects the dots in this way. It is nevertheless entirely possible that an alternative mechanism exists, which physiologically links D₃ to UVB regarding their effect on circadian rhythms.

To our knowledge we are the first to be studying the effect of D₃ (and of course also its interaction with UVB) in CCGs expression in skin cells. Another study, as already mentioned, found a synchronizing effect of D₃ in serum-starved cultured adipose derived stem cells (ADSCs).³³ After administration of D₃ in serum-starved cells, expression of BMAL1 and Per2 was increased, although no statistics were provided. CCGs in adipose cells reacting opposite to dermal/epidermal cells following UVB irradiation was nevertheless observed in Nikkola et al.⁷⁰ and more studies researching differential gene expression profiling of skin cells treated with D₃ would be needed.

The exact mechanisms pertaining to the suppressive effects of D₃ supplementation need to be further elucidated. Per2, along with Neuronal PAS domain 2 (NPAS2) -also a circadian rhythm related gene- were found to be the most significantly differentially expressed genes after transcriptome sequencing of scar tissue in rats undergoing vitamin D deficient diet against control.³⁴ Vitamin D₃'s classic mechanism of regulating gene expression, up to 3% of the human genome, is through its nuclear binding to VDR, formation of the VDR-RXR heterodimer which attaches itself thereafter to the Vitamin D Response Element (VDRE) of target genes driving their expression. That is referred to as the "genomic pathway". Using mice with disrupted intestinal clock (knockout of BMAL1 expression in duodenum), found that, while VDR expression indicated circadian rhythmicity in BMAL1^{+/+} mice, this rhythmicity was disrupted in BMAL1^{-/-} mice. They further confirmed rhythmic recruitment of VDR to the VDRE after administration of D₃, which was again lost under circadian clock disruption.³⁵ Multiple evidence suggests a circadian regulation of calcium metabolism, with Ca levels

showing circadian rhythmicity, which is eliminated under core clock depletion.^{34,82} Expression of the core circadian clock genes in the different tissues is further disrupted in CKD–MBD. (Chronic Kidney Disease – Mineral bone disorder), what can be either/both attributed to uremia influencing the core clock in the hypothalamus, and/or the parallel D₃ disruption under kidney damage.⁸³ In essence, it is possible that restoring vitamin D₃ deficiency vs supplementing additional D₃ can have completely different outcomes, due to saturation of VDR targets limiting effects past a certain point of D₃ increase in serum. It is tempting to hypothesize that serum starvation depletes cells, among others, either from D₃ or its binding protein (DBP), which results in different outcomes (upregulation) in treating them with D₃, compared to ours (downregulation). In fact, a study comparing supplementation of D₃ in FBS-containing cultures found that presence of serum increased D₃ concentrations needed for activation of core VDR-target gene CYP24A1 in osteoblastic cells and that effect is DBP-dependent.⁸⁴ Interestingly, while DBP indeed impacts D₃-mediated gene activation, bioactivity of D₃ is not compromised from DBP depletion in vivo.⁸⁴ Our parallel work of measuring VDR and VDR-target gene activation under these conditions and time points, might shed light into whether the results indicating suppression of CCGs under D₃ in non-radiated samples. Dose dependent effects should also be taken into account, pertaining to altering effects after potential saturation of VDR. Future studies should further evaluate how different concentrations of D₃, but also how depletion of VDR, affect CCG expression. This should be further weighted in, in regards to potential clinical application, whether such applications could exist or not, as *per os* administration of vitamin D has not been proven to impact processes within the skin.⁸⁵ Last but not least, it can be stipulated that D₃ increase acts as a signaling of UVB damage, even in the absence of UVB, “cheating” the system into activating the CCG anti-UVB response system and thereby countering the “expected UVB upregulation” by suppressing CCG expression. D₃ has, anyway, been long known for its protective role against UVB insults.^{86,87} More, regarding D₃-mediated photoprotectivity are discussed later.

BMAL1 shows a weaker expression profile in SCL-1 compared to HaCaT/NHEK. Low-dosed UVB radiation affects BMAL1 expression differently based on cell type, showing higher activation in NHEK than HaCaT and a suppression in SCL-1.

Extending our observations to the differences between keratinocytes of different p53 status and thereby also of different stage across the photocarcinogenicity pathway, we found a strong difference of BMAL1 expression between NHEK/HaCaT and SCL-1 cells. BMAL1 was profoundly lower expressed in cancerous SCL-1 compared to the models of normal keratinocyte clocks (HaCaT and NHEK). Although no study has to our knowledge explicitly

researched circadian rhythms of cutaneous Squamous Cell Carcinoma (cSCC), there have been investigations of other forms of cancer in which significant disruption of CCGs was also reported, with examples extending in Head and Neck SCC (downregulation)⁸⁸, Gastric Cancer (upregulation)⁸⁹, Breast cancer (variable depending on type of cancer)⁹⁰ etc. The exact aetiology of why several cancers indicated altered circadian rhythms is not yet fully understood. The biggest question remains regarding causality: does circadian clock disruption predispose against cancer, or is malignant transformation accompanied by circadian disruption and/or obstruction of synchronizing signaling pathways? In regards to the cancer inducing effects of clock disruption, there is already sufficient *in vitro* and *in vivo* evidence supporting this theory. In experimental settings such a concept has been corroborated by studies in which circadian clocks in cell cultures or mice were artificially disrupted and then cancer inducing effects were studied and compared. Regarding skin and UV damage, evidence suggests circadian disruption makes skin more susceptible to UVB-radiation and limits its UVB-associated damage repair efficiency. This was proved both in rodent¹² and human²³ experimental models. Addressing those effects in a clinical setting, the most obvious research model involves the studying of correlations between shift-work (directly related to disrupted circadian rhythms) and cancer formation potential. In a recent meta-analysis, the risk of several common cancers in women (breast, digestive system, lung and skin cancer) was shown to be significantly increased through shift-work.⁹¹ However, contrasting evidence against the correlation of skin cancer and shift-work also exists.^{92,93} A lack of circadian rhythmicity is nevertheless evident in advanced cancers; there is merit of it being both a cause and a result of cancer formation. The answer is most probably somewhere in-between. As explained, our specific cell selection was in part to model the three stages of carcinogenesis (normal -> precancerous -> cancerous) in regards to their respective p53 status (NHEK; p53 wild-type; normal, HaCaT; mutated p53; precancerous, SCL-1; p53 null phenotype; cancerous). In regards to their overall expression we found no difference between NHEK and HaCaT ($p=0,492$), while they both strongly differed from SCL-1 expression of circadian genes in regards to BMAL1 expression, while interestingly the expression of Per2 did not show any statistically significant differences between the three cells ($p=0,521$). Taken into account that BMAL1 constitutes the positive arm of the circadian clock, while Per2 is referred to as the “clock inhibitor”, suppression of BMAL1 without similar influence on Per2 in SCC is indicative of clock inhibiting effects of carcinogenesis, as evidenced also by the SCL-1’s relative ill CCG activity. On the other hand, a recent retrospective study found p53 overexpression in more than 80% of cSCC cases, which was also linked to the risk of recurrence.⁶¹ This is indicative of the heterogeneity of the expression profiles of malignant tumors. As Per2 holds a significant role in the crosstalk between the p53- and circadian clock pathway, it is interesting how despite the differences in BMAL1 expression between these cells, Per2 expression was similar between cells despite their different p53 status.

Of course, drawing conclusions regarding the role of p53 solely based on cell type would be risky, as especially between NHEK and SCL-1 the differences extend further than just the p53 phenotype. At the same time the already discussed downregulation effect of D₃ on Per2 in non-radiated HaCaT as opposed to no influence in BMAL1 gene activity, could further support the involvement of a Per2/p53 pathway in D₃-dependent photoprotectivity and skin cancer, owing to the lately suggested relationship between p53 and VDR.³⁷ Further in vivo experimentation could associate differences in expression of Per2 between sample tissue, coming from normal skin vs actinic keratosis vs cSCC and how this can be associated with p53 expression in the same samples. Such an investigation could constitute an interesting future research project.

Furthermore, we found altered reactions of CCGs against UVB stimulus between the different tested cells. For HaCaT and NHEK low-dose UVB radiation resulted in upregulation of BMAL1 after 12h, with significantly stronger effect for the NHEKs compared to HaCaT, while in SCL-1 the effect was significantly suppressive. Regarding Per2, UVB mediated a significant upregulation of the gene in all 3 cells, with no difference in regards to the magnitude of the influence. Upregulation of NHEK by UVB seems to contradict the 2 studies published on the matter^{25,70}, in which a downregulation of all tested CCGs followed, within a 24h interval post-UVB radiation. Of course, as already discussed, differences in our experimental model regarding pre-treatment synchronization and the use of serum should also be taken into consideration pertaining to our results contrasting those, albeit limited, found in the literature. Differences could also be circumstantial, owing to the testing of only one time point in this instance, rather than an overall representative picture extending to several time points inside one or more consecutive circadian periods (as was done in the first part of the experiment).

CCGs have been shown to be implicated in protective mechanisms against UV-induced stress. PER proteins were shown to be mediating a suppressive effect on matrix metalloproteinase-1 (MMP-1) in HaCaT KCs, a result of chronic UV exposure and causing agent of DNA-Damage, thereby regulating a UV-stress response mechanism.⁹⁴ Per2 was furtherly shown to be delaying p53 degradation and therefore favoring induction of p53 target genes.⁸⁰ Per2 and p53 are however antiphasic suggesting a more complex molecular pathway explaining their complex relationship. In essence, we hypothesize that BMAL1 short term activation in HaCaT and NHEK could be part of its response mechanisms, a way to signalize the presence of the insulting agent and thereby mobilize the other response mechanisms. In malignant cells, disrupted clocks showed an altered response, as a matter of the overall disruption of their response mechanisms against UV-stress. This all describes a picture of an action/reaction with induction of CCGs being the probable result of a favorable response against the UV stressor, while their suppression being rather indicative of a systems' failure. Depending on the phase at time of

radiation we can thereby expect either outcome; in unsynchronized cultures like ours, differences between independent experiments cannot always be avoided by simply applying the same experimental conditions. In the future, the hereby tested effects should be repeated in synchronized cells, for example either with Dexamethasone, serum shock, or serum-starvation pretreatment. Interestingly, the one replication of the whole 11 time points experimental design for SCL-1 indicated a much stronger suppressing effect of UVB and D₃ in regards to BMAL1 and a phase shift in Per2. The combined effects of D₃ and UVB did not show in that case any self-cancelling effect like the one mentioned in HaCaT KCs. While safe conclusions can in no way be drawn from only one replicate, combining those results with the ones from Experiment 1B we can hypothesize again that malignant cells, owing to their lack of stable response mechanisms against external stress, are more vulnerable against regulation from both UVB and D₃ and that perhaps the same mechanisms with which D₃ seems to protect the clock against UVB might be eliminated in malignant transformed cells. This can be in part due to differences in p53 expression, but most probably also because of many other unknown factors.

The role of p53 is important in applying knowledge of keratinocyte cell cultures to draw conclusions regarding epidermal physiology, but extending *in vitro* results into practice should be done with caution. Gene profiling of UVB-treated cultured keratinocytes was different to *in vivo* samples of human epidermis.⁹⁵ Cultured KCs responded to UVB through the apoptotic and cell-cycle arresting pathways, meanwhile epidermal KCs prominently upregulated genes related to damage repair. The role of p53 was of special interest, since despite p53 protein accumulation several of the p53 target genes were not affected in the *in vivo* samples. This also raises questions regarding the applicability of DNA-damage experiments in KC cultures (more on that later.)

The unclear role of 1,25(OH)₂D₃ in UVB-induced DNA-damage response and repair in our study model.

In the next part of our investigation, we focused away from gene expression and dived into DNA damage and repair as part of our research. The interaction of UVB and D₃ have been long studied in the realm of DNA damage, repair and photocarcinogenicity. We chose to measure those effects, through the measurement of two known UVB-induced photoproducts: CPDs and 6-4PPs. We selected those two photoproducts, because of them being the most abundant UVB induced DNA lesions, being directly linked to keratinocyte photocarcinogenicity and their repair being solely dependent on a single repairing system (NER).¹⁶

We started up with test Experiment 2, in which we also weighed in the factor of time of radiation in cell cultures in an effort to emulate similar results performed in mice, where UVB administered in different times during the day (morning/afternoon) had a different effect regarding DNA damage induction and repair,¹² while also introducing D₃ as the extra variable to consider. We therefore used the same time points as in the above-mentioned study (¹²), but received inconsistent results and no obvious difference between samples irradiated at 18:00 vs samples irradiated at 00:00. Most probably that was related to our cells having unsynchronized circadian rhythms, owing to their lack of a central pacemaker as is the case in complex organisms. It would be interesting to test those same conditions in cell cultures after synchronization of their rhythms to see if effects found in vivo are reproducible. Correlating effects in synchronized but still independent peripheral clocks with those in complex organisms could provide insight into the significance of intercellular and systemic circadian signaling in DNA-damage repair processes of individual cells. Had we introduced this variable (circadian synchronization) in our model, we would thereafter have serious limitations in comparing our results to those of the first experiment. Because of that, we did not follow up with more replicates of this experiment, but rather used it as a tool to select between our proposed assays for DNA-damage quantification. Concluding, we selected ELISA for being a standardized method, since the differences, which we would have to compare, would require a more sensitive method than the Dot Blot Assay proved to be. An interesting finding was the significantly different results based on time of pretreatment with D₃ before UVB. Treating cells with D₃ 12h prior to UVB radiation vs 6h prior to UVB, vs immediately post-UVB indicated significant differences in regards to CPD content for all time points following UVB radiation until 12h after its administration. Further exploring how time of pretreatment influences protectiveness of D₃ against UVB could be another interesting phenomenon to investigate in future research.

In the next part of our investigation, we introduced two further substances: (1) calcifediol a precursor of calcitriol [1,25(OH)₂D₃; here abbreviated as D₃] which has been described as a potent VDR-inhibitor, and (2) CH-223191 a potent Aryl hydrocarbon Receptor (AhR) inhibitor. (see in 2.6.5 for more) Extending from the effects of D₃ and UVB on the circadian rhythms we focused on the actual DNA-damage and reparation, the role of VDR and AhR and the differences between HaCaT and NHEKs. As discussed, we believe that the effects observed in CCGs expression after UVB, D₃ and UVB+D₃ are at least in part due to direct influences on the DNA, in the form of DNA damages and cellular toxicity. At the same time, the AhR / circadian clock crosstalk are known since many years,^{45,49} but most recently a further crosstalk between both the VDR and AhR pathway were evidenced,⁵² while also novel non-calcemic D₃ analogs were shown to have AhR as their prime target receptor.⁵³ Investigating alternative non-VDR mediated effects of D₃ was thereby also part of goals in this part of our project.

We decided to measure DNA damage, 1h vs 24h for CPDs and 1h vs 3h for 6-4PPs. Measuring them in those specific time points had two main goals: (1) DNA damage close to the time of treatment (1h after treatment in this case), would represent the damage inducing effects, in which differences between the conditions would have to be due to effects on the damage inducing mechanisms, rather than the -more time consuming- influence on the repairing process. (2) the second time points (24h after treatment for CPDs and 3h for 6-4PPs) would, on the other hand, represent a post-repair damage profile of the cellular genome. The specific time points for CPDs were chosen due to previous experience of our laboratory with similar experimental protocols, but also based on findings in the literature indicating a 60-70% reduction of post-UVB CPD content between sampling times of immediately post-radiation (0-1h) and 24h after treatment.⁹⁶ For 6-4PPs the respective time points representing “initial” vs “post-repair damage” were as explained much closer to the time of treatment. That is because of repair in 6-4PPs happening a lot faster, with the majority of the damage being already repaired within hours.⁹⁷

For both CPDs and 6-4PPs in HaCaT keratinocytes we had no important new findings. As expected, the effect of “time”, meaning the 1h vs 24h after treatment, was significant, which can be attributed to a repairing of the caused DNA damage from the NER repairing system. This corroborates similar findings in the literature.⁹⁶ While both are solely repaired from the NER repairing system, evidence suggests that faster repair of 6-4PPs might be due to a preferential binding of the DNA-Damage Binding protein 2 (DDB2) to 6-4PPs compared to CPDs.⁹⁸ Quantifying UV induced DNA damage and repair, coupled with an overall assessment of toxicity with LDH-Assays, we aimed to gain insight into the quality and magnitude of UVB damage, in accordance with our results from the first experiment. Irradiated vs non-irradiated cells, obviously, indicated significantly higher CPD and 6-4PPs content. The significant differences in accordance with time and irradiation, while obviously do not contribute something out of the ordinary, are in support of our experimental model representing actual biologic outcomes, rather than being skewed due to practical impairment. For CPDs looking at *Figure 19* a tendency of reduced DNA damage in D₃ treated irradiated samples vs the the D₃ (-) ones is indicated, suggesting a probable photoprotective effect of D₃, in accordance with what is known in the literature.⁹⁹

A potential damaging effect of 1,25(OH)₂D₃ in NHEK experiments. Increase of 6-4PP but not of CPDs in non-radiated 1,25(OH)₂D₃-treated NHEKs: A limited sample size error or a new pathway?

Our results regarding the effects of D₃ in NHEKs were however inconsistent with the suggested protective effects of D₃ against UVB-induced damage. Irradiated NHEK with D₃ treatment immediately after UVB administration indicated significantly increased CPD content ($p=0,005$) compared to non-D₃-treated samples. With 6-4PPs a similar tendency towards a damaging effect was also observed, with an overall increase in 6-4PPs content even in non-radiated samples ($p=0,009$). What was more interesting, was that even if between non-radiated samples, D₃ (+) contained higher 6-4PP content, the observed effects between irradiated samples were reversed. Indeed, samples that were treated with D₃ immediately post-radiation showed a reduced 6-4PPs content compared to their non-D₃ treated irradiated counterparts. This reminds us of the double-edge effects of D₃ in CCGs, in which administration of D₃ protected against radiation influence, but suggested negative effects when comparing its individual effect against the control. While our limited number of replicates ($n=2$) arguably decreased the power of our outcomes, especially the case of the 6-4PPs increasing 1h after D₃ treatment in the absence of UVB is of great value. It should be noted that both non-radiated D₃ (+) and (-) samples indicating a difference in 6-4PP content, were also measured for their CPD content, in which, as one would expect, DNA-damage levels were at the lowest, almost undetectable levels sensed by ELISA. Therefore, any experimental pitfalls exposing our cells to outside UVB treatment, would also cause differences in CPD content between the samples. Instead, we observed a specific 6-4PP effect of D₃ in those same NHEK samples. This nevertheless, still contradicts results of other studies, which indicate an induction of CPD and 6-4PP repair after D₃ treatment, although much of the literature utilizes protocols with D₃ pretreatment, rather than post-radiation administration of it, like we did.^{99,100} It is therefore highly possible that our results derive from problems with our assay, or of limited validity due to limited replication. At the same time, assessing the effects of UVB + D₃ combination in relation to the relative time of D₃ administration (before/after UVB) becomes once again a point to be elucidated.

Clinical vs Experimental photoprotectivity of 1,25(OH)₂D₃ and the relevance of VDR / AhR chemical antagonization. Is AhR antagonization inducing 6-4PP clearance?

Evidence in favor of photoprotectivity of D₃ in the clinical practice is by any means much more abundant in the literature, than in experimental settings involving cell cultures. The main

problem with cell culture experiments remains that they fail to exactly emulate the respective mechanisms pertaining to oral administration of D₃ in the clinical practice. In essence measuring effects in cells treated with medium containing any of the vitamin D analogs might in reality be of no clinical value, if the actual mechanisms implicated in the metabolism action of Vitamin D supplements or lifestyle changes do work through completely different pathways. Vitamin D deficiency is prevalent in many European populations, and oral supplementation has been suggested as an aiding tool in combating this phenomenon. However, a big disadvantage of the classical Vitamin D supplements are the calcium related side effects, like hypercalcemia, hypercalciuria and kidney stones when administered in high doses and/or together with calcium supplements. Vitamin D supplementation has even recently attracted attention in light of its potential for improving clinical outcome and survival of COVID-19 patients.¹⁰¹ Administration can also be done intravenously, although no difference in efficacy, compared to per os treatment, has been displayed.³² Investigating the efficacy of novel non-calcemic vitamin D analogs as alternative options, could have potential in combating this issue.¹⁰²

In our investigation of the role of VDR in the D₃-mediated effects regarding DNA damage induction and repair, we used the suggested VDR inhibitor calcifediol, as previously described.¹⁰³ Interestingly, no significant difference regarding any of the tested properties: Induction and repair of DNA damage and cellular toxicity, showed any difference after VDR inhibition. Results should, however, be confirmed with other methods of VDR elimination, or an efficiency estimation of the calcifediol's inhibition of VDR should be conducted to be able to assess our results. In our future work, measuring of VDR and VDR target genes in specific rhythmic time points around the clock, could reflect how this substance really affects VDR both in the presence and absence of its D₃ substrate.

Regarding the role of AhR we still, strictly speaking, lacked any results of statistical significance. However, especially regarding the 3h after treatment 6-4PP content of HaCaT keratinocytes under AhR inhibition vs unligated AhR, the difference was only marginally rejected ($p= 0,056$). From *Figure 20*, a reduction of 6-4PP content in AhR (-) HaCaT KCs, compared to AhR (+) can be observed. These results corroborate the reports linking AhR activation to formation and maintenance of skin cancer, through attenuation of DNA repair system and activation of carcinogenic chemicals.⁴⁶ Inhibition of AhR both through chemical inhibition and molecular interference techniques, but also the overexpression of its natural inhibitor AhR-Repressor (AhRR) improved CPD removal, while its activation reduced CPD clearance in an NER-dependent manner.⁴⁷

The two experimental aspects of our project hold special value, as they explore a potentially new way of D₃ protecting against UVB. It has been suggested that most of the observed photoprotective effects of D₃ are irrelevant to D₃'s genomic pathway, since both a non-gene altering analog of D₃ emulated its photoprotective properties and a non-gene altering antagonist of D₃ eliminated those same protective effects.⁸⁶ The effects contributing to D₃ protection against UVB are, nevertheless, most probably VDR mediated, as under depletion of VDR these photoprotective effects are eliminated in skin fibroblasts. Interestingly, this same study challenged the suggested mechanism of D₃ inducing skin protection by upregulating p53, since those same skin fibroblasts, regardless of VDR-depletion, indicated upregulated p53 under D₃ treatment.¹⁰⁴ Skepticism against the relevance of D₃-mediated p53 upregulation in the substance's role as a protective agent has been further faced, following studies in keratinocytes indicating no association between p53 levels and post-UV radiation DNA damage.¹⁰⁵ On the other hand, enough evidence also exists in favor of a crosstalk between VDR and p53 playing an important role in D₃'s suggested photoprotectivity. P53 has been shown to directly regulate VDR, to be associated with decreased UV damage in the presence of D₃ and regulate skin pigmentation, thereby increasing protectivity against UV but also reducing D₃ synthesis as a result.³⁸

In essence, it is established that D₃ counters UVB-radiation's insulting effects, the exact mechanisms still remain largely unknown.

Limitations:

Despite our best efforts, our study has many limitations. The most important one is the limited numbers of biologic replications (n=3 for all experiments, with the exception of Experiment 3 where we had n=2 replicates for NHEKs). Therefore, despite our significance/ p-values being valid, our results are lacking in statistical power (1-2 degrees of freedom in most cases. See the respective results tables). Additionally, our experiments concerning the effects of UVB, D₃ and time on CCGs involved only transcriptome data, meaning that any post-translational changes would not be taken into account in our design. It should be highlighted that no experiments concerning the effects of UVB, let alone its interaction with D₃, on CCGs have been published involving protein quantification over time, to our knowledge. Such experimental designs are obviously very time and fund consuming, but would nevertheless be necessary to completely paint a picture of the role of these conditions in the regulation of the circadian rhythms. Moreover, as mentioned, in our experiments concerning HaCaT keratinocytes and SCL-1 cells we used culture mediums supplemented with a moderate amount of FBS (10%), which could have also impacted relative expression of CCGs, which could have consequently influenced the magnitude and even quality of our results. At the same time, experimentation with serum-starved cells could also have provided us with skewed results, as part of a cell cycle synchronization process explained in detail before. This limitation could potentially apply and therefore explain the relative differences observed between HaCaT and NHEK cells (which were treated serum-free) in their common experiments. Furthermore, we examined effects of conditions on unsynchronized cells, which are obviously not representing exactly the respective conditions skin cells are undergoing as part of a complex organism, in which they are also receiving synchronization signals from the master clock. As discussed, part of our experimentation involved investigating cells in the absence of such signals, as our extending hypothesis involves the skin as a sensing organ of time cues and therefore as part of the central systematic clock circuitry. Therefore, because we wanted to investigate how the skin is involved in the transduction of such signals, we chose to avoid intervening in the synchronization of individual cell clocks. At the same time, as with all experiments on cell cultures, intercellular processes are not taken into account, which in the realm of circadian clock physiology constitutes a very important variable we had to omit.

Implications / Impact of research

As already established, exploring the role of vitamin D₃ constitutes the major target of this research project. Despite that, the actual impact of our work reflects on exploring the role of

skin as an endocrine organ. Being the first to be proving an involvement of Vitamin D₃ in the modulation of CCG expression in a cell culture experimental setting, could pave the way for further experimentation in complex organisms and comparison of the respective effects in and without the presence of a central pacemaker and other hormonal cues. Due to tissue accessibility, in vivo experimentation in human models could be far easier and faster compared to other organs, with minimally invasive methods as proposed. At the same time proving a role of the skin in the systematic communication of timekeeping messages, through vitamin D₃- and/or UVB-dependent processes, could potentially establish skin as a new therapy access point in the form of photo- /photochemical circadian clock modification with applications extending not only to dermatological, but all kind of multidisciplinary translational research and therapeutics. In an era of personalized medicine, all this raises the question: In the realm of therapy customization, apart from the “what” and “who”, should we also investigate the role of **“when”**?

Future Recommendations:

Further experimentation, investigating the role of skin cells in the regulation of the circadian clock and how this relates to the defense mechanisms against external insulting stimuli should be conducted. Studies involving not only mRNA but also protein regulation would further be of great importance in elucidating the mechanisms of circadian clock physiology and the post-transcriptional/post-translational processes that are involved in its regulation. The proven interaction effect of D₃ and UVB should be tested in further in vivo experimentation to compare results from individual peripheral clocks (like in our case), to those in more complex organisms. Of special interest would be not only the investigation of circadian impact of vitamin D₃ supplementation in healthy individuals with potential disruption of circadian clock (e. g. shift workers), but also the circadian clock alterations of vitamin D₃ deficient individuals and how that changes after restoring their deficiency through supplementation. A method of in vivo testing effects on individual circadian clocks, with only minimal invasiveness (using as samples, pulled hair follicles) has been developed,⁷⁶ which could facilitate such experimentation by reducing the single most important limitation of in vivo experimentation: bioethics of invasive sampling procedures. Lastly, the role of the VDR receptor in the observed effects of 1,25(OH)₂D₃ should also be further explored. Already developed VDR knockout rat models could be examined against their normal counterparts, both in terms of their circadian rhythms (CCG expression) and circadian rhythm behavior (locomotor activity, sleep cycles etc.) but also in how UVB and 1,25(OH)₂D₃ treatments influence these effects. We would be highly interested in exploring all those prospects in our future work.

Conclusions:

With our research we aimed to study the skin as a sensory organ and D₃ as its potential signaling agent. While a vast body of research exists regarding the role of CCGs in UVB response we focused our research in the more underexplored effects of UVB radiation on the CCGs themselves and were the first to study these effects both between cells during different stages of photocarcinogenicity and in relation to D₃. We found indeed that UVB significantly increased gene activity of core CCGs BMAL1 and Per2, in a cell-damaging way, as evidenced by a significant increase in cellular toxicity following UVB radiation. We observed an ill BMAL1 expression in cancerous cells and significantly different responses against it between HaCaT, NHEK and SCL-1 cells. While we theorized that D₃ was implicated in the mediation of UVB's effects through its receptor VDR we found it failed to emulate those effects in the absence of UVB. At the same time, we observed a significant interaction effect of UVB*D₃ in regards to Per2 being downregulated in non-radiated samples, indicating that D₃ is indeed implicated in the CC/UVB interplay through alternative ways, with possible involvement of the p53/Per2 pathway. In light of studies challenging the concept of D₃ protecting cells from UVB through alteration of target gene expression, we challenge this and hypothesize a protective and timekeeping role of D₃ in a systematic level. Because of this we are especially interested in investigating the crosstalk between VDR and the circadian clock pathway in complex organisms.

References

1. Konopka, R. J. & Benzer, S. Clock mutants of *Drosophila melanogaster*. *Proc. Natl. Acad. Sci. U. S. A.* **68**, (1971).
2. Reddy, P. *et al.* Molecular analysis of the period locus in *Drosophila melanogaster* and identification of a transcript involved in biological rhythms. *Cell* **38**, (1984).
3. Bargiello, T. A., Jackson, F. R. & Young, M. W. Restoration of circadian behavioural rhythms by gene transfer in *Drosophila*. *Nature* **312**, (1984).
4. Lalchhandama, K. The path to the 2017 Nobel Prize in Physiology or Medicine. *Sci. Vis.* **17**, (2017).
5. Matsui, M. S., Pelle, E., Dong, K. & Pernodet, N. Biological rhythms in the skin. *International Journal of Molecular Sciences* vol. 17 (2016).
6. Plikus, M. V. *et al.* The Circadian Clock in Skin. *J. Biol. Rhythms* **30**, 163–182 (2015).
7. Panda, S. Circadian physiology of metabolism. *Science* vol. 354 (2016).
8. Husse, J., Eichele, G. & Oster, H. Synchronization of the mammalian circadian timing system: Light can control peripheral clocks independently of the SCN clock: Alternate routes of entrainment optimize the alignment of the body's circadian clock network with external time. *BioEssays* **37**, 1119–1128 (2015).
9. Hardman, J. A. *et al.* The Peripheral Clock Regulates Human Pigmentation. *J. Invest. Dermatol.* **135**, 1053–1064 (2015).
10. Al-Nuaimi, Y. *et al.* A meeting of two chronobiological systems: Circadian proteins period1 and bmal1 modulate the human hair cycle clock. *J. Invest. Dermatol.* **134**, 610–619 (2014).
11. Slominski, A. T., Hardeland, R. & Reiter, R. J. When the Circadian Clock Meets the Melanin Pigmentary System. *J. Invest. Dermatol.* **135**, 943–945 (2015).
12. Gaddameedhi, S., Selby, C. P., Kaufmann, W. K., Smart, R. C. & Sancar, A. Control of skin cancer by the circadian rhythm. *Proc. Natl. Acad. Sci. U. S. A.* **108**, 18790–18795 (2011).
13. Janich, P. *et al.* Human epidermal stem cell function is regulated by circadian oscillations. *Cell Stem Cell* **13**, (2013).
14. Narayanan, D. L., Saladi, R. N. & Fox, J. L. Ultraviolet radiation and skin cancer. *International Journal of Dermatology* vol. 49 (2010).
15. Desotelle, J. A., Wilking, M. J. & Ahmad, N. The Circadian Control of Skin and Cutaneous Photodamage†. *Photochem. Photobiol.* **88**, 1037–1047 (2012).
16. Sinha, R. P. & Häder, D. P. UV-induced DNA damage and repair: A review. *Photochem. Photobiol. Sci.* **1**, (2002).
17. Reardon, J. T. & Sancar, A. Nucleotide Excision Repair. *Prog. Nucleic Acid Res. Mol. Biol.* **79**, 183–235 (2005).
18. A. Gaddameedhi, S. Selby, C. P. Kemp, M. G. Ye, R. S. The Circadian Clock Controls Sunburn Apoptosis and Erythema in Mouse Skin. *J Invest Dermatol* **135**, 1119–1127 (2015).
19. Sun, Y., Wang, P., Li, H. & Dai, J. BMAL1 and CLOCK proteins in regulating UVB-induced apoptosis and DNA damage responses in human keratinocytes. *J. Cell. Physiol.* **233**, 9563–9574 (2018).
20. Kawamura, G. *et al.* Cooperative interaction among BMAL1, HSF1, and p53 protects mammalian cells from UV stress. *Commun. Biol.* **1**, 4–9 (2018).
21. Geyfman, M. *et al.* Brain and muscle Arnt-like protein-1 (BMAL1) controls circadian cell proliferation and susceptibility to UVB-induced DNA damage in the epidermis. *Proc. Natl. Acad. Sci. U. S. A.* **109**, 11758–11763 (2012).
22. Nikkola, V. *et al.* Circadian Time Effects on NB-UVB-Induced Erythema in Human Skin In Vivo. *J. Invest. Dermatol.* **138**, 464–467 (2018).
23. Sarkar, S. & Gaddameedhi, S. UV-B-Induced Erythema in Human Skin: The Circadian Clock Is Ticking. *J. Invest. Dermatol.* **138**, 248–251 (2018).

24. Yousef, E., Mitwally, N., Noufal, N. & Tahir, M. R. Shift work and risk of skin cancer: A systematic review and meta-analysis. *Sci. Rep.* **10**, 1–11 (2020).
25. Kawara, S. *et al.* Low-dose ultraviolet B rays alter the mRNA expression of the circadian clock genes in cultured human keratinocytes. *J. Invest. Dermatol.* **119**, 1220–1223 (2002).
26. Bee, L. *et al.* Nucleotide excision repair efficiency in quiescent human fibroblasts is modulated by circadian clock. *Nucleic Acids Res.* **43**, 2126–2137 (2015).
27. Negelspach, D. C., Kaladchibachi, S. & Fernandez, F. The circadian activity rhythm is reset by nanowatt pulses of ultraviolet light. *Proc. R. Soc. B Biol. Sci.* **285**, (2018).
28. Kolarski, D. *et al.* Controlling the Circadian Clock with High Temporal Resolution through Photodosing. *J. Am. Chem. Soc.* **141**, 15784–15791 (2019).
29. Reichrath, J., Saturnus, R. & Vogt, T. Endocrine actions of vitamin D in skin: Relevance for photocarcinogenesis of non-melanoma skin cancer, and beyond. *Mol. Cell. Endocrinol.* **453**, 96–102 (2017).
30. Jagoda, S. V. & Dixon, K. M. Protective effects of 1,25 dihydroxyvitamin D 3 and its analogs on ultraviolet radiation-induced oxidative stress: a review. *Redox Rep.* **25**, 11–16 (2020).
31. Pawlowska, E., Wysokinski, D. & Blasiak, J. Nucleotide excision repair and vitamin D—Relevance for skin cancer therapy. *Int. J. Mol. Sci.* **17**, 1–21 (2016).
32. Saturnus, R., Vogt, T. & Reichrath, J. A critical appraisal of strategies to optimize vitamin d status in germany, a population with a western diet. *Nutrients* **11**, 1–22 (2019).
33. Gutierrez-Monreal, M. A., Cuevas-Diaz Duran, R., Moreno-Cuevas, J. E. & Scott, S. P. A role for 1 α ,25-dihydroxyvitamin D3 in the expression of circadian genes. *J. Biol. Rhythms* **29**, 384–388 (2014).
34. Mengatto, C. M., Mussano, F., Honda, Y., Colwell, C. S. & Nishimura, I. Circadian rhythm and cartilage extracellular matrix genes in osseointegration: A genome-wide screening of implant failure by vitamin D deficiency. *PLoS One* **6**, (2011).
35. Kawai, M. *et al.* Intestinal clock system regulates skeletal homeostasis. *JCI insight* **4**, 1–16 (2019).
36. Maguire, O. & Campbell, M. J. Vitamin D and p53 - Differentiating their relationship in AML. *Cancer Biology and Therapy* vol. 10 (2010).
37. Reichrath, J., Reichrath, S., Vogt, T. & Römer, K. Crosstalk between vitamin d and p53 signaling in cancer: An update. in *Advances in Experimental Medicine and Biology* vol. 1268 (2020).
38. Reichrath, J., Reichrath, S., Heyne, K., Vogt, T. & Roemer, K. Tumor suppression in skin and other tissues via cross-talk between vitamin D- and p53-signaling. *Frontiers in Physiology* vol. 5 JUN (2014).
39. Miki, T., Matsumoto, T., Zhao, Z. & Lee, C. C. P53 regulates Period2 expression and the circadian clock. *Nat. Commun.* **4**, (2013).
40. Hassan, A., Ahmad, J., Ashraf, H. & Ali, A. Modeling and analysis of the impacts of jet lag on circadian rhythm and its role in tumor growth. *PeerJ* **2018**, (2018).
41. Jiang, W. *et al.* The circadian clock gene Bmal1 acts as a potential anti-oncogene in pancreatic cancer by activating the p53 tumor suppressor pathway. *Cancer Lett.* **371**, (2016).
42. Zhou, L., Yu, Y., Sun, S., Zhang, T. & Wang, M. Cry 1 regulates the clock gene network and promotes proliferation and migration via the Akt/P53/P21 pathway in human osteosarcoma cells. *J. Cancer* **9**, (2018).
43. Lamia, K. A. Ticking time bombs: Connections between circadian clocks and cancer. *F1000Research* vol. 6 (2017).
44. Esser, C., Bargon, I., Weighardt, H., Haarmann-Stemmann, T. & Krutmann, J. Functions of the aryl hydrocarbon receptor in the skin. *Semin. Immunopathol.* **35**, 677–691 (2013).
45. Shimba, S. & Watabe, Y. Crosstalk between the AHR signaling pathway and circadian rhythm. *Biochem. Pharmacol.* **77**, 560–565 (2009).

46. Hidaka, T., Fujimura, T. & Aiba, S. Aryl Hydrocarbon Receptor Modulates Carcinogenesis and Maintenance of Skin Cancers. *Front. Med.* **6**, 1–7 (2019).
47. Pollet, M. *et al.* The AHR represses nucleotide excision repair and apoptosis and contributes to UV-induced skin carcinogenesis. *Cell Death Differ.* **25**, 1823–1836 (2018).
48. Luecke, S., Wincent, E., Backlund, M., Rannug, U. & Rannug, A. Cytochrome P450 1A1 gene regulation by UVB involves crosstalk between the aryl hydrocarbon receptor and nuclear factor κ B. *Chem. Biol. Interact.* **184**, 466–473 (2010).
49. Anderson, G., Beischlag, T. V., Vinciguerra, M. & Mazzocchi, G. The circadian clock circuitry and the AHR signaling pathway in physiology and pathology. *Biochem. Pharmacol.* **85**, 1405–1416 (2013).
50. Jaeger, C. & Tischkau, S. A. Role of Aryl Hydrocarbon Receptor in Circadian Clock Disruption and Metabolic Dysfunction. *Environ. Health Insights* **10**, 133–141 (2016).
51. Takami, M., Fujimaki, K., Nishimura, M. I. & Iwashima, M. Cutting Edge: AhR Is a Molecular Target of Calcitriol in Human T Cells. *J. Immunol.* **195**, 2520–2523 (2015).
52. Matsunawa, M. *et al.* Vitamin D Receptor Activation Enhances Benzo[a]pyrene Metabolism via CYP1A1 Expression in Macrophages. *Drug Metab. Dispos.* **40**, 2059–2066 (2012).
53. Slominski, A. T. *et al.* Differential and overlapping effects of 20,23(OH)₂ D₃ and 1,25(OH)₂ D₃ on gene expression in human epidermal keratinocytes: Identification of AHR as an alternative receptor for 20,23(OH)₂ D₃. *Int. J. Mol. Sci.* **19**, (2018).
54. Slominski, A. T. *et al.* ROR α and ROR γ are expressed in human skin and serve as receptors for endogenously produced noncalcemic 20-hydroxy- and 20,23-dihydroxyvitamin D. *FASEB J.* **28**, 2775–2789 (2014).
55. Slominski, A. T. *et al.* Vdr and Inverse Agonists on Ror A and Ror γ . 42–56 (2018) doi:10.1016/j.jsbmb.2016.09.024.ENDOGENOUSLY.
56. Guillaumond, F., Dardente, H., Giguère, V. & Cermakian, N. Differential control of Bmal1 circadian transcription by REV-ERB and ROR nuclear receptors. *J. Biol. Rhythms* **20**, (2005).
57. Boukamp, P. *et al.* Normal keratinization in a spontaneously immortalized aneuploid human keratinocyte cell line. *J. Cell Biol.* **106**, (1988).
58. Spörl, F. *et al.* A circadian clock in hacaT keratinocytes. *J. Invest. Dermatol.* **131**, 338–348 (2011).
59. Le, M., Mothersill, C. E., Seymour, C. B., Rainbow, A. J. & McNeill, F. E. An Observed Effect of p53 Status on the Bystander Response to Radiation-Induced Cellular Photon Emission. *Radiat. Res.* **187**, (2017).
60. Boukamp, P. *et al.* Phenotypic and genotypic characteristics of a cell line from a squamous cell carcinoma of human skin. *J. Natl. Cancer Inst.* **68**, (1982).
61. Campos, M. A. *et al.* Prognostic significance of RAS mutations and P53 expression in cutaneous squamous cell carcinomas. *Genes (Basel)*. **11**, (2020).
62. Kim, S. H. *et al.* Novel compound 2-methyl-2H-pyrazole-3-carboxylic acid (2-methyl-4-o- tolylazo-phenyl)-amide (CH-223191) prevents 2,3,7,8-TCDD-induced toxicity by antagonizing the aryl hydrocarbon receptor. *Mol. Pharmacol.* **69**, (2006).
63. Castoldi, A. *et al.* Calcifediol-loaded liposomes for local treatment of pulmonary bacterial infections. *Eur. J. Pharm. Biopharm.* **118**, (2017).
64. Zheng, W. *et al.* Vitamin D-induced vitamin D receptor expression induces tamoxifen sensitivity in MCF-7 stem cells via suppression of Wnt/ β -catenin signaling. *Biosci. Rep.* **38**, (2018).
65. S.A. Deepak *et al.* Real-Time PCR: Revolutionizing Detection and Expression Analysis of Genes. *Curr. Genomics* **8**, (2007).
66. Smith, S. M., Wunder, M. B., Norris, D. A. & Shellman, Y. G. A simple protocol for using a LDH-Based cytotoxicity assay to assess the effects of death and growth inhibition at the same time. *PLoS One* **6**, (2011).
67. Sullivan, L. M., Weinberg, J. & Keaney, J. F. Common statistical pitfalls in basic science research. *Journal of the American Heart Association* vol. 5 (2016).

68. Introduction to analysis of variance: design, analysis, and interpretation. *Choice Rev. Online* **39**, (2001).
69. Park, S., Lee, E. S., Park, N. H., Hwang, K. & Cho, E. G. Circadian expression of TIMP3 is disrupted by UVB irradiation and recovered by green tea extracts. *Int. J. Mol. Sci.* **20**, (2019).
70. Nikkola, V. *et al.* Ultraviolet B radiation modifies circadian time in epidermal skin and in subcutaneous adipose tissue. *Photodermatol. Photoimmunol. Photomed.* **35**, (2019).
71. Olejníková, L., Polidarová, L. & Sumová, A. Stress affects expression of the clock gene *Bmal1* in the suprachiasmatic nucleus of neonatal rats via glucocorticoid-dependent mechanism. *Acta Physiol.* **223**, (2018).
72. Ahmed, R. *et al.* Replicative senescent human cells possess altered circadian clocks with a prolonged period and delayed peak-time. *Aging (Albany, NY)*. **11**, (2019).
73. Materna, L. *et al.* Idiopathic hypersomnia patients revealed longer circadian period length in peripheral skin fibroblasts. *Front. Neurol.* **9**, (2018).
74. Sinturel, F. *et al.* Cellular circadian period length inversely correlates with HbA1c levels in individuals with type 2 diabetes. *Diabetologia* **62**, (2019).
75. Brown, S. A. *et al.* The period length of fibroblast circadian gene expression varies widely among human individuals. *PLoS Biol.* **3**, (2005).
76. Yamaguchi, A. *et al.* A simple method using ex vivo culture of hair follicle tissue to investigate intrinsic circadian characteristics in humans. *Sci. Rep.* **7**, 6824 (2017).
77. Kuo, T. T. & Ladurner, A. G. Exploiting the Circadian Clock for Improved Cancer Therapy: Perspective From a Cell Biologist. *Front. Genet.* **10**, (2019).
78. Chen, M. *et al.* Serum starvation induced cell cycle synchronization facilitates human somatic cells reprogramming. *PLoS One* **7**, (2012).
79. Kaneko, H., Kaitsuka, T. & Tomizawa, K. Response to Stimulations Inducing Circadian Rhythm in Human Induced Pluripotent Stem Cells. *Cells* **9**, (2020).
80. Walton, Z. E., Altman, B. J., Brooks, R. C. & Dang, C. V. Circadian Clock's Cancer Connections. *Annual Review of Cancer Biology* vol. 2 (2018).
81. Farshadi, E., van der Horst, G. T. J. & Chaves, I. Molecular Links between the Circadian Clock and the Cell Cycle. *Journal of Molecular Biology* vol. 432 (2020).
82. Jubiz, W., Canterbury, J. M., Reiss, E. & Tyler, F. H. Circadian rhythm in serum parathyroid hormone concentration in human subjects: correlation with serum calcium, phosphate, albumin, and growth hormone levels. *J. Clin. Invest.* **51**, (1972).
83. Egstrand, S., Olgaard, K. & Lewin, E. Circadian rhythms of mineral metabolism in chronic kidney disease-mineral bone disorder. *Current Opinion in Nephrology and Hypertension* vol. 29 (2020).
84. Zella, L. A., Shevde, N. K., Hollis, B. W., Cooke, N. E. & Pike, J. W. Vitamin D-binding protein influences total circulating levels of 1,25-dihydroxyvitamin D3 but does not directly modulate the bioactive levels of the hormone in vivo. *Endocrinology* **149**, (2008).
85. Bikle, D. D. Protective actions of vitamin D in UVB induced skin cancer. *Photochemical and Photobiological Sciences* vol. 11 (2012).
86. Song, E. J. *et al.* 1 α ,25-Dihydroxyvitamin D3 reduces several types of UV-induced DNA damage and contributes to photoprotection. *J. Steroid Biochem. Mol. Biol.* **136**, 131–138 (2013).
87. Dixon, K. M. *et al.* Vitamin D and death by sunshine. *Int. J. Mol. Sci.* **14**, 1964–1977 (2013).
88. Hsu, C. M., Lin, S. F., Lu, C. T., Lin, P. M. & Yang, M. Y. Altered expression of circadian clock genes in head and neck squamous cell carcinoma. *Tumor Biol.* **33**, (2012).
89. Hu, M. L. *et al.* Deregulated expression of circadian clock genes in gastric cancer. *BMC Gastroenterol.* **14**, (2014).
90. Kochan, D. Z. & Kovalchuk, O. Circadian disruption and breast cancer: An epigenetic link? *Oncotarget* **6**, (2015).

91. Yuan, X. *et al.* Night shift work increases the risks of multiple primary cancers in women: A systematic review and meta-analysis of 61 articles. *Cancer Epidemiology Biomarkers and Prevention* vol. 27 (2018).
92. Heckman, C. J., Kloss, J. D., Feskanich, D., Culnan, E. & Schernhammer, E. S. Associations among rotating night shift work, sleep and skin cancer in Nurses' Health Study II participants. *Occup. Environ. Med.* **74**, (2017).
93. Schernhammer, E. S., Razavi, P., Li, T. Y., Qureshi, A. A. & Han, J. Rotating night shifts and risk of skin cancer in the nurses' health study. *J. Natl. Cancer Inst.* **103**, (2011).
94. Yeom, M., Lee, H. I., Shin, S., Park, D. & Jung, E. PER, a circadian clock component, mediates the suppression of MMP-1 expression in HaCaT keratinocytes by cAMP. *Molecules* **23**, 1–14 (2018).
95. Enk, C. D. *et al.* The UVB-induced gene expression profile of human epidermis in vivo is different from that of cultured keratinocytes. *Oncogene* **25**, (2006).
96. Mouret, S., Charveron, M., Favier, A., Cadet, J. & Douki, T. Differential repair of UVB-induced cyclobutane pyrimidine dimers in cultured human skin cells and whole human skin. *DNA Repair (Amst)*. **7**, (2008).
97. Mitchell, D. L. THE RELATIVE CYTOTOXICITY OF(6–4) PHOTOPRODUCTS AND CYCLOBUTANE DIMERS IN MAMMALIAN CELLS. *Photochem. Photobiol.* **48**, (1988).
98. Dreze, M. *et al.* Monitoring repair of UV-induced 6-4-photoproducts with a purified DDB2 protein complex. *PLoS One* **9**, (2014).
99. Trémezaygues, L., Seifert, M., Vogt, T., Tilgen, W. & Reichrath, J. 1,25-Dihydroxyvitamin D3 modulates effects of ionizing radiation (IR) on human keratinocytes: In vitro analysis of cell viability/proliferation, DNA-damage and -repair. *J. Steroid Biochem. Mol. Biol.* **121**, (2010).
100. Chaiprasongsuk, A. *et al.* Protective effects of novel derivatives of vitamin D 3 and lumisterol against UVB-induced damage in human keratinocytes involve activation of Nrf2 and p53 defense mechanisms. *Redox Biol.* **24**, (2019).
101. Annweiler, C. *et al.* Vitamin D and survival in COVID-19 patients: A quasi-experimental study. *J. Steroid Biochem. Mol. Biol.* **204**, (2020).
102. Piotrowska, A. *et al.* Vitamin D and its low calcemic analogs modulate the anticancer properties of cisplatin and dacarbazine in the human melanoma A375 cell line. *Int. J. Oncol.* **54**, 1481–1495 (2019).
103. Zheng, W. *et al.* Vitamin D-induced vitamin D receptor expression induces tamoxifen sensitivity in MCF-7 stem cells via suppression of Wnt/-catenin signaling. *Biosci. Rep.* **38**, (2018).
104. Sequeira, V. B. *et al.* The role of the vitamin D receptor and ERp57 in photoprotection by 1 α ,25-dihydroxyvitamin D 3. *Mol. Endocrinol.* **26**, (2012).
105. Sequeira, V. B. *et al.* Opening of chloride channels by 1 α ,25-dihydroxyvitamin D 3 contributes to photoprotection against UVR-induced thymine dimers in keratinocytes. *J. Invest. Dermatol.* **133**, (2013).

Publications

Regulation of circadian clock genes by UVB radiation and Vitamin D: A pilot study in human epidermal keratinocytes during different stages of skin photocarcinogenesis. L Lamnis, A Stark, H Palm, T Vogt and J Reichrath. *ANTICANCER RESEARCH* 42: 2193-2222 (2022). doi:10.21873/anticancer.15702

(Abstract for Poster in the joint Symposia “Vitamin D in Prevention and Therapy” and “Biologic Effects of Light”, May 2022)

Acknowledgements

First and foremost, I would like to thank my mentor in this journey, Prof. Dr. Jörg Reichrath for granting me the opportunity to work in such a project and supporting me with great patience through countless hours of discussions. It is only rare for research mentors to devote such amounts of time and energy to beginner researchers like myself. Mrs Alexandra Stark played an equally important role in facilitating this project, through her direct mentorship and support in regards to the practical aspects of experiments and the organization in a lab setting. Special thanks goes to my colleague and co-researcher Mr. Christoforos Christofi for his assistance and mental support in many difficult situations. Additionally, Prof. Römer and Prof. Marcus Grimm provided great feedback regarding the organization of the project and its conclusions. The Institute of Experimental Neurology and Mrs Anna Lauer especially should be noted for their contribution regarding the performance of LDH Toxicity Assays. Last but not least, I would like to give special thanks to all friends and family who supported me mentally through the hardships of doing research abroad amid a global pandemic.

Aus datenschutzrechtlichen Gründen wird der Lebenslauf in der elektronischen Fassung der Dissertation nicht veröffentlicht.

Tag der Promotion: 02. Juni 2023

Dekan: Prof. Dr. med. Michael D. Menger

Berichterstatter: Prof. Dr. Jörg Reichrath

Prof. Dr. Sandra Iden

Prof. Dr. Lorenz Thurner